FUNCTIONAL CHARACTERIZATION OF ASYMMETRIC CELL DIVISION ASSOCIATED GENES IN HEMATOPOIETIC STEM CELLS AND BONE MARROW FAILURE SYNDROMES

BY

DEREK C. H. CHAN, BSc (Honours)

A Thesis
Submitted to the School of Graduate Studies
In Partial Fulfillment of the Requirement
For the Degree
Doctorate of Philosophy

McMaster University

McMaster University Bachelor of Science (2012) Hamilton, Ontario
McMaster University Doctorate of Philosophy (2019/20) Hamilton, Ontario

Title: Functional characterization of asymmetric cell division associated genes in hematopoietic stem cells and bone marrow failure syndromes
Author: Derek C. H. Chan, BSc (Honours)
Supervisor: Kristin Hope, PhD
Number of Pages: 135

Abstract

Hematopoietic stem cells (HSCs) are critical to the development of the hematopoietic system during ontogeny and maintaining hematopoiesis under steady-state. Several genes implicated in asymmetric cell division (ACD) have been found to influence HSC self-renewal in normal hematopoiesis and various leukemias. From a separate survey of genes associated with ACD, I now present the results from dedicated functional studies on two genes – Arhgef2 and Staufen1 – in HSCs and identify their potential contributions to benign hematopoietic disorders. Specifically, I present evidence that demonstrates a conserved role of Arhgef2 in orienting HSC division, the loss of which leads to HSC exhaustion that may underlie and contribute to the pathogenesis of Shwachman-Diamond syndrome. I also identify Staufen1 as a critical RNA-binding protein (RBP) in HSC function, downregulation of which elicits expression signatures consistent with clinical anemias reminiscent of aplastic anemia and/or paroxysmal nocturnal hemoglobinuria. I end by reviewing how RBPs function in HSCs and discuss future research directions that could further elucidate how bone marrow failure syndromes arise at the stem cell level.

Acknowledgements

There exists a famous African proverb that states that "it takes a village to raise a child." My village has been my family, whose support of my pursuit of a MD/PhD has been beyond measure. Without them, I would not be able to become who I am and achieve what I have done today. God, Mom, Dad, Sis – I will always be deeply grateful for your love, patience, affirmation and encouragement in me. To you, I dedicate this thesis. Jesús and Jeremy, thank you for your close friendships over these many years. Words cannot express how much you have made my life better during my time going through this program. Through both highs and lows, I would not have had it any other way – thank you.

As for my scientific career and journey, two other quotes come to mind. These are from Louis Pasteur, a French microbiologist, who stated that "in the field of observation, chance favours the prepared mind" and the other from Isaac Newton, an English mathematician and physicist, who previously noted that "if I have seen further, it is by standing on the shoulders of Giants." Much of my work presented in this thesis could only be completed because of the opportunity I received to hone a prepared mind that caught onto clues, coupled with the know-how and technologies brought forward by others in the past. To Kristin – thank you for granting me this chance to pursue a research career in hematology and for instilling in me high standards of scientific endeavour. Through your lab, I have been able to deeply understand the details of blood production, develop my own hypotheses on how blood disorders occur and execute experiments that perhaps no other person has done to date. I hope to be able to bring much of what I have learned in your lab with me as I continue to conduct research in hematology in the future. Sheila and Hans – thank you for your wise remarks throughout my committee meetings. Your

comments over the years have been practical and conceptually informative and I have learned much from seeing how you carry out your own careers as clinician-scientists.

Of lab members and friends, Nick H – thank you for being a bold example of forward honesty when others pushed on their personal agendas. Ana – I will never forget how much you helped me on long nights in the lab when experimental demands pushed our limits. Laura – for your experimental partnership and advocacy for me. Josh – for carrying forward my work here to completion. Nick W – for your support in my experiments and your openness with me. Damian – for your partnership in helping to make sense of large datasets. Nadeem and Saleem – for keeping me grounded and being real. Victor – for your support of my imaging ideas and pursuits. Yu, Lina and Ruilin – for your proteomics support instrumental to my project here. Minomi – for going the extra mile on flow sorts with me. All of you have made my life in lab more humane and have impressed upon me memorable moments of teamwork and spirit.

Finally, to all the patients I have had the privilege to learn from and care for in the past intervening years of my medical education – thank you for your trust in me as a medical student. The daily ebb and flow of our interactions have continually renewed in me a greater sense of responsibility to why I began this journey in the first place. It has been an honour for me to serve and bear witness in your journeys and at times of great need. Importantly, your stories and lives inspire me to believe in and search for better ways to understand, treat and perhaps cure diseases one day. I look forward to how I will continue to grow personally and professionally as a pediatric clinician-scientist in the years ahead.

Table of Contents

List of Figures and Tables

Chapter 2:

Chapter 3:

Chapter 4:

List of Abbreviations and Symbols

(Excludes all gene and technique references in the Chapter 4 review – please see associated chapter contents and Table 1 for details)

7-AAD	7-aminoactinomycin D
293FT	Fast-growing, highly transfectable clonal human embryonal kidney cell line
293GPG	Retroviral packaging human embryonal kidney cell line
Actb	Actin beta
ACD	Asymmetric cell division
Adar1	Adenosine deaminase, double-stranded RNA-specific
Alu	Short interspersed nuclear element; repetitive and transposable DNA among primates
AML	Acute myeloid leukemia
AML1-ETO	Fusion protein adjoining RUNX1 and RUNX1T1 genes; used as a genetically defined and driven type of leukemia
Anln	Anillin actin binding protein
Arhgef2	Rho/Rac guanine nucleotide exchange factor 2 (same gene reference as Lfc)
B220	Protein tyrosine phosphatase, receptor type, C (also known as CD45R)
B2m	Beta-2-microglobulin
B6.SJL	Congenic mouse model carrying pan-leukocyte CD45.1 marker backcrossed to C57Bl/6 background
Bcl11a	B-cell lymphoma/leukemia 11a
BCR-ABL	Chimeric mutation of two genes: the breakpoint cluster region protein and the Abelson murine leukemia viral oncogene homolog 1; used as a genetically defined and driven type of leukemia
Bicoid	Segment polarity protein providing positional cues for *Drosophila* head and thoracic segment development
Bora	Protein aurora borealis; aurora kinase A activator
C57Bl/6	Inbred strain of laboratory mouse; carries the pan-leukocyte CD45.2 marker
CD	Cluster of differentiation (e.g. CD4, CD8, CD45, CD150, CD48, CD34, CD38, CD55, CD59)
Cdk5rap2	Cdk5 regulatory subunit associated protein 2
CDS	Coding sequence
CFU	Colony-forming unit
Chd7	Chromodomain-helicase-DNA-binding protein 7
Cit	Citron Rho-interacting serine/threonine kinase

c-Kit	Tyrosine-protein kinase (also known as CD117 or mast/stem cell factor receptor)
Clec7a	C-type lectin domain containing 7a
CML	Chronic myeloid leukemia
CMP	Common myeloid progenitor
CMV	Cytomegalovirus (used in reference to its promoter sequence)
Cntrl	Centriolin
Cre	Type 1 topoisomerase from bacteriophage P1; causes recombination of loxP sites
Cyba	Cytochrome B-245 alpha chain
DAVID	Database for annotation, visualization and integrated discovery
DEAD	Amino acid sequence: Asp-Glu-Ala-Asp; used in reference to family of RNA helicases
DEG	Differential expressed gene
DNA	Deoxyribonucleic acid
dsRBD	Double-stranded RNA-binding domain
dsRBP	Double-stranded RNA-binding protein
dsRNA	Double-stranded RNA
Dynlt1	Dynein light chain Tctex-type 1 (same gene reference as Tctex-1)
E2f1	E2F transcription factor 1 (E2 recognition site: 5'-TTTC[CG]CGC-3')
EGFP	Enhanced green fluorescent protein
Eif4e	Eukaryotic translation initiation factor 4E
Eif4h	Eukaryotic translation initiation factor 4H
Emsy	BRCA2-interacting transcriptional repressor
ER	Endoplasmic reticulum
FBS	Fetal bovine serum
Fbx05	F-box only protein 5
Fc	Fragment, crystallizable region; receptor on surface of many leukocytes
Fcgr	Fc fragment of IgG receptor (e.g. Fcgr2a, Fcgr3a, Fcgr3b)
FL	Fetal liver
Flt3	Fms related tyrosine kinase 3
Fpr1	Formyl peptide receptor 1
Gapdh	Glyceraldehyde-3-phosphate dehydrogenase
Gata	DNA sequence "GATA"; used in reference to transcription factor family that binds to this sequence (e.g. Gata1, Gata2)
GEF	Guanine nucleotide exchange factor
GEMM	Colonies derived from multipotent progenitors (granulocytic, erythroid, monocyte, macrophage)

Gfi1	Growth factor independent 1 transcriptional repressor
GO	Gene ontology
GP+E-86	Ecotropic retroviral packaging murine fibroblast cell line
Gr-1	Granulocytic marker comprised of both Ly6C and Ly6G membrane molecules
Gurken	Determinant of anterior-posterior and dorsal-ventral axes of *Drosophila* egg
H2B	Histone H2B
Hipk2	Homeodomain-interacting protein kinase 2
Hlf	Hepatic leukemia factor
HSC	Hematopoietic stem cell
HSPC	Hematopoietic stem and progenitor cell
Hunchback	Gap class segmentation protein controlling *Drosophila* head development
Ifn-γ (or -g)	Interferon gamma
Ifngr	Interferon gamma receptor (e.g. Ifngr1, Ifngr2)
Igf2bp	Insulin-like growth factor 2 mRNA-binding protein; RBP family
IgG	Immunoglobulin G
IL	Interleukin (e.g. murine and human IL3, IL6, IL1B)
IPA	Ingenuity pathway analysis
IRES	Internal ribosome entry site
Irf7	Interferon regulatory factor 7
Ki-67	Nuclear antigen encoded by Mki67 gene; cellular marker of proliferation
LAMA-84	Human immortalized chronic myeloid-megakaryocytic leukemia cell line
Lfc	Lbc's first cousin (same gene reference as Arhgef2)
Lin	Lineage
Lis1	Lissencephaly 1 (same gene reference as PAFAH1B1)
LoxP	Locus of x-over P1; a 34-base pair site derived from bacteriophage P1
LK	$Lin^{-}Sca\text{-}1^{-}c\text{-}Kit^{+}$, denoting myeloid progenitor
LS	$Lin^{-}Sca\text{-}1^{+}c\text{-}Kit^{-}$, denoting lymphoid progenitor
LSC	Leukemic stem cell
LSK	$Lin^{-}Sca\text{-}1^{+}c\text{-}Kit^{+}$
Ltbr	Lymphotoxin beta receptor
LT-HSC	Long term-hematopoietic stem cell (i.e. LSK SLAM: $Lin^{-}Sca\text{-}1^{+}c\text{-}Kit^{+}$ $CD150^{+}CD48^{-}$)
Ly9	Lymphocyte antigen 9
K562	Human immortalized erythro-myeloid leukemia cell line
m6a	N^{6}-methyladenosine
Mac-1	Macrophage-1 antigen, a complement receptor consisting of CD11b and CD18

MAPK	Mitogen activated protein kinase
mCherry	Monomeric red fluorescent protein
Meis1	Myeloid ecotropic viral integration site 1
MEP	Megakaryocyte-erythroid progenitor
mIL	Murine interleukin (e.g. mIL-3, mIL-6)
miR	MicroRNA (e.g. miR-30, miR-223)
miR-E	Optimized microRNA-30 backbone restoring conservation of 3' element
MLP	Multi-lymphoid progenitor
MPP	Multipotent progenitor
mRNA	Messenger RNA
Mrtf	Myocardin-related transcription factor
mSCF	Murine stem cell factor
MSCV	Murine stem cell virus (used in reference to its long terminal repeat promoter)
mTPO	Murine thrombopoietin
Myb	Proto-oncogene, transcription factor family
Myc	Proto-oncogene, BHLH transcription factor
Nanos	Maternal RNA-binding protein controlling posterior development and is required for *Drosophila* germ cell proliferation and self-renewal
Nanos1	Translational repressor essential for *Xenopus* primordial germ cell development
Nfe2l2	Nuclear factor, erythroid 2 like 2
Nlrp3	NLR family pyrin domain containing 3
NMD	Nonsense-mediated decay
NOD	Non-obese diabetic
NSG	NOD/SCID/IL2R$\gamma^{-/-}$
Oskar	Maternal effect protein that organizes germ plasm and directs posterior localization of *Nanos* mRNA and Staufen in *Drosophila* egg
$p54^{nrb}$	Non-POU domain-containing octamer binding protein (also known as NonO)
Pafah1b1	Platelet activating factor acetylhydrolase 1b regulatory subunit 1 (same gene reference as Lis1)
Pbrm1	Polybromo 1
Piga	Phosphatidylinositol glycan class A
PCR	Polymerase chain reaction
PKR	Protein kinase R; eukaryotic translation initiation factor 2 alpha kinase 2 (also known as Eif2ak2)
Prkdc	Protein kinase, DNA-activated, catalytic subunit
Ptger2	Prostaglandin E receptor 2

Pum1	Pumilio RNA binding family member 1
Pum2	Pumilio RNA binding family member 2
qPCR	Quantitative polymerase chain reaction
Rab20	Ras-related protein; functions in apical endocytosis/recycling
RAS	Small GTPase family of related proteins
RBC	Red blood cell
RBP	RNA-binding protein
RhoA	Ras homolog family member A; small GTP binding protein
RhoB	Ras homolog family member B; small GTP binding protein
Rho^{lo}	Rhodamine-123, mitochondrial dye (low levels indicating efficient cellular efflux)
rMATS	Replicate multivariate analysis of transcript splicing
RNA	Ribonucleic acid
RNAi	RNA interference
RNA-seq	RNA-sequencing
RNP	Ribonucleoprotein
rRNA	Ribosomal RNA
Rtel1	Regulator of telomere elongation helicase 1
Sca-1	Stem cell antigen-1 (also known as Ly6a)
SCID	Severe combined immunodeficient
scRNA-seq	Single cell RNA-sequencing
SDS	Shwachman-Diamond syndrome
shRNA	Short hairpin RNA
SLAM	Signaling lymphocyte activation molecule (reference to family of receptors, most often $CD150^{+}CD48^{-}$ combination for HSCs)
SMD	Staufen-mediated decay
snoRNA	Small nucleolar RNA
Srf	Serum response factor
Stat1	Signal transducer and activator of transcription 1
Stau1	Staufen double-stranded RNA binding protein 1
Stau2	Staufen double-stranded RNA binding protein 2
Tctex-1	Light chain of cytoplasmic dynein (same gene reference as Dynlt1)
Ter-119	Erythroid-specific antigen (also known as Ly-76)
THP-1	Human immortalized monocytic leukemia cell line
Thy-1	Thy-1 cell surface antigen/membrane glycoprotein (also known as CD90)
TMT	Tandem mass tag
Tuba	Alpha tubulin (same gene reference as α-tubulin)

Upf1	Up-frameshift 1; monomeric RNA helicase and ATPase
UPLC	Ultra-performance liquid chromatography
UTR	Untranslated region
Vamp8	Vesicle associated membrane protein 8
VegT	Transcription factor required for *Xenopus* mesendoderm formation
Vera	Vegetal-1 mRNA-binding protein; regulates *Xenopus* mRNA transport and localization (ortholog to Igf2bp RBP family)
Vg1	Vegetal-1; maternal growth signalling factor with vegetal localization in *Xenopus* blastomeres important for dorsal mesoderm specification
WBM	Whole bone marrow
WT	Wildtype
Xbp1	X-box-binding protein 1; transcription factor that regulates the unfolded protein response during ER stress
Xdazl1	RNA-binding protein required for *Xenopus* primordial germ cell differentiation
ZsGreen	Zoanthus green fluorescent protein

Declaration of Academic Achievement

I designed and executed all research, analyzed the data, and wrote all sections of this thesis presented herein, with exceptions to the following:

Chapter 2: Lfc/Arhgef2 fetal liver data and SBDS-ARHGEF2 rescue experimental work was carried out by Ana Vujovic and Joshua Xu respectively. Cailin Joyce and Carl Novina acted as collaborators for the SDS single cell RNA-sequencing data in this project.

Chapter 3: RNA-sequencing and analysis was performed by Patrick Gendron from the Institute for Research in Immunology and Cancer at the University of Montreal. Lina Liu, Ruilin Wu and Dr. Yu Lu ran mass spectrometry-based proteomic samples. Damian Tran assisted with overlaying RNA-seq and proteome datasets.

Dr. Kristin Hope supervised the projects, helped with data interpretation and reviewing/editing of manuscripts. All other specific contributions and additional acknowledgements are included in the respective chapters.

Chapter 1: Introduction

On the origins of blood formation in the bone marrow

The discovery that adult blood formation originated within the bone marrow first emerged in 1868, at a time when the advent of microscopes permitted early observations of cells within living organisms. Ernst Neumann and Giulio Bizzozero, both pathologists, curiously peered down their microscopes during this new window of opportunity and identified nucleated red blood cells as the precursors of erythropoiesis in the bone marrow after eliciting its contents from the human, rabbit, chicken and pigeon (Neumann, 1868; Bizzozero, 1868). Both individuals recognized that the bone marrow also produced white blood cells, which led Neumann to postulate that a common cell of origin may exist within the hematopoietic system (Bizzozero, 1869; Neumann, 1870). Incidentally, the term 'stem cell' (or 'stammzelle') was coined by the biologist Ernst Haeckel around this time, who transferred this concept from his drawings of phylogenetic trees (referred to as 'stammbäume' for family or stem trees) to describe the unicellular ancestor of all multicellular organisms (Haeckel, 1868; Haeckel, 1874). Later on, the introduction of aniline dye staining revealed further morphological differences between blood cells (Ehrlich, 1877; Pappenheim, 1898a; Pappenheim, 1898b), fueling speculation on the maturation sequence of blood cell lineages from a common ancestor. Yet while the notion of a common blood stem cell drew support from others during this time, the lack of further evidence for its unifying existence led to intense debate that continued well into the 1900s.

The discovery and characterization of hematopoietic repopulating cells

World War II (1939–1945) arrived and with it a new era of highly focused war-related research. Following the detonation of atomic bombs over Hiroshima and Nagasaki, it became clear that the lethal effects of whole body irradiation were due to the elimination of a functional hematopoietic system that led to bone marrow failure. Lead shielding of the bones or spleen prevented irradiation deaths in mice, as did bone marrow transplants from non-irradiated donors (Jacobson *et al.*, 1951). When transplanted cells were tracked by way of unique chromosomal markers or enzymes present among donor strains, it was found that radiation sickness was not rescued by secreted factors that repaired radiation lesions in the affected host, but rather by donor cell-driven engraftment and regeneration of hematopoiesis (Ford *et al.*, 1956; Nowell *et al.*, 1956).

Based on these insights, James Till, a radiation physicist, and Ernest McCulloch, a hematologist-oncologist, teamed up to quantify the effects of irradiation on the loss of hematopoietic cells. In the process of transplanting a graded number of bone marrow cells into irradiated recipient mice, they autopsied those that received doses insufficient to confer radioprotection and noticed discrete nodules in their spleens (Till and McCulloch, 1961). Histological examinations revealed that each nodule consisted of a rapidly proliferative colony of mainly undifferentiated cells, but also cells within the erythroid, monocyte, granulocyte and megakaryocyte lineages. After multi-staging their irradiation procedures around transplants and identifying that trackable chromosomal abnormalities in a colony were found throughout most of its constituent cells *in situ*, their teams importantly demonstrated that each colony was clonal (Becker *et al.*, 1963). Subsequent work showed that these colony-forming units in the spleen were renewable (Siminovitch *et al.*, 1963) and that they also gave rise to lymphocytes (Wu *et al.*, 1968), providing

the first clear line of evidence to support the existence of a common ancestral cell of origin and importantly solidifying the unitarian theory of hematopoiesis.

Prospective isolation of hematopoietic stem cells

Inspired by this work, and aided by the development of hybridoma-produced monoclonal antibodies (Kohler and Milstein, 1975) and the fluorescence-activated cell sorter (Hulett *et al.*, 1969), Irving Weissman, a pathologist, then led a group of researchers to derive several limiting dilution-based clonal progenitor assays. With studies that began in lymphocytes, their group first identified a subset of bone marrow cells with a Thy-1^{-} cell surface profile that efficiently homed to mouse thymus and generated T cells (Lepault and Weissman, 1981; Lepault *et al.*, 1983). They found that Thy-1^{lo} bone marrow populations gave rise to long term B lineage *in vitro* cultures (Muller-Sieburg *et al.*, 1986) and that by using other additional lineage (Lin) markers (B220, Gr-1, Mac-1, CD4, CD8) to refine this population by way of negative selection, their group could enrich a population of Lin^{-}Thy-1^{lo} cells that produced all major hematopoietic lineages (multipotency) and conferred long-term survival to irradiated mice over serial transplantations (self-renewal) (Muller-Sieburg *et al.*, 1986). With the addition of the Sca-1 marker, which was originally found to mark bone marrow precursors of thymus lymphocytes among other hematolymphoid subsets (Aihara *et al.*, 1986), they prospectively enriched a population of Lin^{-} Thy-1^{lo}Sca-1^{+} cells with an estimated hematopoietic stem cell (HSC) frequency of 1 in 30 (representing ~0.05% of mononuclear bone marrow cells) that could rescue 50% of irradiated recipients (Spangrude *et al.*, 1988). With further refinements, including the addition of erythroid Te-119 marker for Lin^{-} negative selection (Ikuta *et al.*, 1990), and the addition of the c-Kit^{+} surface receptor (which was found to bind the important stem cell factor required for HSC maintenance),

their group further enriched for HSCs as marked by the $Lin^{-}Thy\text{-}1^{lo}Sca\text{-}1^{+}c\text{-}Kit^{+}$ profile at a HSC frequency range of ~1 in 5–10 (Ikuta and Weissman, 1992; Morrison and Weissman, 1994). About a decade later, Sean Morrison, a stem cell biologist who carried some of this earlier work in Weissman's group, led his own group to further HSC purification efforts by identifying a separate family of signaling lymphocyte activation molecule (SLAM) markers of the $CD150^{+}CD48^{-}$ combination that yielded a HSC frequency of ~1 in 4.8 cells. Notably, when used together in combination, $Lin^{-}Sca\text{-}1^{+}c\text{-}Kit^{+}$ $CD150^{+}CD48^{-}$ (LSK SLAM) cell populations yielded a HSC frequency of ~1 in 2.1, significantly enriching HSCs to near purity (Kiel *et al.*, 2005).

Similar early initiatives in human HSC isolation began with the $Lin^{-}Thy\text{-}1^{+}CD34^{+}$ population of fetal cells that were found to be enriched for their ability to initiate long-term co-cultures on supportive stromal cells while maintaining outputs of both B-lymphoid and myeloid cells (Baum *et al.*, 1992). This population could reconstitute human thymuses and engraft in transplanted bones within severe combined immunodeficient (SCID) recipient mice that carried a $Prkdc^{SCID}$ mutation (Baum *et al.*, 1992), rendering B and T cells of the host mouse dysfunctional due their inability to rearrange antigen presenting receptor genes to mount an adaptive humoral and cellular immune response (McCune *et al.*, 1988). Subsequent work demonstrated that further HSC enrichment could be achieved with the addition of $CD38^{-}$ to $Lin^{-}CD34^{+}$ cells from cord blood and bone marrow (Terstappen *et al.*, 1991; Hao *et al.*, 1995; Bhatia *et al.*, 1997; Hao *et al.*, 1998; Miller *et al.*, 1999), repopulating multilineage hematopoiesis in non-obese diabetic (NOD)/SCID recipient mice at a HSC frequency of ~1 in 600 (Bhatia *et al.*, 1997) (This NOD/SCID mouse strain provided additional functional deficits in NK cells, absence of circulating complement and immature macrophages (Shultz *et al.*, 1995) to the SCID-mediated dysfunctions in B and T cells, allowing for increased uptake of xenografts). Groups led by

Weissman and separately by John Dick, another renowned stem cell biologist, improved on this work again, further enriching for HSCs in cord blood with the addition of a $CD90^{+}CD45RA^{-}$ profile (CD90 is also known as Thy1) that yielded a frequency ranging from 1 in 10–20 cells (Majeti *et al.*, 2007; Notta *et al.*, 2011). Addition of the integrin marker $CD49f^{+}$ with efficient efflux of the mitochondrial dye rhodamine-123 (Rho^{lo}) rendered Dick's group able to readout HSCs at single cell resolution in NOD/SCID/IL2R$\gamma^{-/-}$ (NSG) mice (Notta *et al.*, 2011), a strain which provided an even more sensitive background for xenografts given the additional defects of absent lymphocytes, NK cells and other aspects of innate immunity (Yahata *et al.*, 2002; Ito *et al.*, 2002; Traggiai *et al.*, 2004; Shultz *et al.*, 2005; Ishikawa *et al.*, 2005).

The classical model of the hematopoietic hierarchy

Initiatives that overlapped with these annotative efforts to enrich for HSCs also identified what marked downstream progenitors, their sequence during repopulation, and their lineage outputs. By the year 2000, these efforts led to an early depiction of a hierarchical hematopoietic tree, where the first branch point downstream of HSCs segregated lymphoid outputs apart from myeloid potential before going down additional bifurcations that led into unipotent progenitors. Later refinements with additional cell surface markers modified this hierarchy, keeping myeloid and lymphoid potentials together further down the tree (Adolfsson *et al.*, 2005; Doulatov *et al.*, 2010), moving megakaryocytic branching higher up (Yamamoto *et al.*, 2013; Sanjuan-Pla *et al.*, 2013) and subdividing the multipotent progenitor compartment into distinct populations (Oguro *et al.*, 2013; Cabezas-Wallscheid *et al.*, 2014; Pietras *et al.*, 2015). Evident within this stream of work was an appreciation that the HSC compartment was more functionally and molecularly heterogeneous than previously recognized (Müller-Sieburg *et al.*, 2002; Müller-Sieburg *et al.*,

2004; Dykstra *et al.*, 2007; Wilson *et al.*, 2008; Foudi *et al.*, 2009; Benveniste *et al.*, 2010; Challen *et al.*, 2010; Morita *et al.*, 2010; Benz *et al.*, 2012; Yamamoto *et al.*, 2013; Oguro *et al.*, 2013).

An emerging landscape of continuous hematopoietic differentiation

In the last decade, technological advancements permitting single cell analyses introduced opportunities to detail HSC heterogeneity at an unprecedented clonal resolution. Expression profile correlations using single cell RNA-sequencing (scRNA-seq) with HSC self-renewal have uncovered a predominant representation of genes that negatively regulate cell cycle, consistent with work that have previously indicated that quiescent HSCs are also those that harbor enduring ability to drive and contribute to hematopoiesis in transplanted settings (Wilson *et al.*, 2008). Analyses from scRNA-seq have also demonstrated that a majority of cells within the HSC compartment progress through a gradual continuum of low lineage priming (Velten *et al.*, 2017) before adopting distinct and nearly exclusive modules as unipotent progenitors (Yamamoto *et al.*, 2013; Notta *et al.*, 2016). These results could importantly explain lineage-biased outputs seen in functional experiments earlier on, and are at least validated in the example of megakaryocyte-biased HSCs in both settings of transplantation (Sanjuan-Pla *et al.*, 2013; Grover *et al.*, 2016; Carrelha *et al.*, 2018) and in native hematopoiesis (Rodriguez-Fraticelli *et al.*, 2018). An emerging model depicts human HSCs as a fluid cloud state that directly gives rise to committed progenitors without much hierarchy in between. Interestingly, some of these lineage-biased or restricted stem cells appear to be able to regain other lineage potentials in serial transplantations (Carrelha *et al.*, 2018; Yamamoto *et al.*, 2018), highlighting a certain level of plasticity that exists within HSCs. More broadly, scRNA-seq analyses have detailed trajectories of lymphoid, erythroid and granulocytic/monocytic lineages and are now refining the different pathways that lead to the

production of the various terminally differentiated hematopoietic cells, providing complementary data relatively consistent with *in situ* barcoding studies to date (Sun *et al.*, 2014; Pei *et al.*, 2017; Rodriguez-Fraticelli *et al.*, 2018). However, a complete understanding of the hematopoietic system structure still remains to be achieved, as limitations with current scRNA-seq technologies preclude detection of lowly expressed genes and foregoes equivalent degrees of data integration with protein levels, epigenetic status and metabolic profiles among other considerations.

Asymmetric cell division in development and hematopoiesis

In redefining the hematopoietic system and the various differentiation trajectories that flow from HSCs, one approach that has provided insights into their biology involves examining what occurs during HSC division when two resultant daughter cells are produced that either maintain stemness (symmetric self-renewal), differentiate into more committed progenitors (symmetric commitment), or alternatively give rise to one HSC and one more committed progenitor (asymmetric cell division (ACD)). A conceptual advantage with this axis of study, and specifically regulators of ACD, is that understanding how cell polarity is established to differentially influence cell fate decisions during division runs largely independent from how the hematopoietic system may be structured, its differentiation trajectories and/or clonal dynamics.

Initial evidence highlighting the importance of proper cell polarization to developmental outcome originated from early studies in ascidians, amphibians and insects, where it was found that localization mechanisms and polarity establishment were tightly coordinated during embryonic patterning, cellular morphogenesis and cellular migration (Zernicka-Goetz, 2002; Knoblich, 2008; de la Torre-Ubieta and Bonni, 2011; Woodham and Machesky, 2014). However, this concept was

not linked to hematopoiesis until the early 1990s, when Peter Lansdorp, a hematologist and geneticist, led a group that cultured individual human cord blood HSCs and progenitor cells (HSPCs), and characterized the lineage outputs of the resulting daughter cells by colony forming assays to demonstrate that roughly 3–17% of divisions were functionally asymmetric (Mayani *et al.*, 1993). Subsequent studies reiterated this finding, with work that favoured either intrinsic (Mayani *et al.*, 1993; Brummendorf *et al.*, 1998, Huang *et al.*, 1999) or extrinsic (Punzel *et al.*, 2003; Takano *et al.*, 2004) influences that could alter the frequency of ACDs in HSPCs. While the identification of asymmetrically segregated proteins among HSPCs followed (Beckmann *et al.*, 2007), insights on the linkage of cell division to molecular aspects of cell fate decision-making in this process were not made until a genetic reporter mouse of the Notch signaling pathway was generated (Wu *et al.*, 2007). This model permitted the visual identification of ACD among HSPCs in real time and importantly demonstrated that both intrinsic and extrinsic cues are able to alter divisional preferences and daughter cell fates. With advances made in genetics that permitted modulation of gene expression levels by way of short hairpin RNAs to knock down transcripts and/or to constitutively overexpress genes, a formalized and more systematic approach to testing whether putative intrinsic regulators of ACD functionally regulated HSC activity was taken by a several members of a group led by Guy Sauvageau, an immunologist and virologist, whose work identified several 'hit' genes that altered HSC activity (Faubert *et al.*, 2004; Hope *et al.*, 2010; Ting *et al.*, 2012). Some of these ACD-associated genes have since led to translational insights into both normal HSCs and in diseases like acute myeloid leukemia (AML) (Kharas *et al.*, 2010; Ito *et al.*, 2010; Heidel *et al.*, 2013; Park *et al.*, 2014; Zimdahl *et al.*, 2014; Park *et al.*, 2015; Taggart *et al.*, 2016; Rentas *et al.*, 2016; Naudin *et al.*, 2017; Hattori *et al.*, 2017; Mizukawa *et al.*, 2017; Mohr *et al.*, 2018). Other work has linked altered levels of ACD in HSCs with specific metabolic pathways (Ito *et al.*, 2012), contractile forces (Shin *et al.*, 2014) and aging (Florian *et al.*, 2012). Most

recently, Timm Schroeder and Dirk Loeffler, a biosystems duo, led an approximate decade-long project that continually observed single HSC daughter cells to integrate markers of ACD with markers indicative of HSC activation and differentiation (Loeffler *et al.*, 2019). With the use of advanced imaging platforms, they could reproducibly measure signal intensity differences within a two-fold range, producing a model of asymmetric inheritance of degradative lysosomal components (which includes CD63 and Numb) and Notch1, where the recipient of higher levels of these determinants maintained markers of HSC function and quiescence (autophagy, mitochondrial clearance), whereas the other daughter cell underwent differentiation (increased translational, metabolic activity and upregulation of CD71) (Loeffler *et al.*, 2019). Taken together, these longstanding strides have directly demonstrated that HSCs participate in ACDs and that several ACD-related genes influence HSC activity in various settings and in malignancies like AML.

Summary of Intent

The former of the previously mentioned successes (**Chapter 1**) inspired the main objective of this work, which was to study how other ACD-associated genes may functionally regulate HSCs and to be able to understand their role in hematopoiesis. In the following chapters, I detail distilled stories on how a mitotic spindle orientation factor previously described to alter ACDs in neural cortical precursors is essential to establishing hematopoiesis *in vivo* with direct implications with the bone marrow failure syndrome Shwachman-Diamond syndrome (**Chapter 2**); how a mammalian RNA-binding protein (RBP) paralog previously described to asymmetrically segregate during division in other model organisms is critical to HSC activity, that when downregulated, reveals expression signatures potentially reflective of clinical anemias such as aplastic anemia and/or paraoxysmal nocturnal hemoglobinuria (**Chapter 3**); and review the current understanding of RBPs in hematopoiesis to date, which also includes their role in leukemias and the emerging technologies relevant to studying post-transcriptional regulation (**Chapter 4**). I finally conclude by discussing implications arising from this work and future directions worth taking to build on these findings (**Chapter 5**). Notably, in contrast to other lines of work that have focused on malignancies like AML, both the overarching theme and novel connection found in this thesis therefore links ACD-associated genes with the understudied area of bone marrow failure syndromes as benign blood disorders for the first time. As such, I hope that you will enjoy reviewing this work as I have done in thinking about these genes for quite some time.

References

1. Adolfsson J, Månsson R, Buza-Vidas N, Hultquist A, Liuba K, Jensen CT, et al. 2005. Identification of Flt3+ lympho-myeloid stem cells lacking erythro-megakaryocytic potential a revised road map for adult blood lineage commitment. *Cell*. 121:295–306.
2. Aihara Y, Bühring HJ, Aihara M, Klein J. 1986. An attempt to produce "pre-T" cell hybridomas and to identify their antigens. *Eur J Immunol*. 16:1391–1399.
3. Baum CM, Weissman IL, Tsukamoto AS, Buckle AM, Peault B. 1992. Isolation of a candidate human hematopoietic stem-cell population. *Proc Natl Acad Sci U S A*. 89:2804–2808.
4. Becker AJ, McCulloch EA, Till JE. 1963. Cytological demonstration of the clonal nature of spleen colonies derived from transplanted mouse marrow cells. *Nature*. 197:452–454.
5. Beckmann J, Scheitza S, Wernet P, Fischer JC, Giebel B. 2007. Asymmetric cell division within the human hematopoietic stem and progenitor cell compartment: identification of asymmetrically segregating proteins. *Blood*. 109:5494–5501.
6. Benveniste P, Frelin C, Janmohamed S, Barbara M, Herrington R, Hyam D, et al. 2010. Intermediate-term hematopoietic stem cells with extended but time-limited reconstitution potential. *Cell Stem Cell*. 6:48–58.
7. Benz C, Copley MR, Kent DG, Wohrer S, Cortes A, Aghaeepour N, et al. 2012. Hematopoietic stem cell subtypes expand differentially during development and display distinct lymphopoietic programs. *Cell Stem Cell*. 10:273–283.
8. Bhatia M, Wang JC, Kapp U, Bonnet D, Dick JE. 1997. Purification of primitive human hematopoietic cells capable of repopulating immune-deficient mice. *Proc Natl Acad Sci U S A*. 94:5320–5325.
9. Bizzozero G. 1868. Sulla funzione ematopoetica del midollo del ossa. *Zentralbl Med Wissensch*. 6:885.
10. Bizzozero G. 1869. Sul midollo delle ossa. *Il Morgagni*. 11:465–481;617–646.
11. Brummendorf TH, Dragowska W, Zijlmans JMJM, Thornbury G, Lansdorp PM. 1998. Asymmetric cell divisions sustain long-term hematopoiesis from single-sorted human fetal liver cells. *J Exp Med*. 188:1117–1124.
12. Cabezas-Wallscheid N, Klimmeck D, Hansson J, Lipka DB, Reyes A, Wang Q, et al. 2014. Identification of regulatory networks in HSCs and their immediate progeny via integrated proteome, transcriptome, and DNA methylome analysis. *Cell Stem Cell*. 15:507–522.
13. Carrelha J, Meng Y, Kettyle LM, Luic TC, Norfo R, Alcolea V, et al. 2018. Hierarchically related lineage-restricted fates of multipotent haematopoietic stem cells. *Nature*. 554:106–111.

14. Challen GA, Boles NC, Chambers SM, Goodell MA. 2010. Distinct hematopoietic stem cell subtypes are differentially regulated by TGF-β1. *Cell Stem Cell*. 6:265–278.
15. de la Torre-Ubieta L, Bonni A. 2011. Transcriptional regulation of neuronal polarity and morphogenesis in the mammalian brain. *Neuron*. 72:22–40.
16. Doulatov S, Notta F, Eppert K, Nguyen LT, Ohashi PS, Dick JE. 2010. Revised map of the human progenitor hierarchy shows the origin of macrophages and dendritic cells in early lymphoid development. *Nat Immunol*. 11:585–593.
17. Dykstra B, Kent D, Bowie M, McCaffrey L, Hamilton M, Lyons K, et al. 2007. Long-term propagation of distinct hematopoietic differentiation programs *in vivo*. *Cell Stem Cell*. 1:218–229.
18. Ehrlich P. 1877. Beitrage zur kenntnis der anilinfärbungen und ihrer verwendung in der mikroskopischen technik. *Arch Mikr Anat*. 13:263–277.
19. Florian MC, Dörr K, Niebel A, Daria D, Schrezenmeier H, Rojewski M, et al. 2012. Cdc42 activity regulates hematopoietic stem cell aging and rejuvenation. *Cell Stem Cell*. 10:520–530.
20. Ford CE, Hamerton JL, Barnes DW, Loutit JF. 1956. Cytological identification of radiation-chimaeras. *Nature*. 177:452–454.
21. Foudi A, Hochedlinger K, Van Buren D, Schindler JW, Jaenisch R, Carey V, et al. 2009. Analysis of histone 2B-GFP retention reveals slowly cycling hematopoietic stem cells. *Nat Biotechnol*. 27:84–90.
22. Grover A, Sanjuan-Pla A, Thongjuea S, Carrelha J, Giustacchini A, Gambardella A, et al. 2016. Single-cell RNA sequencing reveals molecular and functional platelet bias of aged haematopoietic stem cells. *Nat Commun*. 7:11075.
23. Haeckel E. 1868. Natürliche Schöpfungsgeschichte. Georg Reimer, Berlin.
24. Haeckel E. 1874. Anthropogenie (1st edition). Wilhelm Engelmann, Leipzig.
25. Hao QL, Shah AJ, Thiemann FT, Smogorzewska EM, Crooks GM. 1995. A functional comparison of $CD34^{+}CD38^{-}$ cells in cord blood and bone marrow. *Blood*. 86:3745–3753.
26. Hao QL, Smogorzewska EM, Barsky LW, Crooks GM. *In vitro* identification of single $CD34^{+}CD38^{-}$ cells with both lymphoid and myeloid potential. *Blood*. 91:4145–4151.
27. Hattori A, Tsunoda M, Konuma T, Kobayashi M, Nagy T, Glushka J, et al. 2017. Cancer progression by reprogrammed BCAA metabolism in myeloid leukaemia. *Nature*. 545:500–504.
28. Heidel FH, Bullinger L, Arreba-Tutusaus P, Wang Z, Gaebel J, Hirt C, et al. 2013. The cell fate determinant Llgl1 influences HSC fitness and prognosis in AML. *J Exp Med*. 210:15–22.

29. Hope KJ, Cellot S, Ting SB, MacRae T, Mayotte N, Iscove NN, et al. 2010. An RNAi screen identifies Msi2 and Prox1 as having opposite roles in the regulation of hematopoietic stem cell activity. *Cell Stem Cell*. 7:101–113.
30. Huang S, Law P, Francis K, Palsson BO, Ho AD. 1999. Symmetry of initial cell divisions among primitive hematopoietic progenitors is independent of ontogenic age and regulatory molecules. *Blood*. 94:2595–2604.
31. Hulett HR, Bonner WA, Barrett J, Herzenberg LA. 1969. Cell sorting: automated separation of mammalian cells as a function of intracellular fluorescence. *Science*. 166:747–749.
32. Ikuta K, Kina T, MacNeil I, Uchida N, Peault B, Chien YH, et al. 1990. A developmental switch in thymic lymphocyte maturation potential occurs at the level of hematopoietic stem cells. *Cell*. 62:863–74.
33. Ikuta K, Weissman IL. 1992. Evidence that hematopoietic stem cells express mouse c-kit but do not depend on steel factor for their generation. *Proc Natl Acad Sci U S A*. 89:1502–1506.
34. Ishikawa F, Yasukawa M, Lyons B, Yoshida S, Miyamoto T, Yoshimoto G, et al. 2005. Development of functional human blood and immune systems in NOD/SCID/IL2 receptor γ chainnull mice. *Blood*. 106:1565–1573.
35. Ito K, Carracedo A, Weiss D, Arai F, Ala U, Avigan DE, et al. 2012. A PML-PPAR-δ pathway for fatty acid oxidation regulates hematopoietic stem cell maintenance. *Nat Med*. 18:1350–1358.
36. Ito M, Hiramatsu H, Kobayashi K, Suzue K, Kawahata M, Hioki K, et al. 2002. NOD/SCID/γ_c^{null} mouse: an excellent recipient mouse model for engraftment of human cells. *Blood*. 100:3175–3182.
37. Ito T, Kwon KY, Zimdahl B, Congdon KL, Blum J, Lento WE, et al. 2010. Regulation of myeloid leukaemia by the cell-fate determinant Musashi. *Nature*. 466:765–768.
38. Jacobson LO, Simmons EL, Marks EK, Eldredge JH. 1951. Recovery from radiation injury. *Science*. 113:510–511.
39. Kharas MG, Lengner CJ, Al-Shahrour F, Bullinger L, Ball B, Zaidi S, et al. 2010. Musashi-2 regulates normal hematopoiesis and promotes aggressive myeloid leukemia. *Nat Med*. 16:903–908.
40. Kiel MJ, Yilmaz OH, Iwashita T, Yilmaz OH, Terhorst C, Morrison SJ. 2005. SLAM family receptors distinguish hematopoietic stem and progenitor cells and reveal endothelial niches for stem cells. *Cell*. 121:1109–1121.
41. Knoblich JA. 2008. Mechanisms of asymmetric cell division. *Cell*. 132:583–597.

42. Kohler G, Milstein C. 1975. Continuous cultures of fused cells secreting antibody of predefined specificity. *Nature*. 256:495–497.
43. Lepault F, Coffman RL, Weissman IL. 1983. Characteristics of thymus-homing bone marrow cells. *J Immunol*. 131:64–69.
44. Lepault F, Weissman IL. 1981. An *in vivo* assay for thymus-homing bone marrow cells. Nature. 293:151–154.
45. Loeffler D, Wehling A, Schneiter F, Zhang Y, Müller-Bötticher N, Hoppe PS, et al. 2019. Asymmetric lysosome inheritance predicts activation of haematopoietic stem cells. *Nature*. 573:426–429.
46. Majeti R, Park CY, Weissman IL. 2007. Identification of a hierarchy of multipotent hematopoietic progenitors in human cord blood. *Cell Stem Cell*. 1:635–645.
47. Mayani H, Dragowska W, Lansdorp PM. 1993. Lineage commitment in human hemopoiesis involves asymmetric cell division of multipotent progenitors and does not appear to be influenced by cytokines. *J Cell Physiol*. 157:579–586.
48. McCune JM, Namikawa R, Kaneshima H, Shultz LD, Lieberman M, Weissman IL. 1988. The SCID-hu mouse: murine model for the analysis of human hematolymphoid differentiation and function. *Science*. 241:1632–1639.
49. Miller JS, McCullar V, Punzel M, Lemischka IR, Moore KA. 1999. Single adult human CD34+/Lin–/CD38– progenitors give rise to natural killer cells, B-lineage cells, dendritic cells, and myeloid cells. *Blood*. 93:96–106.
50. Mizukawa B, O'Brien E, Moreira DC, Wunderlich M, Hochstetler CL, Duan X, et al. 2017. The cell polarity determinant CDC42 controls division symmetry to block leukemia cell differentiation. *Blood*. 130:1336–1346.
51. Mohr J, Dash BP, Schnoeder TM, Wolleschak D, Herzog C, Tubio Santamaria N, et al. 2018. The cell fate determinant Scribble is required for maintenance of hematopoietic stem cell function. *Leukemia*. 32:1211–1221.
52. Morita Y, Ema H, Nakauchi H. 2010. Heterogeneity and hierarchy within the most primitive hematopoietic stem cell compartment. *J Exp Med*. 207:1173–1182.
53. Morrison SJ, Weissman IL. 1994. The long-term repopulating subset of hematopoietic stem cells is deterministic and isolatable by phenotype. *Immunity*. 1:661–673.
54. Muller-Sieburg CE, Whitlock CA, Weissman IL. 1986. Isolation of two early B lymphocyte progenitors from mouse marrow: a committed pre-pre-B cell and a clonogenic Thy-1-lo hematopoietic stem cell. *Cell*. 44:653–62.
55. Müller-Sieburg CE, Cho RH, Karlsson L, Huang JF, Sieburg HB. 2004. Myeloid-biased hematopoietic stem cells have extensive self-renewal capacity but generate diminished lymphoid progeny with impaired IL-7 responsiveness. *Blood*. 103:4111–4118.

56. Müller-Sieburg CE, Cho RH, Thoman M, Adkins B, Sieburg HB. 2002. Deterministic regulation of hematopoietic stem cell self-renewal and differentiation. *Blood*. 100:1302–1309.
57. Naudin C, Hattabi A, Michelet F, Miri-Nezhad A, Benyoucef A, Pflumio F, et al. 2017. PUMILIO/FOXP1 signaling drives expansion of hematopoietic stem/progenitor and leukemia cells. *Blood*. 129:2493–2506.
58. Neumann E. 1868. Ueber die Bedeutung de Knochenmarkers für die Blutbildung. *Zentralbl Med Wissensch*. 6:689.
59. Neumann E. 1870. Ein fall von leukämie mit erkrankung des knochenmarkes. *Arch Heilk*. 11:1–14.
60. Notta F, Doulatov S, Laurenti E, Poeppl A, Jurisica I, Dick JE. 2011. Isolation of single human hematopoietic stem cells capable of long-term multilineage engraftment. *Science*. 333:218–221.
61. Notta F, Zandi S, Takayama N, Dobson S, Gan OI, Wilson G, et al. 2016. Distinct routes of lineage development reshape the human blood hierarchy across ontogeny. *Science*. 351:aab2116.
62. Nowell PC, Cole LJ, Habermeyer JG, Roan PL. 1956. Growth and continued function of rat marrow cells in x-radiated mice. *Cancer Res*. 16:258–261.
63. Oguro H, Ding L, Morrison SJ. 2013. SLAM family markers resolve functionally distinct subpopulations of hematopoietic stem cells and multipotent progenitors. *Cell Stem Cell*. 13:102–116.
64. Pappenheim A. 1898a. Abstammung und entstehung der roten blutzelle. *Virchow's Archiv Pathol Anat*. 151:89–158.
65. Pappenheim A. 1898b. Von den gegenseitigen beziehungen der verschiedenen farblosen blutzellen zu einander. *Virchow's Archiv Pathol Anat*. 159:40–85.
66. Park SM, Deering RP, Lu Y, Tivnan P, Lianoglou S, Al-Shahrour F, et al. 2014. Musashi-2 controls cell fate, lineage bias, and TGF-β signaling in HSCs. *J Exp Med*. 211:71–87.
67. Park SM, Gönen M, Vu L, Minuesa G, Tivnan P, Barlowe TS, et al. 2015. Musashi2 sustains the mixed-lineage leukemia-driven stem cell regulatory program. *J Clin Invest*. 125:1286–1298.
68. Pei W, Feyerabend TB, Rössler J, Wang X, Postrach D, Busch K, et al. 2017. Polylox barcoding reveals haematopoietic stem cell fates realized *in vivo*. *Nature*. 548:456–460.
69. Pietras EM, Reynaud D, Kang YA, Carlin D, Calero-Nieto FJ, Leavitt AD, et al. 2015. Functionally distinct subsets of lineage-biased multipotent progenitors control blood production in normal and regenerative conditions. *Cell Stem Cell*. 17:35–46.

70. Punzel M, Liu D, Zhang T, Eckstein V, Miesala K, Ho AD. 2003. The symmetry of initial divisions of human hematopoietic progenitors is altered only by the cellular microenvironment. *Exp Hematol*. 31:339–347.
71. Rentas S, Holzapfel N, Belew MS, Pratt G, Voisin V, Wilhelm BT, et al. 2016. Musashi-2 attenuates AHR signalling to expand human haematopoietic stem cells. *Nature*. 532:508–511.
72. Rodriguez-Fraticelli AE, Wolock SL, Weinreb CS, Panero R, Patel SH, Jankovic M, et al. 2018. Clonal analysis of lineage fate in native haematopoiesis. *Nature*. 553:212–216.
73. Sanjuan-Pla A, Macaulay IC, Jensen CT, Woll PS, Luis TC, Mead A, et al. 2013. Platelet-biased stem cells reside at the apex of the haematopoietic stem-cell hierarchy. *Nature*. 502:232–236.
74. Shin JW, Buxboim A, Spinler KR, Swift J, Christian DA, Hunter CA, et al. 2014. Contractile forces sustain and polarize hematopoiesis from stem and progenitor cells. *Cell Stem Cell*. 14:81–93.
75. Shultz LD, Lyons BL, Burzenski LM, Gott B, Chen X, Chaleff S, et al. 2005. Human lymphoid and myeloid cell development in NOD/LtSz-scid IL2Rγnull mice engrafted with mobilized human hemopoietic stem cells. *J Immunol*. 174:6477–89.
76. Shultz LD, Schweitzer PA, Christianson SW, Gott B, Schweitzer IB, Tennent B, et al. 1995. Multiple defects in innate and adaptive immunologic function in NOD/LtSz-scid mice. *J Immunol*. 154:180–191.
77. Siminovitch L, McCulloch EA, Till JE. 1963. The distribution of colony-forming cells among spleen colonies. *J Cell Physiol*. 62:327–336.
78. Spangrude GJ, Heimfeld S, Weissman IL. 1988. Purification and characterization of mouse hematopoietic stem cells. *Science*. 241:58–62.
79. Sun J, Ramos A, Chapman B, Johnnidis JB, Le L, Ho YJ, et al. 2014. Clonal dynamics of native haematopoiesis. *Nature*. 514:322–327.
80. Taggart J, Ho TC, Amin E, Xu H, Barlowe TS, Perez AR, et al. 2016. MSI2 is required for maintaining activated myelodysplastic syndrome stem cells. *Nat Commun*. 7:10739.
81. Takano H, Ema H, Sudo K, Nakauchi H. 2004. Asymmetric division and lineage commitment at the level of hematopoietic stem cells: inference from differentiation in daughter cell and granddaughter cell pairs. *J Exp Med*. 199:295–302.
82. Terstappen LW, Huang S, Safford M, Lansdorp PM, Loken MR. 1991. Sequential generations of hematopoietic colonies derived from single nonlineage-committed CD34+CD38– progenitor cells. *Blood*. 77:1218–1227.
83. Till JE, McCulloch EA. 1961. A direct measurement of the radiation sensitivity of normal mouse bone marrow cells. *Radiat Res*. 14:213–222.

84. Ting SB, Deneault E, Hope K, Cellot S, Chagraoui J, Mayotte N, et al. 2012. Asymmetric segregation and self-renewal of hematopoietic stem and progenitor cells with endocytic Ap2a2. *Blood*. 119:2510–2522.
85. Traggiai E, Chicha L, Mazzucchelli L, Bronz L, Piffaretti JC, Lanzavecchia A, et al. 2004. Development of a human adaptive immune system in cord blood cell-transplanted mice. *Science*. 304:104–107.
86. Velten L, Haas SF, Raffel S, Blaszkiewicz S, Islam S, Hennig BP, et al. 2017. Human haematopoietic stem cell lineage commitment is a continuous process. *Nat Cell Biol*. 19:271–281.
87. Wilson A, Laurenti E, Oser G, van der Wath RC, Blanco-Bose W, Jaworski M, et al. 2008. Hematopoietic stem cells reversibly switch from dormancy to self-renewal during homeostasis and repair. *Cell*. 135:1118–1129.
88. Woodham EF, Machesky LM. 2014. Polarized cell migration: intrinsic and extrinsic drivers. *Curr Opin Cell Biol*. 30:25–32.
89. Wu AM, Till JE, Siminovitch L, McCulloch EA. 1968. Cytological evidence for a relationship between normal hemotopoietic colony-forming cells and cells of the lymphoid system. *J Exp Med*. 127:455–464.
90. Wu M, Kwon HY, Rattis F, Blum J, Zhao C, Ashkenazi R, et al. 2007. Imaging hematopoietic precursor division in real time. *Cell Stem Cell*. 1:541–554.
91. Yahata T, Ando K, Nakamura Y, Ueyama Y, Shimamura K, Tamaoki N, et al. 2002. Functional human T lymphocyte development from cord blood $CD34^+$ cells in nonobese diabetic/Shi-scid, IL-2 receptor γ null mice. *J Immunol*. 169:204–209.
92. Yamamoto R, Morita Y, Ooehara J, Hamanaka S, Onodera M, Rudolph KL, et al. 2013. Clonal analysis unveils self-renewing lineage-restricted progenitors generated directly from hematopoietic stem cells. *Cell*. 154:1112–1126.
93. Yamamoto R, Wilkinson AC, Ooehara J, Lan X, Lai CY, Nakauchi Y, et al. 2018. Large-scale clonal analysis resolves aging of the mouse hematopoietic stem cell compartment. *Cell Stem Cell*. 22:600–607.
94. Zernicka-Goetz M. 2002. Patterning of the embryo: the first spatial decisions in the life of a mouse. *Development*. 129:815–829.
95. Zimdahl B, Ito T, Blevins A, Bajaj J, Konuma T, Weeks J, et al. 2014. Lis1 regulates asymmetric division in hematopoietic stem cells and in leukemia. *Nat Genet*. 46:245–252.

Chapter 2: Arhgef2 regulates mitotic spindle orientation in hematopoietic stem cells and is essential for productive hematopoiesis

Derek C. H. Chan,[1,2] Ana Vujovic,[1] Joshua Xu,[1,2] Victor Gordon,[1] Nicholas Wong,[1] Laura P. M. H. de Rooij,[1] Cailin E. Joyce,[3–5] Jose La Rose,[6] María-José Sandí,[6] Bradley W. Doble,[1] Carl D. Novina,[3–5] Robert K. Rottapel,[6–9] and Kristin J. Hope[1]

[1]Stem Cell and Cancer Research Institute, Department of Biochemistry and Biomedical Sciences, McMaster University, Hamilton, Ontario, Canada; [2]Michael G. DeGroote School of Medicine, Faculty of Health Sciences, McMaster University, Hamilton, Ontario, Canada; [3]Department of Cancer Immunology and Virology, Dana-Farber Cancer Institute, Boston, Massachusetts, USA; [4]Department of Medicine, Harvard Medical School, Boston, Massachusetts, USA; [5]Broad Institute of Harvard and MIT, Cambridge, Massachusetts, USA; [6]Princess Margaret Cancer Centre, University Health Network, Toronto, Ontario, Canada; [7]Department of Medical Biophysics, University of Toronto, Toronto, Ontario, Canada; [8]St. Michael's Hospital, Division of Rheumatology, Department of Medicine, University of Toronto, Toronto, Ontario, Canada; and [9]Department of Immunology, University of Toronto, Toronto, Ontario, Canada

Abstract

How hematopoietic stem cells (HSCs) coordinate their divisional axis relative to supportive niche cells and whether or not their divisional orientation is important for stem cell-driven hematopoiesis is poorly understood. Single cell RNA sequencing data from patients with Shwachman-Diamond syndrome (SDS), an inherited bone marrow failure with high risk of transformation to myelodysplastic syndrome (MDS) and leukemia, shows that ARHGEF2, a RhoA-specific guanine nucleotide exchange factor (GEF) and determinant of mitotic spindle orientation, is specifically downregulated in SDS hematopoietic stem and progenitor cells (HSPCs). We demonstrate that transplanted Lfc/Arhgef2$^{-/-}$ bone marrow yields impaired hematopoietic recovery and a production deficit of long-term HSCs, phenotypes that are not due to differences in numbers of transplanted HSCs, their cell cycle status, level of apoptosis, progenitor output or homing ability. Using live imaging of dividing HSPCs, we show an increased frequency of misoriented divisions in the absence of Lfc/Arhgef2. ARHGEF2 knockdown in human HSCs also impairs their ability to regenerate hematopoiesis, culminating in significantly smaller xenografts. Together, these data demonstrate a conserved role for Lfc/Arhgef2 in orienting HSPC division and suggest that HSCs divide in certain orientations to establish hematopoiesis, the loss of which may underlie HSC dysfunction in certain bone marrow failure syndromes.

Introduction

Stem and progenitor cells across diverse species and organ systems can use both symmetric and asymmetric modes of division to achieve balanced expansion and differentiation during development. During embryogenesis, hematopoietic stem cells (HSCs) emerge in response to an asymmetric signal within the hemogenic endothelium[1] and transit through both the fetal liver and spleen before reaching and colonizing the perinatal bone marrow.[2] HSCs rapidly proliferate in this niche before becoming mostly quiescent,[3] allowing their more proliferative downstream progeny, which follow complex lineage pathways,[4–6] to productively drive native hematopoiesis.[7–12] Numerous regulators of HSC activity that are either cell-autonomous[13] or produced extrinsically by the niche[2] have been identified to date; however, little is known about how HSCs divide and how their cell fate decisions are coupled to a divisional axis when establishing hematopoiesis in either native or transplant settings.

Dividing stem cells in other tissue types are known to couple their cell polarity axis with a properly oriented mitotic spindle to allow for appropriate acquisition of intracellular stem versus commitment fate determinants among daughter cells.[14] Orientation of the mitotic spindle relative to stem cell-supportive niche signals is therefore critical for establishing cell polarity as well as directing fate decisions through the placement of prospective daughter cells in niche-proximal versus niche-distal conformations. For example, neural precursors in the developing brain undergo an early expansion phase, during which fate decisions are largely symmetric as a result of divisions occurring parallel to the ventricular zone apical neuroepithelium.[15,16] A switch occurs in the subsequent neurogenic phase when the divisions of these expanded precursors become oblique and/or perpendicular, leading to the production of a differentiated progenitor cell that

further contributes to proper cortical neurogenesis and layering.[17] Within the intestine, dividing crypt base columnar stem cells perpendicularly align their mitotic spindles to the apical lumen, generating asymmetric daughter cell fates, whereas dividing cells in positions higher up along the crypt assume parallel orientations.[18] Similarly, in early epidermal development, perpendicular mitotic divisions are employed to properly specify epithelial stratification and differentiation.[19]

Whether similar principles hold true for the hematopoietic system remains to be determined. In the zebrafish, hematopoietic stem and progenitor cells (HSPCs) are found anchored to a mesenchymal stromal cell and achieve asymmetry of cell fates when they divide so as to displace one daughter cell away from this niche.[20] Mammalian adult hematopoietic precursors are also known to divide in specific ways depending on their surrounding signaling milieu; a pro-renewal environment promotes symmetric expansion and a pro-differentiation environment biases for asymmetric division.[21–23] We and others have shown that HSC maintenance and activity are influenced by several known intrinsic effectors of polarity establishment and asymmetrically associated cell fate determinants.[24–32] However, in distinct cell types and species, not all such factors appear to have the same mechanism or degree of action as initially described in model organisms.[32,33] Nonetheless, one study to date that supports the importance of proper spindle orientation regulation in mammalian HSCs involves Lis1/Pafah1b1, a dynein-binding microtubule capturing protein that influences murine HSPC divisions and the inheritance of cell fate determinants in both normal hematopoietic and leukemia contexts.[34] In this study however, neither the functional importance of LIS1/PAFAH1B1 in human HSPCs nor an accounting of whether its altered expression is observed in non-malignant hematopoietic disorders were explored.

Here, we describe Lfc/Arhgef2, a RhoA-specific GEF and determinant of mitotic spindle orientation, as an important regulator of mammalian hematopoiesis *in vivo*. We present evidence that hematopoiesis driven in the Lfc/Arhgef2$^{-/-}$ background heavily relies on LT-HSCs and primitive progenitors and that a productive deficit is present at these levels within the hematopoietic hierarchy. We validate this functional link in human HSC-derived xenografts and directly show that Lfc/Arhgef2 regulates spindle orientation in HSPCs. We further show that ARHGEF2 is specifically downregulated in HSC and primitive progenitor subsets from bone marrow samples of patients diagnosed with Shwachman-Diamond syndrome (SDS). Our findings demonstrate the importance of mitotic spindle orientation in HSPC function and suggest that depletion of *ARHGEF2* in humans may contribute to clinical bone marrow failure.

Materials and Methods

Colony forming unit, proliferation, cell cycle and apoptosis assays

1.2 x 10^4 whole bone marrow (WBM) from Lfc/Arhgef2$^{fl/fl}$ and Lfc/Arhgef2$^{-/-}$ mice were plated in biological triplicate in MethoCult GF M3434 (STEMCELL Technologies) and colonies scored at 12–14 days. Lin$^-$Sca-1$^+$c-Kit$^+$ (LSK) HSPCs were sorted and cultured for up to 7 days in HyClone Dulbecco's High Glucose Modified Eagle Medium (GE Healthcare Life Sciences) supplemented with 10% FBS (Gibco), 100 ng/mL mSCF, 100 ng/mL mTPO, 10 ng/mL mIL-3 and 10 ng/mL mIL-6. K562 cells were cultured in IMDM (Thermo Fisher) supplemented with 10% FBS (Wisent Bioproducts) and 100 U/mL Pen/Strep (Thermo Fisher). Transductions were carried out by adding lentiviruses with 5 μg/mL polybrene (Sigma) for 3 days prior to *in vitro* assays. For cell cycle analyses, cells were fixed with Cytofix/Cytoperm solution (BD), permeabilized with Perm/Wash buffer (BD Biosciences) and stained with Ki-67-PE-Cy7 (BD) and 7-AAD (BD).

Apoptosis was measured through staining with Annexin V-FITC (BD) in binding buffer (BioLegend) and 7-AAD.

Mouse bone marrow and fetal liver transplantation

Non-competitive hematopoietic transplants were carried out in lethally irradiated (1100 cGy, Gammacell 40 Exactor, Best Theratronics) 8- to 12-week-old B6.SJL recipient mice. 1 x 10^6 WBM or 3 x 10^5 E14.5 fetal liver (FL) cells from Lfc/Arhgef2$^{fl/fl}$ or Lfc/Arhgef2$^{-/-}$ CD45.2$^+$ donor mice were injected via tail vein. Competitive transplants were carried out using the same parameters but involved injecting either a 1:1 or 2:1 mixture of Lfc/Arhgef2$^{-/-}$:C57Bl/6 WBM cells. Donor engraftment levels were serially monitored by tail vein blood collection and flow cytometry analysis using antibodies described below. Bone marrow transplant periods were ≥16 weeks in duration; secondary transplants were performed with doses of 1.5 x 10^6 primary WBM cells. Kaplan-Meier survival analysis was calculated on the non-competitive transplant cohorts. Homing experiments were conducted by injecting 5 x 10^4 Lin$^-$ cells into lethally irradiated recipients and reisolating recipient bone marrow 16 hours later for flow cytometry analysis.

Isolation of primary human HSCs and flow cytometry

Patient samples were obtained with informed consent and approved by the research ethics board at McMaster University. Umbilical cord blood cells were collected, lineage depleted and flow cytometrically analyzed as previously published.[33] Antibodies against mouse antigens included: CD45.2 v450 (BD); Lineage eFluor 450 (eBioscience), Alexa Fluor 700 (BioLegend); Sca-1 APC (eBioscience), PerCP-Cy5.5 (eBioscience); c-Kit PE-Cy7 (BD); CD150 PE (BioLegend); CD48 FITC (BD), APC (eBioscience); and CD11b PE, Gr-1 APC-Cy7, B220 APC, CD4 PE, CD8a APC-

Cy7 (BD). Sorting was performed on a MoFlo XDP (Beckman Coulter), routine acquisition on a LSRII (BD) and flow analysis completed using FlowJo v10.0.7 (Tree Star Inc.).

Lentiviral constructs, knockdown and overexpression validation, and virus production

Third generation shRNA sequences against human ARHGEF2 and SBDS were selected based on high sensor assay rankings[35] and cloned into lentiviral vectors pZIP-SFFV-ZsGreen-Puro (TransOMIC Technologies) or pZIP-SFFV-tNGFR-Puro re-adapted to contain a miR-E delivery scaffold.[35] qPCR validation of knockdown was performed on leukemia cell lines with the following primers: ARHGEF2 (left 5'-TACCTGCGGCGAATTAAGAT-3', right 5'-AAACAGCCCGACCTTCTCTC-3'; Roche Universal ProbeLibrary #22); EIF4H (left 5'-CGTGGATCCAACATGGATTT-3', right 5'-GGAGTCGTGGTCTCTGTGCT-3'; Roche Universal ProbeLibrary #35); and ACTB (Assay ID: Hs01060665_g1, Thermo Fisher). Human ARHGEF2 cDNA (NM_001162384.1) was subcloned into the pUMG-LV5 lentiviral expression vector (a gift from Maria Mesuraca). Western blot validation of knockdown was performed using antibodies against human ARHGEF2 (Abcam, ab201687) and ACTB (Santa Cruz Biotechnology, sc-81178). Lentiviruses were produced by co-transfection of the vector with viral packaging plasmids pMD2.G and psPAX2 (a gift from Didier Trono, Addgene #12259 and #12260) into 293FT cells (Fisher Scientific).

Cord blood infection and xenotransplantation experiments

5 x 10^4 $CD34^+$ human cord blood HSPCs were cultured in StemSpan SFEM II (STEMCELL Technologies) supplemented with 100 ng/mL hSCF, 100 ng/mL hFLT3, 20 ng/mL hTPO and 20 ng/mL hIL-6 for 16–20 hours. Lentivirus encoding shRNAs against Luciferase or ARHGEF2 were added and transduced cultures kept another 3 days before gene transfer values were measured by

flow cytometry and 1/5 of day 0 equivalent cultures transplanted intrafemorally into each sublethally-irradiated (315 cGy) NSG recipient mouse. Bone marrow aspirates were taken from the opposite femur between 8–10 weeks post-transplant; bilateral iliac crests, femurs and tibias were processed to evaluate the bone marrow ≥16 weeks post-transplant using flow cytometry.

Live cell imaging of mitotic spindle orientation

For fluorescent labeling, H2B-EGFP and mCherry-α-tubulin were cloned from pLKO-H2B-EGFP (a gift from Daniel Schramek) and mCh-alpha-tubulin (a gift from Gia Voeltz, Addgene #49149) vectors into a MSCV retroviral backbone. These constructs were cotransfected with pGP1 and pHCMV-G packaging plasmids into 293GPG packaging cells. Viral supernatant was added to the GP+E-86 packaging line and $EGFP^{+}mCherry^{+}$ producers sorted for co-culture with mouse LSKs over 3 days in equally mixed HyClone DMEM (GE Healthcare Life Sciences) and StemSpan SFEM (STEMCELL Technologies) media supplemented with 10% FBS (Gibco) and the aforementioned murine cytokines. Sorted $CD45.2^{+}EGFP^{+}mCherry^{+}$ cells were plated onto retronectin coated chambered glass bottom μ-slides (Ibidi, 80447 and 80827). Live cell fluorescence images were acquired using a scanning laser confocal microscope with a 60x oil immersion objective (Nikon Eclipse Ti2). 15 μm stacks were obtained over 21 steps at 0.7 μm per step. Images were processed using ImageJ2[36] on the Fiji platform[37] where they were cropped to focus on dividing cells and rotated such that the plane of division was parallel to the X-axis of the image. Once aligned, the angle of division was visualized using an orthogonal view of the XZ plane. The angle of division was measured between the X-axis and the uppermost centrosome with the lowermost centrosome being used as the vertex of the angle.

Results

ARHGEF2 is significantly downregulated in HSCs within patients with SDS

Defects at the stem and progenitor level underlie aspects of the severe paucity of hematopoiesis characteristic in inherited bone marrow failure syndromes.[38-44] In exploring possible molecular mechanisms underpinning these disorders, we analyzed a recently generated dataset of single cell RNA sequencing on $CD34^+$ bone marrow HSPCs of patients diagnosed with SDS[45] and observed that ARHGEF2 was downregulated in SDS HSC/MPPs (FDR = 0.0029) and common myeloid progenitors (CMPs) (FDR = 0.0087) when compared to the same cell subsets found in healthy individuals (Figure 1A-C). ARHGEF2 represented 1 of 229 genes found to be significantly and differentially reduced in expression in the HSC/MPPs of patients with SDS out of approximately 11,000 detected genes. Previous reports have demonstrated Lfc/Arhgef2 as a unique GEF that associates with, helps assemble and orients the mitotic spindle.[46-48] In the mammalian neural system, downregulation of Lfc/Arhgef2 led to impaired neurogenesis and maintained precursors in a cycling state.[48] In cord blood (CB) $CD34^+$ cells, capitalizing on shRNA-mediated knockdown of SBDS, a known pathogenic driver in SDS, we show that the *ARHGEF2* transcript levels mirror the reduction in *SBDS* mRNA (Figure 1D, E). Moreover, while overexpression of ARHGEF2 did not alter early apoptosis levels in K562 cells targeted with shLuciferase, a trend of enhanced cell survival at the day 3 time point was observed with SBDS knockdown and ectopic ARHGEF2 expression, suggesting that ARHGEF2 may be dependent on and/or an important effector of disrupted SBDS activity (Figure 1D, F). Based on these combined data, we hypothesized that as it does in neural progenitors, Lfc/Arhgef2 similarly regulates HSC function and division within the hematopoietic system.

Lfc/Arhgef2$^{-/-}$ mice undergo compromised embryonic development and exhibit mild hematopoietic alterations at native steady-state

To directly investigate the effects of loss of function of Lfc/Arhgef2 in mammalian hematopoiesis, we capitalized on a previously validated Lfc/Arhgef2$^{-/-}$ mouse model[49] to first characterize the nature of steady-state hematopoiesis in its absence (Figure 2A). While Lfc/Arhgef2$^{-/-}$ mice were viable, litter sizes were noticeably reduced and serial heterozygous crosses yielded significantly fewer Lfc/Arhgef2$^{-/-}$ mice than expected (Figure 2B, *Top*). In developing embryos, we observed an overall decrease in the percentage and absolute number of Lfc/Arhgef2$^{-/-}$ fetal liver HSCs relative to controls (Figure 2B, *Bottom*). Among viable adult Lfc/Arhgef2$^{-/-}$ mice, native peripheral blood analysis revealed approximately 25% fewer circulating platelets (Figure 2C), but no other significant differences in the number of leukocytes. These parameters were unchanged in both younger (4 months) and maturing adult (8 months) mice. Immunophenotyping of Lfc/Arhgef2$^{-/-}$ adult bone marrow revealed a higher myeloid-to-lymphoid ratio that was maintained at the terminal end of the hierarchy (Figure 2D). There were significantly fewer lineage-negative cells (Figure 2E), characterized by fewer restricted (Lin$^-$CD150$^-$CD48$^+$) and lymphoid (Lin$^-$Sca-1$^+$c-Kit$^-$, LS) progenitors (Figure 2F) and a corresponding relative increase in myeloid (Lin$^-$Sca-1$^-$c-Kit$^+$, LK) progenitors within the lineage-negative compartment (Figure 2F). However, neither HSPCs (Lin$^-$Sca-1$^+$c-Kit$^+$, LSK) nor long-term HSCs (LSK CD150$^+$CD48$^-$, LT-HSCs) were significantly different between knockout and control adult bone marrow samples (Figure 2G). Overall, these data indicate that while Lfc/Arhgef2$^{-/-}$ embryonic development is compromised and signs of thrombocytopenia are present in viable Lfc/Arhgef2$^{-/-}$ mice, adult steady-state hematopoiesis is stable and only mildly altered in mice where the blood system is sufficiently established.

Lfc/Arhgef2$^{-/-}$ bone marrow HSPCs do not show significant alterations in their total myeloid colony output, proliferation, cell cycle or apoptosis status

To measure progenitor outputs, we performed colony forming unit (CFU) assays of whole bone marrow. While we did notice a slight decrease in the proportion of CFU-G, the remainder of all myeloid progenitors including CFU-GEMMs were present in similar numbers in Lfc/Arhgef2$^{-/-}$ bone marrow as compared to Lfc/Arhgef2$^{fl/fl}$ controls (Figure 3A). When measured at two distinct time points in culture, Lfc/Arhgef2$^{-/-}$ LSK HSPCs did not differ in their proliferation rates (Figure 3B, *Left*), cell cycle status (Figure 3B, *Middle*, *Right*), or levels of early and late apoptosis (Figure 3C). These results argue against severe defects in either spindle stability (e.g. lack of and/or multipolar spindles) and DNA damage (e.g. aneuploidy, chromatin bridges) in these cells and show that apart from defects in granulocyte colony numbers, Lfc/Arhgef2$^{-/-}$ HSPCs are functionally comparable to control HSPCs in their overall myeloid progenitor outputs, division kinetics, apoptosis and growth.

Lfc/Arhgef2$^{-/-}$ fetal liver and bone marrow insufficiently reconstitute the blood system, more heavily relies on and shows production deficits in HSCs

We next sought to verify that the decrease of phenotypic fetal liver HSCs was also apparent at the functional level by transplanting matched doses of E14.5 fetal liver cells isolated from Lfc/Arhgef2$^{fl/fl}$ and Lfc/Arhgef2$^{-/-}$ embryos into lethally-irradiated congenic recipients (Figure 4A). Within two weeks, the vast majority of recipients of Lfc/Arhgef2$^{-/-}$ cells became moribund, while all mice having received Lfc/Arhgef2$^{fl/fl}$ cells survived until the experimental 16-week post-transplant endpoint (Figure 4B). In 2 of the 6 Lfc/Arhgef2$^{-/-}$ recipients that survived until 10 days post-transplant, we noted a relative decrease in the percentage of peripheral CD45.2^{+} and Gr-1^{+} granulocytic engraftment, with the lowest of engrafted of these becoming moribund shortly after

this sampling (Figure 4C). Together, this data indicates a significant impairment in functional repopulating HSCs within the fetal liver of Lfc/Arhgef2$^{-/-}$ mice.

To functionally test the hematopoietic reconstitution capacity of Lfc/Arhgef2$^{-/-}$ bone marrow, we performed competitive and non-competitive serial transplantation assays *in vivo* (Figure 4A). In noncompetitive transplants, the majority of mice receiving Lfc/Arhgef2$^{-/-}$ bone marrow showed evidence of anemia and became moribund, whereas recipients of Lfc/Arhgef2$^{fl/fl}$ bone marrow did not display signs of hematopoietic insufficiency and/or delayed recovery (Figure 4D, E). Similar phenotypes and increased mortality were also evident in secondary transplant settings (Figure 4E). Importantly, this post-transplant failure phenotype was not due to compromised homing abilities, since as early as 16 hours post-transplantation, Lfc/Arhgef2$^{-/-}$ Lin^{-} cells homed to recipient bone marrow with an efficiency comparable to Lfc/Arhgef2$^{fl/fl}$ Lin^{-} cells (Figure 4F). However, within the grafts of the recipients of Lfc/Arhgef2$^{-/-}$ bone marrow that remained at the end of secondary transplants, Lin^{-}CD150^{+}CD48^{-} HSCs were significantly exhausted in comparison to those found in control grafts (Figure 4G). Competitive primary transplants of Lfc/Arhgef2$^{-/-}$ bone marrow against wildtype bone marrow further demonstrated significantly impaired reconstitution at both equivalent (1:1) doses and when biased (2:1) to give an advantage to Lfc/Arhgef2$^{-/-}$ bone marrow (Figure 4H). Interestingly, LT-HSCs were found to be significantly overrepresented in the few remaining Lfc/Arhgef2$^{-/-}$ cells compared to Lfc/Arhgef2$^{fl/fl}$ controls within grafts of secondary transplants (Figure 4I), highlighting a clear production deficit of downstream cells at the most primitive level. These findings demonstrate that in the absence of Lfc/Arhgef2, transplant-driven hematopoiesis heavily relies on LT-HSCs and primitive progenitors and that functional deficits existing at these levels lead to reduced hematopoietic engraftment and a subsequent increased mortality within recipient mice.

Lfc/Arhgef2$^{-/-}$ HSPCs exhibit a significantly increased frequency of misoriented divisions

Since Lfc/Arhgef2 has been uniquely characterized to function by orienting the mitotic spindle, we used a previously published live cell imaging method to measure the angle of division of mouse HSPCs.[34] LSK cells were labelled with H2B-EGFP and mCherry-α-tubulin and plated on retronectin covered chambered slides. By acquiring confocal z-stacks of dividing cells and generating orthogonal projections of cell division events at telophase, we verified that wildtype LSK HSPCs preferentially divide parallel (between 0 and 10°) to this underlying substrate (Figure 5A). However, while Lfc/Arhgef2$^{-/-}$ LSK HSPCs also yielded parallel division events, we observed a significantly increased frequency of non-parallel angles that reached as high as 60° (Figure 5B). These results indicate that while altered divisional preferences do not largely compromise HSPC survival and division kinetics *in vitro*, the post-transplant failure phenotypes measured *in vivo* could potentially be explained by dysregulated fate decisions as a result of misoriented divisions. Our results are thus consistent with the concept that Lfc/Arhgef2 is essential for regulating HSC divisional orientation and effective lineage differentiation within their niche during the establishment of hematopoiesis.

ARHGEF2 knockdown in human HSCs compromises hematopoietic xenografts

To elucidate if ARHGEF2 function is conserved in human hematopoiesis, we performed immunofluorescence staining on several myeloid leukemia cell lines and confirmed that ARHGEF2 localizes at the microtubule apparatus during division (Figure 6A). To determine the functional effects of ARHGEF2 downregulation in human hematopoiesis, shRNAs against either ARHGEF2 or a Luciferase control were introduced into cord blood CD34^{+} HSPCs (Figure 6B, C). Similar to results derived from Lfc/Arhgef2$^{-/-}$ mice, cells with reduced ARHGEF2 proliferated

comparably or was slightly dampened relative to controls (Figure 6D). Myeloid CFU assays yielded no significant differences in multipotent progenitor colonies and significantly decreased monocytic progenitors, while the total colony number remained equivocal across settings (Figure 6E). These data suggest that ARHGEF2 knockdown in human hematopoietic progenitors imparts only mild defects at the lineage-restricted level. Finally, using two separate and efficient shRNAs against ARHGEF2, *in vivo* analyses of intrafemorally xenotransplanted NSG recipient mice at 16 weeks post-transplant showed significantly diminished hematopoietic grafts with a paucity of $CD15^{+}$ myeloid output observed in the residual xenografts of mice receiving ARHGEF2 knockdown cells compared to controls (Figure 6F, G). Considered with our murine data, this clear *in vivo* phenotype in the human context demonstrates the cross-species importance of ARHGEF2 to the regenerative and productive capacity of HSCs and may implicate ARHGEF2-regulated spindle orientation in human hematopoiesis (Figure 6H).

Discussion

In addition to its role in modulating RhoA activity at mitotic spindles,[46–48] two studies to date have shown that Lfc/Arhgef2 associates with microtubules through the dynein light chain Dynlt1/Tctex-1[49–50] and participates in a positive feedback loop in RAS transformed cells to potentiate MAPK signaling independent of its RhoGEF activity.[51] While we cannot rule out the MAPK-regulatory function of Lfc/Arhgef2 underlying our observed phenotypes, the role of this pathway here is unlikely given that MAPK inhibition has been previously shown to have the opposite effect of improving HSC growth and output *in vitro* and *in vivo*.[52–54] Global RhoA dependence has also been tested in the hematopoietic system, however only in the context of conditional deletion within well-established chimeric grafts, where loss of the entire cellular pool

of RhoA does not alter steady-state HSCs, but rather induces bone marrow failure due to significant progenitor loss.[55] Our data using multiple transplant models highlights HSC but not pronounced progenitor deficiencies, suggesting that regulation of RhoA activity at the mitotic spindle by Lfc/Arhgef2 represents an important axis for productive HSC divisions during the critical window over which hematopoiesis is established that may not be obvious at steady-state. In further support of this point, we note that in examining the above-mentioned single cell RNA-sequencing data, ARHGEF2, but not RHOA, is downregulated in primitive pediatric SDS cells (data not shown).[45]

Our finding of decreased fetal liver HSC function in Lfc/Arhgef2$^{-/-}$ mice indicates that fetal hematopoiesis defects may underlie the reduced fraction of Lfc/Arhgef2$^{-/-}$ embryos that reach post-natal viability. Indeed, proper establishment of the hematopoietic system during development requires a minimum number of productive HSC divisions in the fetal liver.[56,57] Thus, only some Lfc/Arhgef2$^{-/-}$ embryos may generate enough effective HSC divisions to allow for sufficient downstream production of functional progenitors to populate the hematopoietic system. Our results *in vivo* using adult HSCs interrogated in two distinct transplant models provide further important insight into the mechanism of Lfc/Arhgef2 loss on HSC decision-making in different bone marrow states. In recipients of competitively transplanted Lfc/Arhgef2$^{-/-}$ cells, wildtype HSCs regenerated hematopoiesis more effectively, placing less of the reconstitution burden on Lfc/Arhgef2$^{-/-}$ HSCs and allowing read-out of their preferred tendency to divide in a manner that promotes accumulation of primitive cells. This elevated HSC frequency may be due to an uncoupling of the cell polarity axis from their orientation of division, leading to a relative retention of stemness determinants in daughter cells. Alternatively, their compromised ability to adopt particular divisional orientations may result in Lfc/Arhgef2$^{-/-}$ daughter cells being

localized in more niche-proximal locations where they would receive enhanced HSC maintenance cues. In the non-competitive transplant setting, where in contrast the long-term regeneration of hematopoiesis is entirely dependent on Lfc/Arhgef2$^{-/-}$ HSCs, the paucity of progenitors generated as a result of the spindle orientation defects leads to a heavier reliance on Lfc/Arhgef2$^{-/-}$ HSC divisions. In this latter context, which importantly mimics the dependencies on HSCs in developmental hematopoiesis, the observed outcome of stem cell loss is likely due to an exhaustion of Lfc/Arhgef2$^{-/-}$ HSCs.

Our observation of similarly defective hematopoietic reconstitution *in vivo* upon transplant of ARHGEF2-depleted human HSCs suggests a conserved function of Lfc/Arhgef2 across species. Downregulation of ARHGEF2 and acutely upon SBDS repression in CD34^{+} cells points to the possibility that repression of ARHGEF2 in SDS patients may contribute to defective HSC-driven hematopoiesis. It is interesting to note that in our Lfc/Arhgef2$^{-/-}$ mouse model we observe native thrombocytopenia, which may indicate an additional role for Lfc/Arhgef2 in regulating megakaryocyte maturation,[58,59] defects in neutrophil chemotaxis,[60] and while not formally characterized yet, bone malformations and clear neurological abnormalities (data not shown), the latter of which may be consistent with other reports outlining cognitive impairments and intellectual disability in patients with ARHGEF2 loss-of-function mutations.[61,62] Importantly, all of these features can be found in patients diagnosed with SDS,[63,64] encouraging future efforts to understand if the loss of ARHGEF2 function contributes to the etiology and pathogenesis of SDS.

In closing, our work highlights implications for how mitotic spindle orientation itself may more broadly affect stem cell division during development and disease. During brain development, centrosomal protein loss-of-function events that influence spindle orientation disrupt the balance

of symmetric and asymmetric divisions leading to microcephaly.[65] Conceptual parallels may therefore also exist between spindle-regulating genes and bone marrow failure syndromes within and beyond SDS. Indeed, the loss of Cdk5rap2, a centrosomal spindle-orienting protein, results in a macrocytic, hypoproliferative anemia and leukopenia ("Hertwig's anaemia") in a heavily irradiated mouse model.[66,67] With the identification of several other spindle-regulating genes implicated in microcephaly, it may be interesting to determine if any of these genes also have roles within bone marrow failure or in disorders that result in tissue insufficiency elsewhere. Finally, the fact that SDS progresses with high frequency to myeloid malignancies where expansion of transformed HSCs is known to be early pathogenic events suggests that spindle orientation dysregulation may also be interesting to explore as a possible contributor to the larger group of disorders that include clonal hematopoiesis, myelodysplastic syndrome and/or leukemia.

Acknowledgements

The authors thank Johann Hitzler and Sheila Singh for important feedback on this work; Minomi Subapanditha for flow cytometry sorting; Lillian Robson, Wendy Whittaker and Norma-Ann Kearns for animal caretaking and maintenance; and Ray Truant for access to the McMaster Biophotonics Facility.

This work was supported by a Canadian Institutes of Health Research (CIHR) MD/PhD Studentship (D.C.), Ontario Graduate Scholarship (D.C.), a CIHR MD/PhD Studentship (J.X.), an Ontario Institute for Cancer Research (OICR) Investigator Award (K.H.) and a CIHR Foundation Grant (R.R.).

Authorship

Contributions: D.C. designed, led and performed the experiments, analyzed and interpreted the data and wrote the manuscript. A.V., J.X. and L.d.R. assisted with animal experiments. V.G. and N.W. assisted with imaging work. C.J. and C.N. designed and completed analyses on sequencing data from patient samples. J.L.R., M.S., and R.R. generated the knockout mouse model. R.R. advised on experimental design. K.H. supervised the project, designed experiments, reviewed the data and wrote the manuscript. All authors reviewed and approved the manuscript.

Conflict-of-interest disclosure: The authors declare no competing financial interests.

Correspondence: Kristin Hope, McMaster University, 1280 Main Street West, Hamilton, Ontario L8S 4K1; E-mail: kristin@mcmaster.ca

Figures

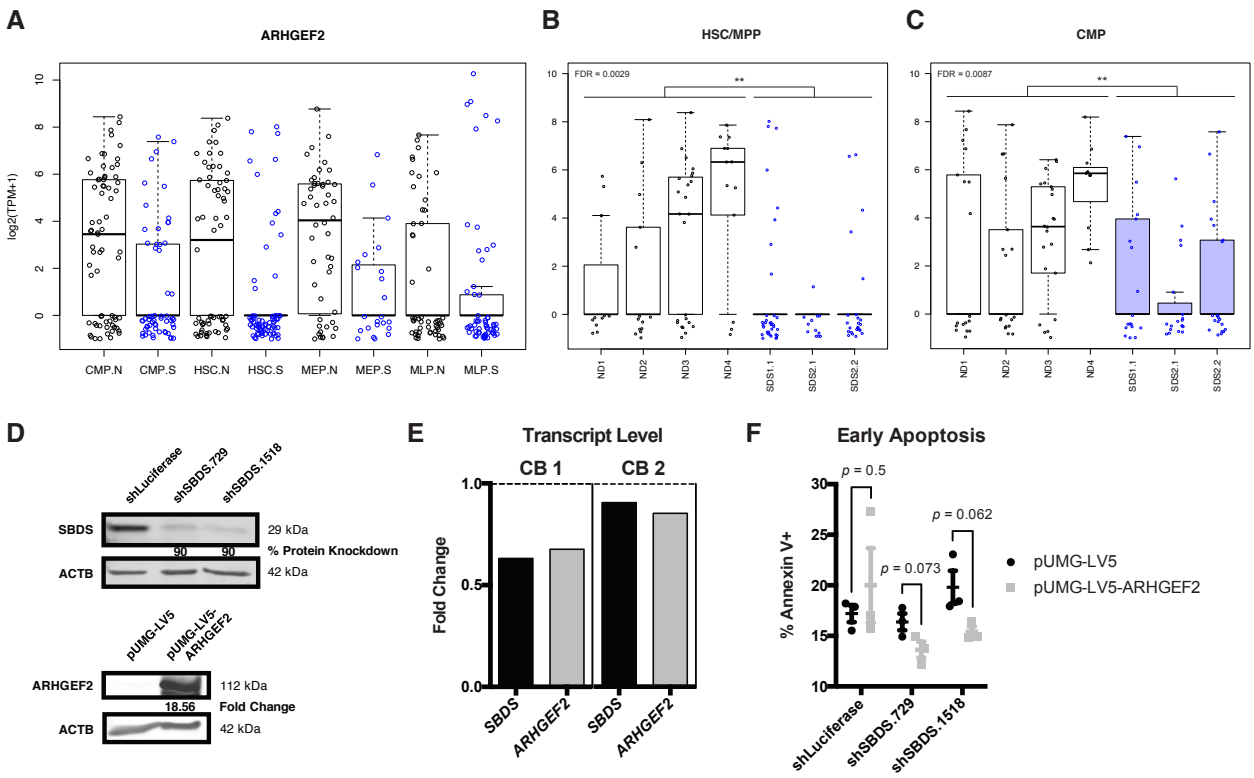

Figure 1. *ARHGEF2* is significantly downregulated in SDS patient HSCs. (A) *ARHGEF2* transcript expression within single HSC, common myeloid progenitors (CMP), megakaryocyte-erythroid progenitors (MEP) and multi-lymphoid progenitor (MLP) cells from $CD34^+$ patient samples from normal (.N, black) or Shwachman-Diamond syndrome (.S, blue) backgrounds. (B–C) *ARHGEF2* transcript expression from individual patient samples within HSC/MPP (B) (**, FDR=0.0029) and CMP (C) (**, FDR=0.0087) populations. ND represents normal donor and SDS represents Shwachman-Diamond syndrome samples respectively. Each data point represents a single cell. (D) (*Top*) Western blot validation of shRNAs targeting SBDS and (*Bottom*) ARHGEF2 overexpression. (E) qPCR assessment of *SBDS* and *ARHGEF2* expression in human $CD34^+$ HSPCs following SBDS knockdown (n = 2 cord blood samples). (F) Flow cytometric evaluation of early apoptosis levels upon concomitant ARHGEF2 overexpression and SBDS knockdown in K562 cells; n = 3 biological replicates evaluated at day 3 of *in vitro* cultures.

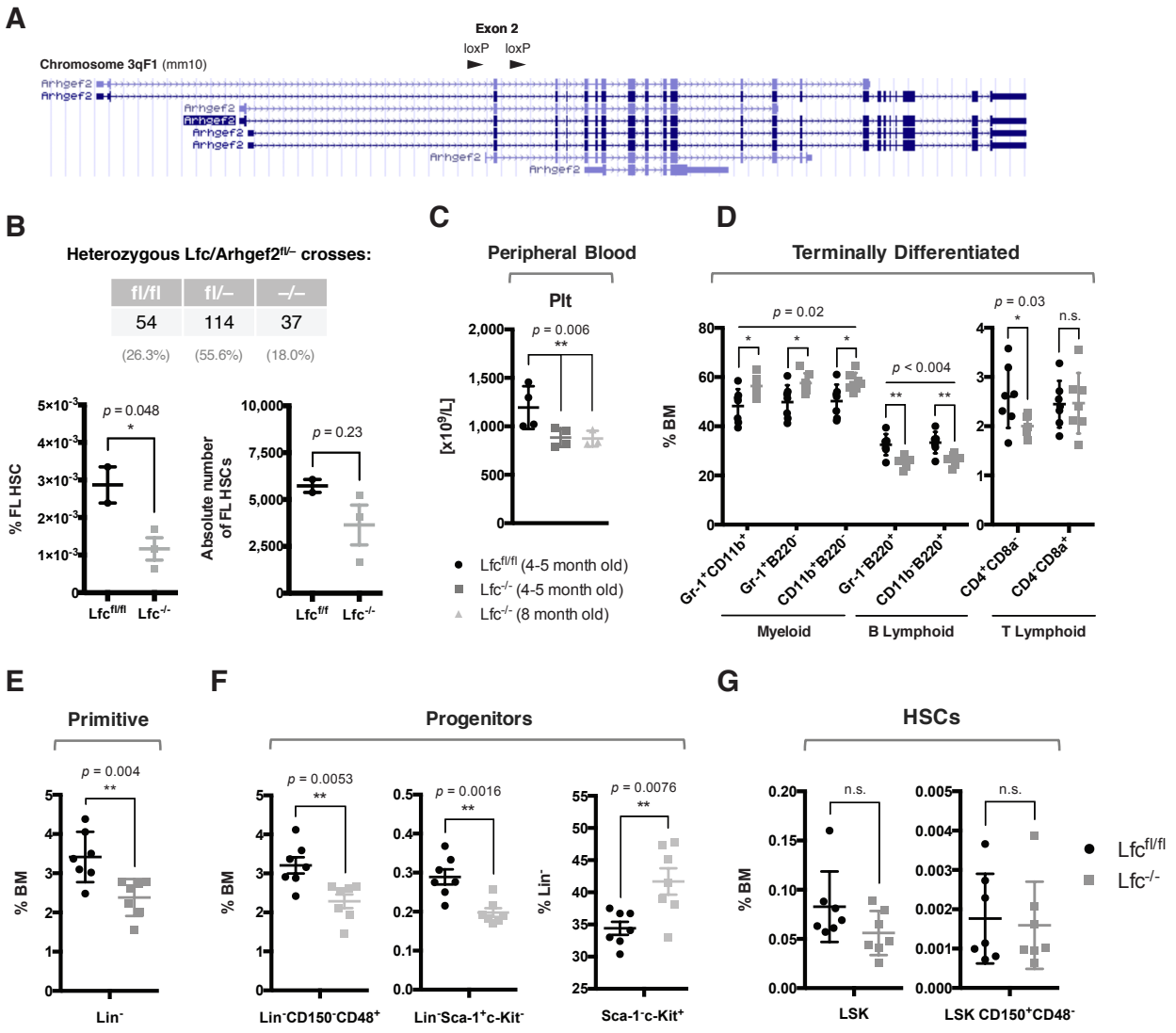

Figure 2. Native Lfc/Arhgef2$^{-/-}$ mice exhibit mildly altered hematopoietic parameters.

(A) Genomic locus of murine Lfc/Arhgef2 annotated with exon 2 flanked with loxP sites. (B) (*Top*) Non-Mendelian ratios observed from heterozygous Lfc/Arhgef2$^{fl/-}$ crosses across 205 born pups. (*Bottom*) Relative percentage and absolute number of fetal liver HSCs (Lin$^-$CD150$^+$CD48$^-$CD11b$^+$) are decreased in Lfc/Arhgef2$^{-/-}$ embryos. (C) Decreased circulating platelets in Lfc/Arhgef2$^{-/-}$ mice (n = 4 mice per age group). (D) Higher myeloid-to-B lymphoid ratios, (E) fewer lineage-negative cell populations and (F) less restricted (*Left*) lymphoid (*Middle*) progenitors in Lfc/Arhgef2$^{-/-}$ bone marrow. (F) (*Right*) Relative increase in myeloid progenitors within lineage-negative compartment of Lfc/Arhgef2$^{-/-}$ bone marrow. (G) (*Left*) LSK HSPCs and (*Right*) LSK+SLAM LT-HSCs are not statistically different in Lfc/Arhgef2$^{-/-}$ mice. (D–G) n = 7 mice per group. (C–G) * $p < 0.05$, ** $p < 0.01$; error bars represent standard error of the mean.

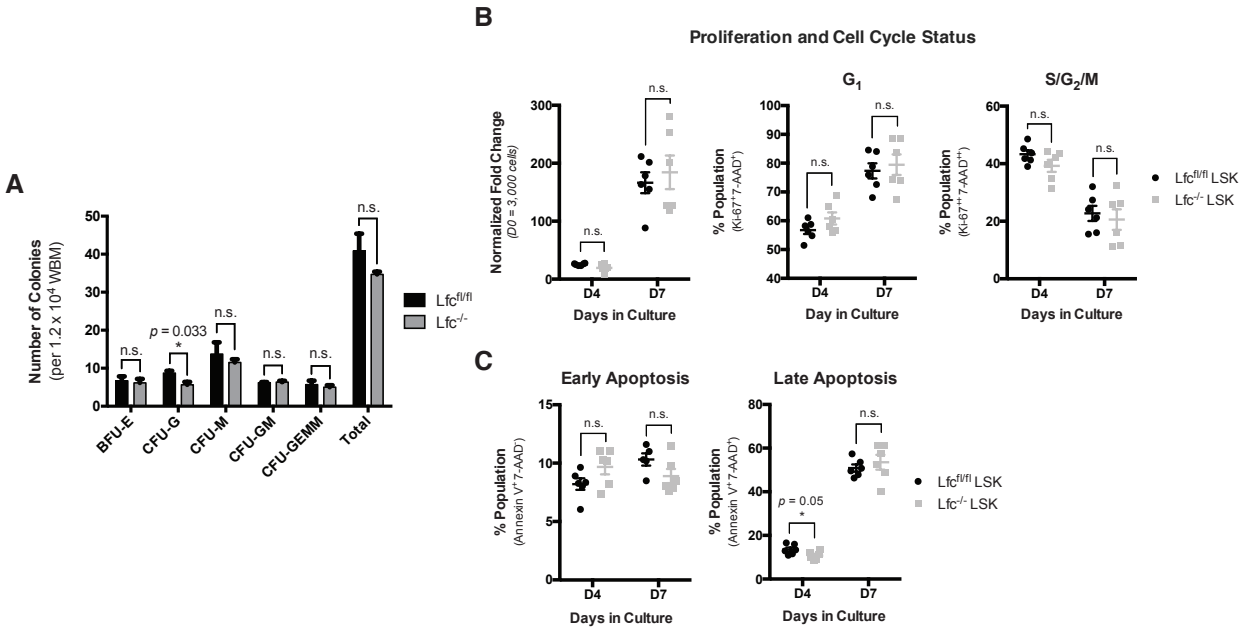

Figure 3. Lfc/Arhgef2$^{-/-}$ bone marrow HSPCs are not altered in their total myeloid colony output, proliferation, cell cycle or apoptosis status. (A) Myeloid colony-forming units from 1.2 x 10^4 whole bone marrow cells plated in biological triplicate enumerated at 12–14 days; (B) (*Left*) LSK HSPCs cultured *in vitro* enumerated for proliferation, (*Middle*) proportional G1 and (*Right*) S/G2/M cell cycle status; and (C) (*Left*) early and (*Right*) late apoptosis at days 4 and 7 in culture. (B–C) n = 6 biological replicates; error bars represent standard error of the mean.

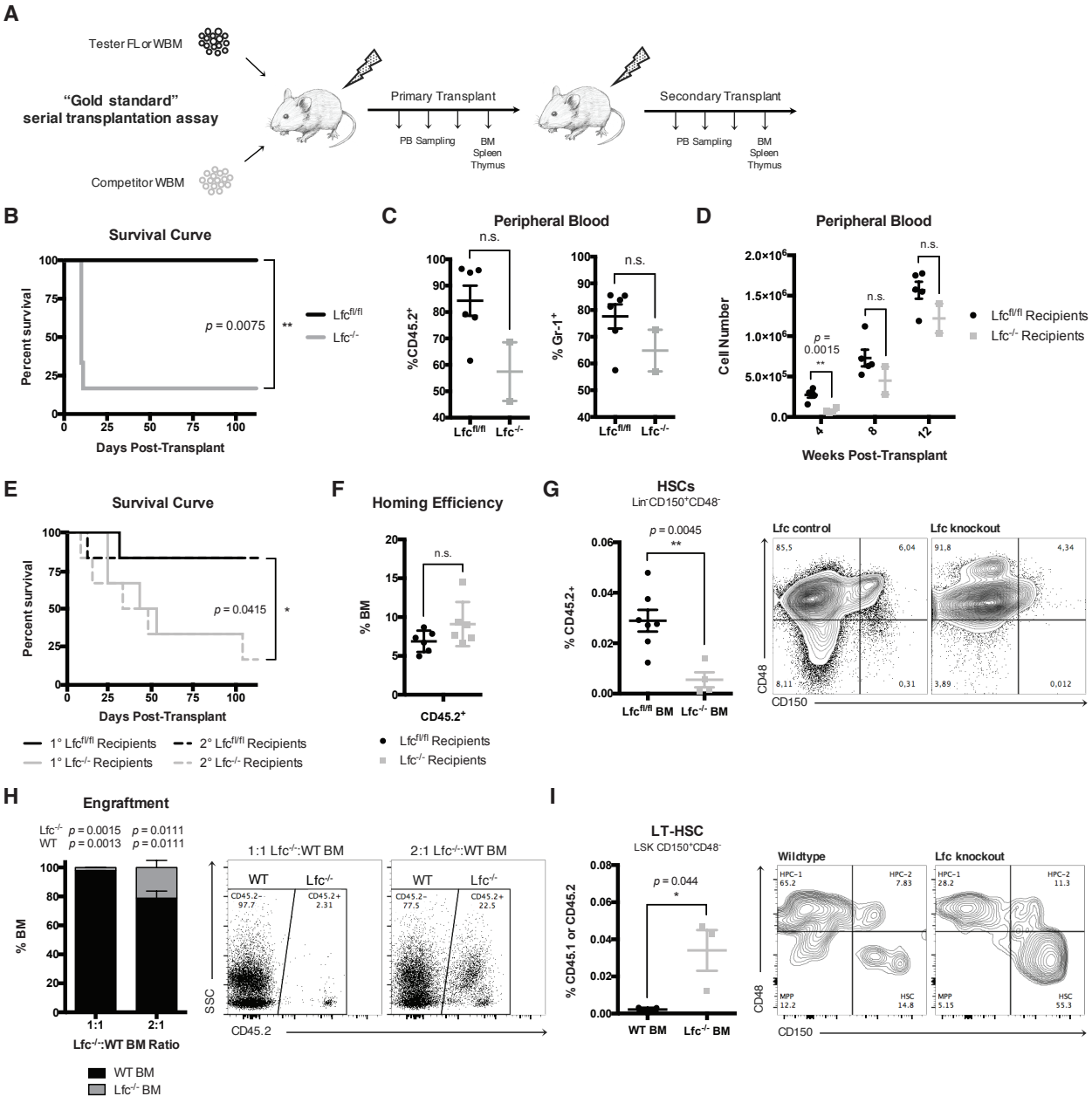

Figure 4. Lfc/Arhgef2$^{-/-}$ fetal liver and bone marrow insufficiently reconstitute the blood system and show productive deficits at the HSC level. (A) Experimental schematic of non-competitive and competitive transplantations. (B) Kaplan-Meier survival curves demonstrating higher mortality among recipients of Lfc/Arhgef2$^{-/-}$ E14.5 fetal liver cells; n = 6 recipients with n = 2 biological Lfc/Arhgef2$^{fl/fl}$ and n = 3 Lfc/Arhgef2$^{-/-}$ fetal liver donors. (C) Decreased levels of peripheral blood engraftment and granulocytic populations as measured in the two remaining recipient mice of Lfc/Arhgef2$^{-/-}$ E14.5 fetal liver cells at Day 10 post-transplant. (D) Insufficient and/or delayed hematopoietic recovery in the peripheral blood of primary transplanted mouse recipients of Lfc/Arhgef2$^{-/-}$ bone marrow. (E) Kaplan-Meier survival curves demonstrating higher mortality among recipients of non-competitively

transplanted Lfc/Arhgef2$^{-/-}$ bone marrow. (F) Comparable homing efficiencies from 5 x 10^4 Lin$^-$ Lfc/Arhgef2$^{-/-}$ bone marrow cells. (G) Lower levels of Lfc/Arhgef2$^{-/-}$ Lin$^-$CD150$^+$CD48$^-$HSCs in secondary non-competitively transplanted bone marrow grafts. (H) Poorer engraftment levels from competing 1:1 and 2:1 Lfc/Arhgef2$^{-/-}$:wildtype doses of bone marrow among primary recipients. (I) Increased proportion of LSK CD150$^+$CD48$^-$ LT-HSCs within secondary grafts among competitively transplanted recipients. Primary non-competitive transplants and homing experiments were with n = 6 recipients/condition using n = 3 biological replicate bone marrow samples. Secondary non-competitive transplants were completed with n = 7 Lfc/Arhgef2$^{fl/fl}$ and n = 4 Lfc/Arhgef2$^{-/-}$ recipients, n = 2 experiments. Primary competitive transplants initiated with n = 3 recipients/dose and secondary competitive analyses conducted with n = 3 recipients from n = 2 primary mice. * $p < 0.05$, ** $p < 0.01$; error bars represent standard error of the mean.

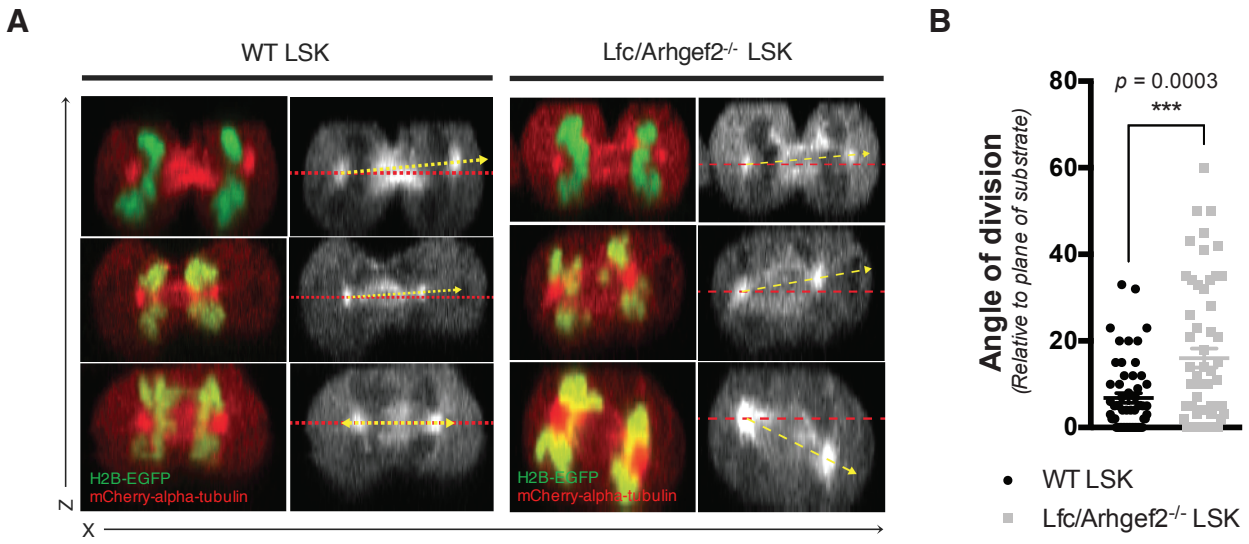

Figure 5. Loss of Lfc/Arhgef2 function disrupts HSPC mitotic spindle orientation.
(A) Representative z-stack stitched images of LSK HSPCs retrovirally transduced with both H2B-EGFP and mCherry-α-tubulin imaged under live cell fluorescence microscopy to capture telophase events. (B) Quantification of cytokinesis events indicate that Lfc/Arhgef2$^{-/-}$ LSK HSPCs exhibit a significantly increased frequency of random divisional orientations whereas wildtype HSPCs preferentially divide parallel to an underlying retronectin substrate. (n = 55 and 56 cells for wildtype and Lfc/Arhgef2$^{-/-}$ backgrounds respectively).

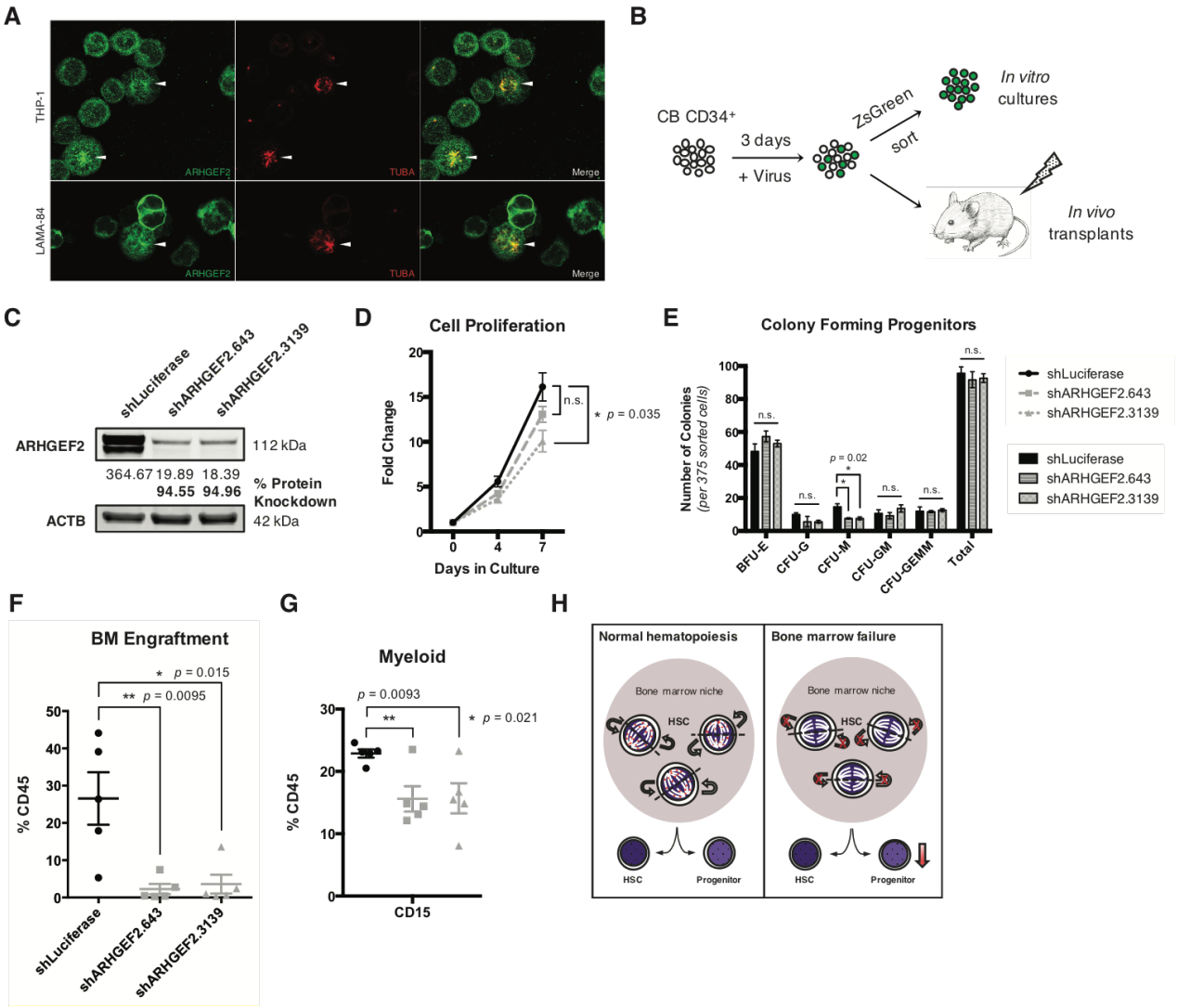

Figure 6. Loss of ARHGEF2 function in CD34$^+$ HSPCs results in significantly diminished xenografts. (A) Immunofluorescent staining showing co-localization of ARHGEF2 and TUBA at the mitotic spindle in THP-1 and LAMA-84 cell lines. (B) Schematic of shRNA knockdown of ARHGEF2 in CD34$^+$ HSPCs *in vivo* and *in vitro*. (C) Protein level knockdown validation of shRNAs against ARHGEF2. (D) Proliferation of CD34$^+$ HSCs *in vitro* over 7 days. (E) Colony output of ARHGEF2 knocked down HSPCs. (F) Decreased engraftment and output of CD15$^+$ myeloid cells (G) derived from CD34$^+$ HSPCs with comparable gene transfer levels receiving shRNAs targeting ARHGEF2, n = 5 recipients each derived from n = 1 cord blood sample. (H) Model summarizing the role of Lfc/Arhgef2 (red dots) actively orienting the HSC mitotic spindle within the niche when establishing hematopoiesis, the loss of which leads to bone marrow failure at the stem cell level. * $p < 0.05$, ** $p < 0.01$; error bars represent standard error of the mean.

References

1. Souilhol C, Gonneau C, Lendinez JG, et al. Inductive interactions mediated by interplay of asymmetric signalling underlie development of adult haematopoietic stem cells. *Nat Commun*. 2016;7:10784.
2. Gao X, Xu C, Asada N, Frenette PS. The hematopoietic stem cell niche: from embryo to adult. *Development*. 2018;145:dev139691.
3. Bowie MB, McKnight KD, Kent DG, McCaffrey L, Hoodless PA, Eaves CJ. Hematopoietic stem cells proliferate until after birth and show a reversible phase-specific engraftment defect. *J Clin Invest*. 2006;116(10):2808–2816.
4. Velten L, Haas SF, Raffel S, et al. Human haematopoietic stem cell lineage commitment is a continuous process. *Nat Cell Biol*. 2017;19(4):271–281.
5. Notta F, Zandi S, Takayama N, et al. Distinct routes of lineage development reshape the human blood hierarchy across ontogeny. *Science*. 2016;351(6269):aab2116.
6. Yamamoto R, Morita Y, Ooehara J, et al. Clonal analysis unveils self-renewing lineage-restricted progenitors generated directly from hematopoietic stem cells. *Cell*. 2013;154(5):1112–1126.
7. Sun J, Ramos A, Chapman B, et al. Clonal dynamics of native hematopoiesis. *Nature*. 2014;514(7522):322–327.
8. Pei W, Feyerabend TB, Rössler J, et al. Polylox barcoding reveals haematopoietic stem cell fates realized *in vivo*. *Nature*. 2017;548(7668):456–460.
9. Rodriguez-Fraticelli AE, Wolock SL, Weinreb CS, et al. Clonal analysis of lineage fate in native haematopoiesis. *Nature*. 2018;553(7687):212–216.
10. Sawai CM, Babovic S, Upadhaya S, et al. Hematopoietic stem cells are the major source of multilineage hematopoiesis in adult animals. *Immunity*. 2016;45(3):597–609.
11. Busch K, Klapproth K, Barile M, et al. Fundamental properties of unperturbed haematopoiesis from stem cells *in vivo*. *Nature*. 2015;518(7540):542–546.
12. Schoedel KB, Morcos MNF, Zerjatke T, et al. The bulk of the hematopoietic stem cell population is dispensable for murine steady-state and stress hematopoiesis. *Blood*. 128(19):2285–2296.
13. Rossi L, Lin KK, Boles NC, et al. Less is more: unveiling the functional core of hematopoietic stem cells through knockout mice. *Cell Stem Cell*. 2012;11(3):302–317.
14. Morrison SJ, Kimble J. Asymmetric and symmetric stem-cell divisions in development and cancer. *Nature*. 2006;441(7097):1068–1074.

15. Fish JL, Kosodo Y, Enard W, Pääbo S, Huttner WB. Aspm specifically maintains symmetric proliferative divisions of neuroepithelial cells. *Proc Natl Acad Sci U S A*. 2006;103(27):10438–10443.
16. Yingling J, Youn YH, Darling D, et al. Neuroepithelial stem cell proliferation requires LIS1 for precise spindle orientation and symmetric division. *Cell*. 2008;132(3):474–486.
17. Postiglione MP, Jüschke C, Xie Y, Haas GA, Charalambous C, Knoblich JA. Mouse inscuteable induces apical-basal spindle orientation to facilitate intermediate progenitor generation in the developing neocortex. *Neuron*. 2011;72(2):269–284.
18. Quyn AJ, Appleton PL, Carey FA, et al. Spindle orientation bias in gut epithelial stem cell compartments is lost in precancerous tissue. *Cell Stem Cell*. 2010;6(2):175–81.
19. Williams SE, Beronja S, Pasolli HA, Fuchs E. Asymmetric cell divisions promote Notch-dependent epidermal differentiation. *Nature*. 2011;470(7334):353–358.
20. Tamplin OJ, Durand EM, Carr LA, et al. Hematopoietic stem cell arrival triggers dynamic remodeling of the perivascular niche. *Cell*. 2015;160(1-2):241–252.
21. Brummendorf TH, Dragowska W, Zijlmans J, Thornbury G, Lansdorp PM. Asymmetric cell divisions sustain long-term hematopoiesis from single-sorted human fetal liver cells. *J Exp Med*. 1998;188:1117–1124.
22. Takano H, Ema H, Sudo K, Nakauchi H. Asymmetric division and lineage commitment at the level of hematopoietic stem cells: inference from differentiation in daughter cell and granddaughter cell pairs. *J Exp Med*. 2004;199:295–302.
23. Wu M, Kwon HY, Rattis F, et al. Imaging hematopoietic precursor division in real time. *Cell Stem Cell*. 2007;1:541–554.
24. Giebel B, Zhang T, Beckmann J, et al. Primitive human hematopoietic cells give rise to differentially specified daughter cells upon their initial cell division. *Blood*. 2006;107(5):2146–2152.
25. Beckmann J, Scheitza S, Wernet P, Fischer JC, Giebel B. Asymmetric cell division within the human hematopoietic stem and progenitor cell compartment: identification of asymmetrically segregating proteins. *Blood*. 2007;109(12):5494–501.
26. Hope KJ, Cellot S, Ting SB, et al. An RNAi screen identifies Msi2 and Prox1 as having opposite roles in the regulation of hematopoietic stem cell activity. *Cell Stem Cell*. 2010;7(1):101–13.
27. Ting SB, Deneault E, Hope K, et al. Asymmetric segregation and self-renewal of hematopoietic stem and progenitor cells with endocytic Ap2a2. *Blood*. 2012;119(11):2510–22.
28. Florian MC, Dörr K, Niebel A, et al. Cdc42 activity regulates hematopoietic stem cell aging and rejuvenation. *Cell Stem Cell*. 2012;10(5):520–30.

29. Heidel FH, Bullinger L, Arreba-Tutusaus P, et al. The cell fate determinant Llgl1 influences HSC fitness and prognosis in AML. *J Exp Med*. 2013;210(1):15–22.
30. Shin JW, Buxboim A, Spinler KR, et al. Contractile forces sustain and polarize hematopoiesis from stem and progenitor cells. *Cell Stem Cell*. 2014;14(1):81–93.
31. Mohr J, Dash BP, Schnoeder TM, et al. The cell fate determinant Scribble is required for maintenance of hematopoietic stem cell function. *Leukemia*. 2018; doi:10.1038/s41375-018-0025-0.
32. Loeffler D, Wehling A, Schneiter F, et al. Asymmetric lysosome inheritance predicts activation of haematopoietic stem cells. *Nature*. 2019;573(7774):426–429.
33. Rentas S, Holzapfel N, Belew MS, et al. Musashi-2 attenuates AHR signaling to expand human haematopoietic stem cells. *Nature*. 2016;532(7600):508–511.
34. Zimdahl B, Ito T, Blevins A, et al. Lis1 regulates asymmetric division in hematopoietic stem cells and in leukemia. *Nat Genet*. 2014;46(3):245–252.
35. Fellmann C, Hoffmann T, Sridhar V, et al. An optimized microRNA backbone for effective single-copy RNAi. *Cell Rep*. 2013;5(6):1704–1713.
36. Rueden CT, Schindelin J, Hiner MC, et al. ImageJ2: ImageJ for the next generation of scientific image data. *BMC Bioinformatics*. 2017;18(1):529.
37. Schindelin J, Arganda-Carreras I, Frise E, et al. Fiji: an open-source platform for biological-image analysis. *Nat Methods*. 2012;9(7):676–682.
38. Goldman FD, Aubert G, Klingelhutz AJ, et al. Characterization of primitive hematopoietic cells from patients with dyskeratosis congenita. *Blood*. 2008;111(9):4523–4531.
39. Dror Y, Freedman MH. Shwachman-Diamond syndrome: an inherited preleukemic bone marrow failure disorder with aberrant hematologic progenitors and faulty marrow microenvironment. *Blood*. 1999;94(9):3048–3054.
40. Maciejewski JP, Selleri C, Sato T, Anderson S, Young NS. A severe and consistent deficit in marrow and circulating primitive hematopoietic cells (long-term culture-initiating cells) in acquired aplastic anemia. *Blood*. 1996;88(6):1983–1991.
41. Maciejewski JP, Anderson S, Katevas P, Young NS. Phenotypic and functional analysis of bone marrow progenitor cell compartment in bone marrow failure. *Br J Haematol*. 1994;87(2):227–234.
42. Scopes J, Bagnara M, Gordon-Smith EC, Ball SE, Gibson FM. Haemopoietic progenitor cells are reduced in aplastic anemia. *Br J Haematol*. 1994;86(2):427–430.
43. Tsai PH, Arkin S, Lipton JM. An intrinsic progenitor defect in Diamond-Blackfan anaemia. *Br J Haematol*. 1989;73(1):112–120.
44. Nathan DG, Clarke BJ, Hillman DG, Alter BP, Housman DE. Erythroid precursors in congenital hypoplastic (Diamond-Blackfan) anemia. *J Clin Invest*. 1978;61(2):489–498.

45. Joyce CE, Saadatpour A, Ruiz-Gutierrez M, et al. TGFβ signaling underlies hematopoietic dysfunction and bone marrow failure in Shwachman-Diamond syndrome. *J Clin Invest*. 2019;130:3821–3826.
46. Benais-Pont G, Punn A, Flores-Maldonado C, et al. Identification of a tight junction–associated guanine nucleotide exchange factor that activates Rho and regulates paracellular permeability. *J Cell Biol*. 2003;160(5):729–740.
47. Bakal CJ, Finan D, LaRose J, et al. The Rho GTP exchange factor Lfc promotes spindle assembly in early mitosis. *Proc Natl Acad Sci U S A*. 2005;102(27):9529–9534.
48. Gauthier-Fisher A, Lin DC, Greeve M, Kaplan DR, Rottapel R, Miller FD. Lfc and Tctex-1 regulate the genesis of neurons from cortical precursor cells. *Nat Neurosci*. 2009;12(6):735–744.
49. Meiri D, Marshall CB, Greeve MA, et al. Mechanistic insight into the microtubule and actin cytoskeleton coupling through dynein-dependent RhoGEF inhibition. *Mol Cell*. 2012;45(5):642–655.
50. Meiri D, Greeve MA, Brunet A, et al. Modulation of Rho guanine exchange factor Lfc activity by protein kinase A-mediated phosphorylation. *Mol Cell Biol*. 2009;29(21)5963–5973.
51. Cullis J, Meiri D, Sandi MJ, et al. The RhoGEF GEF-H1 is required for oncogenic RAS signaling via KSR-1. *Cancer Cell*. 2014;25(2):181–195.
52. Ito K, Hirao A, Arai F, et al. Reactive oxygen species act through p38 MAPK to limit the lifespan of hematopoietic stem cells. *Nat Med*. 2006;12(4):446–451.
53. Jang YY, Sharkis SJ. A low level of reactive oxygen species selects for primitive hematopoietic stem cells that may reside in the low-oxygenic niche. *Blood*. 2007;110(8):3056–3063.
54. Zou J, Zou P, Wang J, et al. Inhibition of p38 MAPK activity promotes *ex vivo* expansion of human cord blood hematopoietic stem cells. *Ann Hematol*. 2012;91(6):813–823.
55. Zhou X, Florian MC, Arumugam P, et al. RhoA GTPase controls cytokinesis and programmed necrosis of hematopoietic progenitors. *J Exp Med*. 2013;210(11):2371–2385.
56. Mikkola HK, Orkin SH. The journey of developing hematopoietic stem cells. *Development*. 2006;133(19):3733–3744.
57. Mahony CB, Bertrand JY. How HSCs colonize and expand in the fetal niche of the vertebrate embryo: an evolutionary perspective. *Front Cell Dev Biol*. 2019;7:34.
58. Pleines I, Hagedorn I, Gupta S, et al. Megakaryocyte-specific RhoA deficiency causes macrothrombocytopenia and defective platelet activation in hemostasis and thrombosis. *Blood*. 2012;119(4):1054–1063.

59. Gao Y, Smith E, Ker E, et al. Role of RhoA-specific guanine exchange factors in regulation of endomitosis in megakaryocytes. *Dev Cell*. 2012;22(3):573–584.
60. Fine N, Dimitriou ID, Rullo J, et al. GEF-H1 is necessary for neutrophil shear stress-induced migration during inflammation. *J Cell Biol*. 2016;215(1):107–119.
61. Ravindran E, Hu H, Yuzwa SA, et al. Homozygous ARHGEF2 mutation causes intellectual disability and midbrain-hindbrain malformation. *PLoS Genet*. 2017;13(4):e1006746.
62. Aleksiūnienė B, Preiksaitiene E, Morkūnienė A, Ambrozaitytė L, Utkus A. A *de novo* 1q22q23.1 interstitial microdeletion in a girl with intellectual disability and multiple congenital anomalies including congenital heart defect. *Cytogenet Genome Res*. 2018;154(1):6–11.
63. Myers KC, Davies SM, Shimamura A. Clinical and molecular pathophysiology of Shwachman-Diamond syndrome: an update. *Hematol Oncol Clin North Am*. 2013;27(1):117–128.
64. Levin TL, Mäkitie O, Berdon WE, Lachman RS. Shwachman-Bodian-Diamond syndrome: metaphyseal chondrodysplasia in children with pancreatic insufficiency and neutropenia. 2015;45(7):1066–1071.
65. Thornton GK, Woods CG. Primary microcephaly: do all roads lead to Rome? *Trends Genet*. 2009;25(11):501–510.
66. Hertwig P. Neue Mutationen und Koppelungsgruppen bei der Hausmaus. *Z Indukt Abstamm Vererbungsl*. 1942;80(1):220–246.
67. Lizarraga SB, Margossian SP, Harris MH, et al. Cdk5rap2 regulates centrosome function and chromosome segregation in neuronal progenitors. *Development*. 2010;137(11):1907–1917.

Chapter 3: Downregulated Staufen1 compromises hematopoietic stem cell activity *in vivo* and elicits expression signatures consistent with clinical anemias

Derek C. H. Chan,[1,2] Lina Liu,[1] Damian Tran,[1] Ana Vujovic,[1] Ruilin Wu,[1] Laura P. M. H. de Rooij,[1] Joshua Xu,[1,2] Yu Lu,[1] Kristin J. Hope[1]

[1]Stem Cell and Cancer Research Institute, Department of Biochemistry and Biomedical Sciences, McMaster University, Hamilton, Ontario, Canada; [2]Michael G. DeGroote School of Medicine, Faculty of Health Sciences, McMaster University, Hamilton, Ontario, Canada

Abstract

Proper regulation of RNA localization, fidelity and translation are fundamental developmental mechanisms that depend on the function of associated RNA-binding proteins (RBPs). Staufen, a member of double-stranded RBPs, mediates asymmetric cell division in neural precursors; however, its role in the hematopoietic system remains unclear. Here, we studied the role of both mammalian paralogs of Staufen and identify that Stau1, but not Stau2, is essential to hematopoietic stem cell (HSC) activity *in vivo*. We also confirm another RBP family known to localize RNAs, Pumilio, as critical regulators of HSC function. Unbiased global profiling of transcriptome and proteome changes with Stau1 downregulation in the primitive hematopoietic compartment reveal expression signatures predictive of an immune/inflammatory-associated anemia, with post-transcriptional pathway analyses highlighting concordant loss of erythroid-promoting transcription factors and cell cycle regulators, gain of an expression state consistent with interferon-γ activity, and discordant regulatory axes coalescing on translational regulation and ribosomal RNA processing. These findings position Stau1 as a guardian of HSC-driven erythropoiesis, with implications potentially relevant to the pathogenesis of aplastic anemia and/or paroxysmal nocturnal hemoglobinuria, and provides a rational foundation for related future investigations in human HSCs and clinical anemias.

Introduction

RNA localization and translational regulation are key mechanisms that directly influence developmental outcomes. In *Drosophila melanogaster*, the precise spatiotemporal translation of mRNA transcripts encoding the cell fate determinants *gurken*, *bicoid*, *oskar* and *nanos* ensures appropriate formation and patterning of dorsoventral and anteroposterior axes in the embryo (Becalska and Gavis, 2009). Similarly, in *Xenopus laevis* oocytes, vegetal pole translation of the determinants *Nanos1*, *Xdazl*, *Vg1* and *VegT* mRNAs are critical for germ cell specification and mesendoderm patterning (King *et al.*, 2005). Recent global analyses have shown that nearly 70% of all tested mRNAs show some pattern of localization in the early *Drosophila* embryo (Lécuyer *et al.*, 2007), with subsequent studies confirming that subcellular RNA localization appears to be the norm rather than the exception for both coding and non-coding RNA species (Jambor *et al.*, 2015; Wilk *et al.*, 2016), indicating that spatiotemporal targeting of transcripts is a widespread means to diversify and/or execute function.

Studies on polarized segregation of mRNAs during asymmetric cell division (ACD) demonstrate that this process depends on the asymmetric distribution and binding capacities of RNA-binding proteins (RBPs). In *Drosophila*, localization of *bicoid* and *oskar* mRNAs requires the binding capacity of the double-stranded RBP (dsRBP) Staufen (St Johnston *et al.*, 1991, Li *et al.*, 1997; Broadus *et al.*, 1998), whereas localized translational repression of *hunchback* mRNA during pattern specification requires the RBP Pumilio (Wreden *et al.*, 1997). In *Xenopus*, vegetal *Vg1* mRNA localization depends on the function of the RBP Vera/Igf2bp (Schwartz *et al.*, 1992). Other members of these historically characterized maternal effect genes, largely categorized into anterior, abdominal or posterior groups based on their localization, are importantly RNA-centric,

with roles that have since been revealed to regulate multiple aspects of RNA processing, stability and/or translation.

In mammals, the roles of Staufen have been more broadly described to not only mediate ACD (Vessey *et al.*, 2012; Kusek *et al.*, 2012), but also elicit RNA decay (Park and Maquat, 2013), regulate splicing (Ravel-Chapuis *et al.*, 2012), initiate adaptive stress responses (Thomas *et al.*, 2009) and alter translational control (Ricci *et al.*, 2014). These additional functions are thought to have arisen from an evolutionary acquisition of genomic *Alu* elements within primates that are recognized and bound by Staufen (Lucas *et al.*, 2018). Interestingly, both mammalian Staufen paralogs – Stau1 and Stau2 – regulate primitive brain development in different ways, as Stau1 containing ribonucleoprotein (RNP) complexes use RNA decay to balance neural stem cell pools with cortical neurogenesis (Moon *et al.*, 2018), while Stau2 RNP complexes localize important fate determinants during ACD to maintain a similar balance between neural precursors and downstream cell types (Vessey *et al.*, 2012; Kusek *et al.*, 2012).

Stau1 and Stau2 both independently and cooperatively elicit RNA decay by recruiting Upf1 to various 3'-untranslated regions (UTRs) (Kim *et al.*, 2005; Park *et al.*, 2013). In some cases, long noncoding RNAs (lncRNAs) harbouring repetitive *Alu* elements bridge and pair with others present in 3'-UTRs to trigger Staufen-mediated decay (SMD) (Gong *et al.*, 2013). Relative expression levels of Stau1 and Stau2 dictate the extent of SMD in competition with the canonical nonsense-mediated decay (NMD) pathway, and together may act as a rheostat in maintaining and/or directing mRNA quality control and fate (Park and Maquat, 2013). In contrast, certain structured 5'-UTRs that recruit Stau1 binding result in enhanced translation (Dugré-Brisson *et al.*, 2005). Stau1 binding to coding sequence (CDS) regions that have greater GC content and/or

propensity to form secondary structures also increase ribosomal loading (Ricci *et al.*, 2014) and enrich for genes that encode for various transcriptional regulators and cell cycle factors.

In situations of oxidative and/or endoplasmic reticulum (ER) stress, cap-independent internal ribosome entry site (IRES)-mediated translation of Stau1 functions to promote cellular recovery by stabilizing polysomes (Dugré-Brisson *et al.*, 2005), dissolving stress granules (Thomas *et al.*, 2009; Ravel-Chapuis *et al.*, 2016) and promoting splicing of mRNAs such as *Xbp1* that protect against ER stress (Sugimoto *et al.*, 2015). Other work has shown RNA binding competition between Stau1 and other dsRBPs, including $p54^{nrb}$ that works to retain RNAs in the nucleus, and protein kinase R (PKR) that acts as a dsRNA sensor to mediate global translational shutdown in settings of viral infection (Elbarbary *et al.*, 2013). Recent studies also detail antagonistic and competitive binding of mRNA targets that are enriched for genes related to apoptosis between Stau1 and adenosine deaminase (Adar1), another dsRBP known for its RNA editing activity (Sakurai *et al.*, 2017; Yang *et al.*, 2017).

Here, we demonstrate that Stau1, but not Stau2, is important for HSC activity *in vivo*. We also confirm recent findings that another RBP family known for localizing RNAs, Pumilio, critically regulates HSC function (Naudin *et al.*, 2017). Interestingly, expression signatures of Stau1 downregulation in the primitive hematopoietic compartment reflect a molecular signature predictive of anemia consistent with an activated immune/inflammatory state, with several altered post-transcriptional direct and/or indirect pathways that may explain this outcome. Our findings suggest possible roles for Stau1 in the pathogenesis of aplastic anemia and/or paroxysmal nocturnal hemoglobinuria, providing rationale for future studies in the human setting to better understand how anemia may arise at a primitive cellular level.

Materials and Methods

Functional assays of HSCs and progenitors

A previously described *in vitro* to *in vivo* series of functional assays for HSC and progenitor activity was followed (Hope *et al.*, 2010) with minor modifications. Briefly, bone marrow was collected from bilateral femurs, tibias and iliac crests from 6- to 8-week-old, sex-balanced B6.SJL mice, lineage-depleted and flow-sorted to obtain a $Lin^{-}CD150^{+}CD48^{-}$ population. Cells were pre-stimulated overnight in StemSpan SFEM media (STEMCELL Technologies) supplemented with mSCF (R&D, 100 ng/mL), mTPO (Peprotech, 100 ng/mL), mIL-3 (Peprotech, 10 ng/mL) and mIL-6 (Peprotech, 10 ng/mL) prior to being transduced with ultracentrifuge-concentrated and filtered lentiviruses for short hairpins (shRNAs) targeting Luciferase, Stau1, Stau2, Pum1 or Pum2 (see following table) expressed in a pZIP-mEF1α-ZsGreen-miR-E backbone (TransOMIC technologies) at a multiplicity of infection of 100 for 3 days. Half-well equivalents were transplanted into each lethally irradiated (1100 cGy, Gammacell 40 Exactor, Best Theratronics) C57Bl/6 recipient mouse with 1 x 10^5 unfractionated recipient bone marrow competitor cells. Peripheral blood analysis was conducted every 4 weeks post-transplant to monitor engraftment levels by measuring $CD45.1^{+}$ cells using flow cytometry. $ZsGreen^{+}$ cells were sorted out of transduced wells and seeded into myeloid-promoting colony-forming unit (CFU) assays using Methocult GF M3434 (STEMCELL Technologies). Colonies from technical duplicates were scored 10–14 days after plating. Antibodies against mouse antigens included the following: CD45.2 v450 (BD); Lineage eFluor 450 (eBioscience), Alexa Fluor 700 (BioLegend); Sca-1 APC (eBioscience), PerCP-Cy5.5 (eBioscience); c-Kit PE-Cy7 (BD); CD150 PE (BioLegend); CD48 FITC (BD), APC (eBioscience); CD11b PE (BD); Gr-1 APC-Cy7 (BD); B220 APC (BD); CD4 PE (BD); and CD8a APC-Cy7 (BD). Bone marrow samples obtained from recipient mice were pre-

treated with Fc block (BD Biosciences). During flow cytometry, cells were discriminated on the basis of size, granularity and viability depending on 7-AAD exclusion as needed. Sorting was performed on a MoFlo XDP (Beckman Coulter), while routine acquisition was performed on a LSRII instrument equipped with FACSDiva software (BD Biosciences). Flow analysis was completed using FlowJo v10.0.7 (Tree Star Inc.).

shRNA	**97-mer**
shLuciferase	TGCTGTTGACAGTGAGCGCCGATATGGGCTGAATACAAATTAGTGAAGCCACAGATGTAATTT GTATTCAGCCCATATCGTTGCCTACTGCCTCGGA
shStau1.1481	TGCTGTTGACAGTGAGCGACCGAGACCATTTTAAAGAGTATAGTGAAGCCACAGATGTATACT CTTTAAAATGGTCTCGGCTGCCTACTGCCTCGGA
shStau1.1584	TGCTGTTGACAGTGAGCGCCCAGGTTGAATACAAAGATTTTAGTGAAGCCACAGATGTAAAAT CTTTGTATTCAACCTGGATGCCTACTGCCTCGGA
shStau1.1585	TGCTGTTGACAGTGAGCGACAGGTTGAATACAAAGATTTTTAGTGAAGCCACAGATGTAAAAA TCTTTGTATTCAACCTGGTGCCTACTGCCTCGGA
shStau1.2864	TGCTGTTGACAGTGAGCGCCCAATAAATGGTAATACTAAATAGTGAAGCCACAGATGTATTTA GTATTACCATTTATTGGTTGCCTACTGCCTCGGA
shStau2.643	TGCTGTTGACAGTGAGCGAAAGATCTTTTATGTTCAGTTATAGTGAAGCCACAGATGTATAAC TGAACATAAAAGATCTTGTGCCTACTGCCTCGGA
shStau2.811	TGCTGTTGACAGTGAGCGCGACGATAAAGATGCAAATAAATAGTGAAGCCACAGATGTATTTA TTTGCATCTTTATCGTCATGCCTACTGCCTCGGA
shPum1.4806	TGCTGTTGACAGTGAGCGCTACAGCCTAGTTAATGTTTAATAGTGAAGCCACAGATGTATTAA ACATTAACTAGGCTGTATTGCCTACTGCCTCGGA
shPum1.4877	TGCTGTTGACAGTGAGCGATGAGAGCCTTTCTAAATGTTATAGTGAAGCCACAGATGTATAAC ATTTAGAAAGGCTCTCACTGCCTACTGCCTCGGA
shPum2.3110	TGCTGTTGACAGTGAGCGCTGCCAGCAATGTAGTAGAAAATAGTGAAGCCACAGATGTATTTT CTACTACATTGCTGGCAATGCCTACTGCCTCGGA
shPum2.4843	TGCTGTTGACAGTGAGCGATAGGATCTGGATCACTTTCAATAGTGAAGCCACAGATGTATTGA AAGTGATCCAGATCCTAGTGCCTACTGCCTCGGA

Sample preparation for next-generation analyses

Bilateral femurs, tibias and iliac crests were collected from 6- to 8-week old, sex-balanced C57Bl/6 mice, crushed, filtered, lysed for RBCs and lineage depleted. Cells were pre-stimulated overnight in StemSpan SFEM II (STEMCELL Technologies) basal media, supplemented with 10% FBS (Gibco), mSCF (R&D, 100 ng/mL), mTPO (Peprotech, 100 ng/mL), mIL-3 (Peprotech, 10 ng/mL) and mIL-6 (Peprotech, 10 ng/mL) prior to being transduced with ultracentrifuge-concentrated and filtered lentiviruses prepared above at a multiplicity of infection of 100 for 5 days. ZsGreen^{+}

cells for each sample were then flow-sorted in the ranges of 1.5 – 3 x 10^6 cells, washed and snap frozen.

RNA-sequencing and analysis

RNA extraction using Trizol LS (Thermo Fisher) was performed on 1 x 10^5 ZsGreen$^+$ sorted cells for each short hairpin. Samples were purified on RNeasy micro columns (Qiagen), quantified by QuBit fluorometer (Thermo Fisher) and assessed for RNA quality with the RNA 6000 pico assay on the BioAnalyzer 2100 (Agilent). Libraries were prepared with the KAPA Stranded mRNA-Seq Kit (KAPA) using Illumina adaptors for PCR amplification of cDNA libraries. Libraries were diluted to 10 nM and normalized by qPCR using the KAPA Library Quantification Kit (KAPA). Libraries were pooled to equimolar concentration and subjected to sequencing on the NextSeq 500 (Illumina) at a depth of 50 million reads per sample (150 cycles, paired-end, 80 base pair length). For data processing, output sequences were trimmed for sequencing adaptors and low quality 3' bases using Trimmomatic v0.35 (Bolger *et al.*, 2014) and aligned to the mouse reference genome mm10 using STAR v2.5.1b (Dobin *et al.*, 2013). Gene and transcript level expressions were obtained both STAR read counts and computed using RSEM (Li and Dewey, 2011) for FPKM and TPM values. Differential expression analyses were carried out using DESeq2 v1.18.1 (Love *et al.*, 2014) to normalize gene read counts. Alternative splicing analyses were conducted using rMATS v4.0.2 (Shen *et al.*, 2014). RNA-seq data was validated by quantitative PCR (qPCR) of select genes using primers designed from the Universal Probe Library (Roche).

Proteomic profiling and analysis

Frozen cell pellets of sorted, biological duplicates of shLuciferase, shStau1.2864 and shStau1.1481 with ≥90% sort purities of ~20 μg were lysed in 50 μL of 8M urea (Sigma-Aldrich) and 100 mM

ammonium bicarbonate (Sigma-Aldrich) each. Lysates were vortexed at 2,800 rpm briefly for 10 seconds, incubated on ice for 10 seconds and repeated for 6 times. Samples were centrifuged at 21,000 x g for 5 minutes at 4°C. Proteins were then reduced using 5 mM tris (2-carboxyethyl) phosphine (Sigma-Aldrich) for 45 minutes at 37°C and alkylated with 10 mM iodoacetamide (Sigma-Aldrich) for 45 minutes at room temperature in the dark. Samples were diluted to lower the urea concentration by 5-fold with 100 mM ammonium bicarbonate (Sigma-Aldrich) and treated with sequencing grade modified trypsin (Promega) at a trypsin:protein (w:w) ratio of 1:50 for overnight digestion at 37°C. Trifluoroacetic acid (Thermo Scientific) was added to reduce pH and samples were desalted with SOLA Solid Phase Extraction 2 mg 96-well plates (Thermo Scientific). Processed peptides were eluted using 200 µL of 80% acetonitrile – 0.1% trifluoroacetic acid solution and speed-vacuum dried using Labconco CentriVap Benchtop Vacuum Concentrator (Kansas City, MO). Tandem Mass Tag (TMT) 6-plex isobaric labelling reagent (Thermo Fisher) was resuspended in liquid chromatography–mass spectrometry grade anhydrous acetonitrile (Sigma-Aldrich) following manufacturer's protocol. Briefly, 0.8 mg of TMT reagent was resuspended in 41 µL of acetonitrile and incubated at room temperature for 10 minutes, during which processed peptide samples were resuspended in 100 mM triethylammonium bicarbonate (Sigma-Aldrich) to 1 µg/µL concentration. Both were mixed with a 4:1 TMT:peptide ratio and incubated at room temperature for 1 hour. Each TMT reaction was quenched with 8 µL of 5% hydroxylamine (Sigma-Aldrich) for 15 minutes at room temperature. TMT-labeled samples were pooled together in equal ratios, separated on inhouse-made traps and analytical columns and delivered by an Ultimate 3000 RSLCNano UPLC system (Thermo Fisher) coupled to a QExactive HF quadrupole–Orbitrap mass spectrometer (Thermo Fisher). Raw output data was processed on Proteome Discoverer v2.2 (Thermo Fisher) to assign and quantify protein identifications; contaminants were filtered out in generated lists.

Post-transcriptional overlay and pathway analyses

Post-transcriptional overlay analyses of genes detected at both the transcript and protein level in shStau1 samples were assembled by ranking genes in each dataset in order of decreasing fold change compared to shLuciferase controls in R v3.5.1, inverted and normalized to a range of 0 to 1. Equivalent values were assigned equivalent ranks. Biological duplicates were consolidated by the average of normalized values. Ranks in both datasets were paired by official gene symbol matching in two-dimensional overlay and used to calculate a Pearson correlation coefficient for gene expression at both detected transcript and protein levels. Genes on this overlay were fractionated by establishing thresholds of 1 standard deviation from the mean along each axis. Gene lists were subjected to gene ontology (GO) analysis of biological process enrichment by both percentage and Benjamini false discovery rates on a *Mus musculus* gene background using DAVID (Dennis *et al.*, 2003). Differential expressed genes (DEGs) (non-adjusted $p < 0.05$) compared to shLuciferase from transcriptomes and proteomes of shStau1.2864 and shStau1.1481 were analyzed using Ingenuity Pathway Analysis (Qiagen) to assess for disease and function associations, upstream regulator analysis, predicted regulator networks and match analysis to compare predictions across all samples.

Results

***Stau1* is more highly expressed in HSC populations than committed progenitors**

To determine the expression profile of Staufen in HSC and progenitor subsets, we first evaluated mouse $Lin^-Sca\text{-}1^+c\text{-}Kit^+$ (LSK) and $Lin^-c\text{-}Kit^+$ (LK) cell populations by quantitative PCR (qPCR) and found that *Stau1* was highly expressed and enriched by 1.7-fold in LSK HSC and progenitors

(HSPCs) over LK progenitors, while *Stau2* was minimally detected in LSK cells at ~2% of *Stau1* expression levels (Figure 1A). Interestingly, whole transcriptome splicing analyses in wildtype mouse HSCs show that among *Stau1* transcript variants, isoforms that maintain an intact and critical RNA-binding domain (dsRBD3) are more highly expressed in HSCs compared to others that have this element disrupted (Figure 1B) (Goldstein *et al.*, 2017). In the human setting, STAU1 is ~2-fold more highly expressed in HSPC populations compared to lineage-restricted progenitors, whereas STAU2 exhibits a basal level of expression in HSPCs that does not significantly differ in downstream progenitors (Figure 1C) (Bagger *et al.*, 2016).

Stau1, Pum1 and Pum2 – but not Stau2 – are essential to primary HSC functions *in vivo*

We characterized the function of Staufen in HSCs by performing RNAi-mediated knockdowns of *Stau1* or *Stau2* in $Lin^{-}CD150^{+}CD48^{-}$ sorted populations and measured their ability to competitively reconstitute lethally-irradiated recipients (Figure 2A). While mid-level (45–75%) knockdown of *Stau1* gave inconsistent results (data not shown), high-level (>90%) knockdown led to significantly lower engraftment levels that dropped to approximately 25% of graft levels present in shLuciferase controls at 16 weeks post-transplant, indicating that effective *Stau1* downregulation compromises primary HSC repopulation *in vivo* (Figure 2B). Endpoint lineages in these grafts were not significantly skewed between myeloid, B and T cell outputs (Figure 2C), although *in vitro* colony-forming unit (CFU) assays showed an increased total myeloid progenitor output with *Stau1* knockdown (Figure 2D). Suspension cultures of $Lin^{-}CD150^{+}CD48^{-}$ cells with downregulated *Stau1* also led to a more rapid acquisition of Lin^{+} markers (Figure 2E) and a deficit in cell proliferation (Figure 2F). In contrast, recipients of $Lin^{-}CD150^{+}CD48^{-}$ HSCs that received high-level (85–95%) knockdown of *Stau2* were only mildly impaired or had increased repopulation activity at the end of 18 weeks in primary transplant settings (Figure 2B),

highlighting functional differences in HSC activity between these two paralogs. Among other hits from the same series of functional experiments, we also found that knockdown (50–95%) of the mammalian paralogs of Pumilio, *Pum1* and *Pum2*, also compromised HSC activity in primary recipients (Figure 2B), while both had no significant differences in their myeloid progenitor colony outputs (Figure 2D) or proliferation (Figure 2F), with these latter results contrasting from what has been reported (Naudin *et al.*, 2017).

Stau1 downregulation compromises HSC-erythroid transcriptional networks and upregulates an immune/inflammatory response signature

Given our phenotype revealing the essentiality of Stau1, but not Stau2, in HSCs and the reporting of a mechanism operating downstream of Pumilio in HSCs (Naudin *et al.*, 2017), we decided to focus efforts on understanding mechanisms underlying Stau1 downregulation in cells within the primitive hematopoietic compartment. Using an unbiased approach, we performed high levels (80–90%) of *Stau1* knockdown in mouse Lin^- cells, flow-sorted transduced populations and subjected these cells to global RNA-sequencing and proteomic measurements (Figure 3A). DEG analyses among mRNA transcripts with strict statistical cut-offs (Benjamini-Hochberg adjusted p-values < 0.05) identified a significant >3-fold depletion of *Myb*, a transcription factor essential for adult erythropoiesis (Mucenski *et al.*, 1991) and HSC self-renewal (Lieu and Reddy, 2009) (Figure 3B). *Thy1*, an early B-cell surface marker used to enrich for HSCs (Muller-Sieburg *et al.*, 1986), was also significantly depleted by >2.8-fold in *Stau1* knockdown samples compared to shLuciferase controls (Figure 3B). Gene ontology (GO) analyses using DAVID (Dennis *et al.*, 2003) performed on significantly downregulated genes (non-adjusted p-value < 0.05) revealed an enrichment of DNA transcription factors, many of which are known to be critical to HSC function (Figure 3C), including *Hlf* (depleted >3.4-fold; Komorowska *et al.*, 2017), *Bcl11a* (depleted >2.2-

fold; Luc *et al.*, 2016), *Gfi1* (depleted >1.9-fold; Zeng *et al.*, 2004; Hock *et al.*, 2004), *Meis1* (depleted >1.6-fold; Kocabas *et al.*, 2012; Unnisa *et al.*, 2012; Ariki *et al.*, 2014; Miller *et al.*, 2016) and *Gata2* (depleted >1.5-fold; Menendez-Gonzalez *et al.*, 2019) (Figures 3C,D). Regulators of cell cycle (*Fbxo5*, *Bora*) and cell division (*Anln*, *Cit*, *Cntrl*) were also significantly depleted in this setting (Figures 3D). In contrast, pathways enriched in genes significantly upregulated (non-adjusted p-value < 0.05) included those involved in transport (*Rab20*, *Rhob*, *Vamp8*), immune (*Ly9*, *B2m*) and inflammatory (*Clec7a*, *Cyba*, *Fpr1*, *Ltbr*) responses (Figure 3D). Alternative splicing analysis using rMATS (Shen *et al.*, 2014) also revealed predominant significant splicing alterations to genes that regulate DNA transcription, covalent chromatin modification (*Emsy*, *Chd7*, *Pbrm1*) and DNA repair (*Rtel1*) (Figure 3E).

The post-transcriptional regulatory axis of Stau1 strongly enriches for translation and ribosomal RNA processing pathways

To identify post-transcriptional pathways regulated by Stau1, we overlaid the transcriptome and proteome by matching genes detected in both datasets and assigned gene rankings by their normalized expression level. This overlay revealed that approximately 75% of variation in protein levels could not be explained by mRNA levels in the setting of *Stau1* downregulation (Pearson correlation coefficient 0.26) (Figure 4A). We stratified relatively concordant, post-transcriptional and discordant expression changes by setting thresholds of one standard deviation from expression means of both datasets and performed GO analyses for term enrichment within each stratum (Figure 4B). Consistent with transcript analyses, concordantly depleted pathways from this overlay included genes that regulated cell cycle, cell division, DNA transcription and DNA repair. Upregulated genes again revealed enrichments for pathways regulating transport, immune and inflammatory responses, along with several components of the immunoproteasome. Post-

transcriptional changes were defined by relatively unchanged levels of mRNA expression but particularly high or low ranked protein expression. Genes particularly elevated at the protein level compared to their corresponding mRNA level enriched for pathways affecting translational regulation (eukaryotic translation initiation factors, ribosomal proteins) and protein transport (Rab family members, adaptor complexes), while those particularly depleted at the protein level significantly enriched for ribosomal RNA (rRNA) processing and ribosome biogenesis (DEAD box polypeptides) as well as RNA splicing. Taken together, this integrated analysis suggests that Stau1 normally may post-transcriptionally function in two different ways: 1) By ensuring appropriate transcript fidelity of several critical hematopoietic transcription factors and cell cycle regulators, while suppressing those that mediate an immune and/or inflammatory response; and 2) more broadly regulating ribosomal maturation alongside translational outputs.

Stau1 downregulation elicits RNA and protein signatures consistent with immune- and inflammatory-associated anemias

To elucidate the significance of this expression landscape and identify possible associations with other factors, we employed Ingenuity Pathway Analysis (Krämer *et al.*, 2014) on DEGs (non-adjusted $p < 0.05$) derived from both transcriptome and proteome datasets. Interestingly, among all disease associations, "anemia" was among the top 5 associations for changes at the transcript level (z-score 2.297; p-value 4.68 x 10^{-5}) (Figure 5A), mainly driven by upregulation of the interferon regulatory factor 7 (*Irf7*), low affinity Fc receptor for multimeric IgG (*Fcgr2a, Fcgr3a/3b*), and downregulation of several key erythroid promoting transcription factors (*Gata1*, *Gata2*, *Myb*) (Figure 5B). Interestingly, *Piga*, loss of which is associated with paroxysmal nocturnal hemoglobinuria, was also on this list. Predicted regulator networks highlighted a signature of activated type II interferon gamma (Ifn-γ) signalling along with downregulated

activity of homeodomain-interacting protein kinase 2 (Hipk2), activity for which would otherwise promote type I interferon responses (Figure 5C) (Cao *et al.*, 2019). Predicted activation of Ifn-γ was also present among DEGs at the protein level, and unsupervised hierarchical clustering placed Ifn-γ activity closely with its downstream transcriptional effector Stat1; microRNA-223 (miR-223), declining levels of which are normally necessary for erythroid commitment (Felli *et al.*, 2009); and the serum response factor (Srf) – myocardin-related transcription factor (Mrtf) axis, which has been reported to regulate cellular adhesion, migration and chemokine signalling (Ragu *et al.*, 2010; Costello *et al.*, 2015) (Figure 5D, middle window). Clustered predictions of repressed regulators included Myc, a concordantly expressed target of Myb (Cogswell *et al.*, 1993; Kumar *et al.*, 2003); and the prostaglandin E receptor 2 (Ptger2), a known positive regulatory axis of HSC function (Hoggatt *et al.*, 2009; Cutler *et al.*, 2013) (Figure 5D, left window). Interestingly, some regulators predicted to be discordant between the transcriptome and proteome datasets also arose. These included those with mild activation at the transcriptome but repression at the proteome level: E2f1, a member of a transcription factor family essential for red blood cell maturation (Li *et al.*, 2003), and Nfe2l2, loss of which is known to result in an immune-mediated hemolytic anemia (Lee *et al.*, 2004)) (Figure 5D, right window). In contrast, those predicted to be mildly repressed at the transcriptome but elevated at the proteome level included the Nlrp3-Il1b axis, known contributors toward an inflammatory-related anemia (Wang *et al.*, 2017). Overall, this expression landscape reflects an anemia signature that mirrors activated Ifn-γ signalling, which is a known detriment to HSCs (de Bruin *et al.*, 2013; Lin *et al.*, 2014; Chen *et al.*, 2015) and clinically associated with aplastic anemia (Zoumbos *et al.*, 1985; Sloand *et al.*, 2002; Solomou *et al.*, 2006). Taken together, this data positions Stau1 as a post-transcriptional modulator of processes in HSCs and primitive progenitors that may underlie anemia pathogenesis, and importantly provides a rational foundation for future phenotypic and mechanistic work in the human setting.

Discussion

In this study, we characterized the function of mammalian Staufen and Pumilio paralogs in HSCs and identified Stau1, Pum1 and Pum2 – but not Stau2 – as essential RBPs to HSC function *in vivo*. By downregulating Stau1 in the primitive hematopoietic compartment, we identified an immune and/or inflammatory-mediated anemia expression signature with several directional gene expression changes reminiscent of aplastic anemia and/or paroxysmal nocturnal hemoglobinuria, both of which remain relatively understudied and poorly understood.

Loss of Stau1 function has been previously modelled in a genetically modified mouse with truncated Stau1 expression, where an IRESβgeo cassette disrupts a critical double-stranded RNA-binding domain (dsRBD3). Affected mice exhibit mild impairments of synaptic development *in vitro* without obvious deficits in viability, development and/or behaviour (Vessey *et al.*, 2008). Studies in the primitive neural compartment have since showed that Stau1 modulates the balance between neural progenitor self-renewal and neurogenesis by eliciting SMD of neurogenic mRNAs (Moon *et al.*, 2018). These findings suggest that while loss of Stau1 function may not prohibit development, its functional relevance may be better appreciated and understood in particular scenarios. Our work in the hematopoietic system parallel these findings by identifying functional defects at the HSC level that lead to downstream processes that may predispose to anemia, which may not intuitively arise from processes present during early development (e.g. chronic anemia of inflammation) and/or elicited unless challenged (e.g. infectious or autoimmune trigger).

In contrast, while Stau2 has been previously identified to regulate the balance of neural stem cell self-renewal and differentiation (Vessey *et al.*, 2012; Kusek *et al.*, 2012), we did not find a similar

dependency of Stau2 in HSCs. Nonetheless, our functional readouts for Stau2 were consistent with other ongoing efforts that include reporting of a genetic loss of Stau2 function mouse model that yields normal hematopoietic parameters (Bajaj *et al.*, 2017). Interestingly, this preliminary work also identified that loss of Stau2 impairs propagation of blast crisis phase chronic myeloid leukemia *in vivo* by altering the balance of symmetric and asymmetric divisions among leukemic stem cells, highlighting functional differences in post-transcriptional regulation between stem cells in normal hematopoiesis and in related counterparts within myeloid leukemia.

Notably, our transcriptome and proteome based analyses provides an unbiased and comprehensive landscape of the post-transcriptional landscape of Stau1 within the primitive hematopoietic compartment. While high cell number requirements of mass spectrometry-driven proteomics limited integrated analyses within more enriched HSC populations, we were able to uncover a molecular predisposition to anemia at a primitive level to direct future areas of phenotypic focus. Our findings of concordantly downregulated enrichment of erythroid promoting transcription factors and cell cycle regulators with Stau1 downregulation is consistent with previous work that identified similar enrichments in the human setting (Ricci *et al.*, 2014) and suggests that Stau1 importantly safeguards the fidelity of these transcripts to ensure they are appropriately translated. Mechanistically, Stau1 may enact these functions directly by promoting the replacement of 5' nuclear-cap structures on target mRNAs with the eukaryotic translation initiation factor eIF4E (Jeong *et al.*, 2019) and/or facilitating efficient translation through its interaction with active ribosomal pools to increase ribosomal loading onto bound transcripts (Ricci *et al.*, 2014). Alternatively, given recent understanding that erythropoiesis is particularly sensitive to ribosome levels (Khajuria *et al.*, 2018), our findings of a predominant post-transcriptional enrichment of ribosomal genes and ribosomal RNAs could suggest a broader

indirect compromise of translation programs brought forward by loss of Stau1 function that could similarly result in anemia.

In contrast, upregulated genes that enriched for immune and/or inflammatory responses reflected a predicted activated Ifn-γ signature, even though Ifng and its cognate receptors Ifngr1 and Ifngr2 were not differentially expressed at either the transcript or protein level in our datasets. It remains possible that other cells produced in culture may generate Ifn-γ that feeds back towards the primitive compartment, but only a portion of downstream components classically activated by Ifn-γ signalling was evident in our datasets. A more intriguing explanation may be that Stau1 normally binds and elicits SMD for genes involved in immune/inflammatory pathways and/or indirectly through other dsRNAs thought to be immunoreactive in HSCs, and when downregulated, then allows for such elements to become activated. Interestingly, a similar concept has been suggested in loss of function studies for the dsRBP Adar1, where its deficiency similarly leads to an upregulated global interferon response conserved in both fetal liver HSCs and erythroid, but not myeloid cells (Hartner *et al.*, 2009). Our findings here parallel this data, where downregulated Stau1 impairs HSC maintenance and leads to a molecular predisposition to anemia, but total myeloid progenitor outputs remained relatively unaltered in both colony assays and at endpoint lineage measurements of transplanted recipients *in vivo*. Given the known association of a particular isoform of Adar1 (p150) that is inducible by interferon, it may be interesting to determine if there also exists a close association of a particular isoform of Stau1 with interferon response, especially since a variant of Stau1 with an intact and critical dsRBD3 is more highly expressed compared to its disrupted form in normal HSCs. In the presence of an immunologic and/or inflammatory signal for example, a disrupted dsRBD3 form of Stau1 could possibly predominate and compound changes that result in anemia.

Finally, this anemia signature reflective of an activated Ifn-γ state is reminiscent and potentially compatible with changes in aplastic anemia and its related entity paroxysmal nocturnal hemoglobinuria. In patients diagnosed with aplastic anemia, IFN-γ levels in the blood become elevated with increased numbers of autoreactive T cells that destroy HSPCs (Zoumbos *et al.*, 1985; Sloand *et al.*, 2002; Solomou *et al.*, 2006). Consistent with hematopoietic studies of mice treated with Ifn-γ that result in decreased *Gata2* expression in LSK cells (Chen *et al.*, 2015), $CD34^+$ cells isolated from patients diagnosed with aplastic anemia similarly show downregulation of *GATA2* and *c-MYB* expression (Zeng *et al.*, 2004), both of which are among the most significantly downregulated changes during loss of Stau1 expression. In paroxysmal nocturnal hemoglobinuria, loss of function mutations of the enzyme encoded by phosphatidylinositol glycan class A (PIGA) renders disrupted cell surface anchoring of complement inhibitors CD55 and CD59, deficiencies of which increases complement-mediated hemolysis of erythrocytes (Takeda *et al.*, 1993). Curiously, significantly downregulated *Piga* expression also occurs with loss of Stau1 expression. Could loss of Stau1 function therefore represent an independent and/or overlapping pathway underlying the pathogenesis of either of these entities? Does the RNA binding profile of Stau1 shift in the presence of viral dsRNAs in ways that disrupt a normal landscape, eliciting an immune/inflammatory response and/or an altered translation program in settings of anemias associated with viral infection? Is Stau1 aberrantly downregulated in hematopoietic cells in cases of aplastic anemia? And if so, could restoring Stau1 function ameliorate the progression of these disorders? Future work to answer these questions would not only be intriguing, but could provide novel insights into these poorly understood disorders and potentially lead to new ways to effectively treat diagnosed patients.

Acknowledgements

The authors thank Sheila Singh and Johann Hitzler for important feedback on this work; Minomi Subapanditha for flow cytometry sorting; Lillian Robson, Wendy Whittaker and Norma-Ann Kearns for animal caretaking and maintenance; and Patrick Gendron for bioinformatics support.

This work was supported by a Canadian Institutes of Health Research (CIHR) MD/PhD Studentship (D.C.), Ontario Graduate Scholarship (D.C.), CIHR Canada Graduate Scholarship – Master's (D.T.), MacData Fellowship (D.T.), CIHR Canada Graduate Scholarship – Doctoral (J.X.), Michael G. DeGroote Doctoral Scholarship of Excellence (J.X.), a Canada Foundation for Innovation – John R. Evans Leaders Fund (CFI-JELF) Award (Y.L.), an Ontario Institute for Cancer Research (OICR) Investigator Award (K.H.), and a CIHR Project Grant (K.H.).

Authorship

D.C. designed, led and performed the experiments, analyzed and interpreted the data and wrote the manuscript. L.L., R.W. and Y.L. processed samples for mass spectrometry-based proteomics. D.T. provided bioinformatics support for dataset overlay. A.V., L.d.R., and J.X. assisted with animal experiments. K.H. supervised the project, designed experiments and reviewed the data.

Conflict-of-interest Disclosure: The authors declare no competing financial interests.

Correspondence: Kristin Hope, McMaster University, 1280 Main Street West, Hamilton, Ontario L8S 4K1; E-mail: kristin@mcmaster.ca

Figures

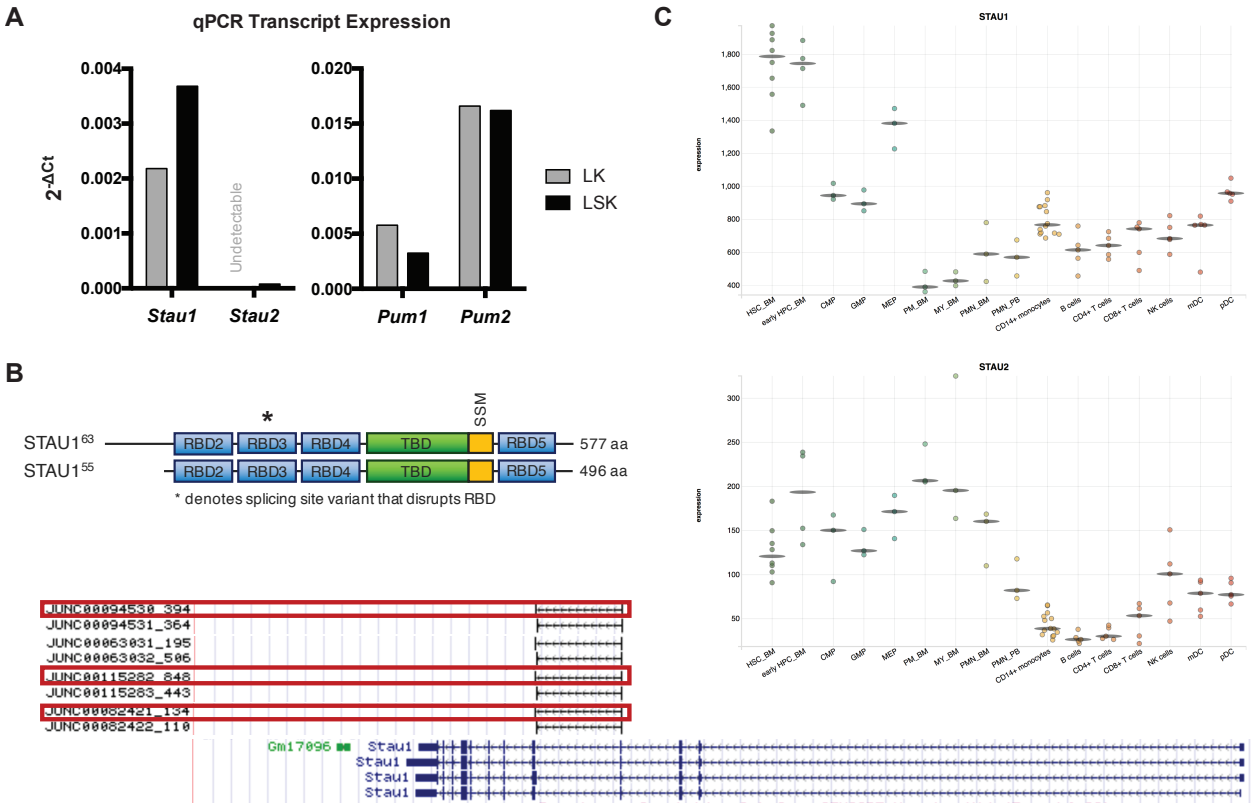

Figure 1: Stau1 is more highly expressed in HSC populations than committed progenitors.
A) qPCR expression profiling of *Stau1*, *Stau2*, *Pum1* and *Pum2* in murine Lin$^-$Sca-1$^-$c$^-$Kit$^+$ (LK, grey bars) and Lin$^-$Sca-1$^-$c$^+$Kit$^+$ (LSK, black bars) cell sorted populations normalized to *Gapdh*. B) (*Top*) Layout of two identified human isoforms of STAU1 from N- (left) to C-terminal (right) with a series double-stranded RNA-binding domains (dsRBDs), a tubulin-binding domain (TBD), and a Staufen-swapping motif (SSM). aa, amino acids. *denotes a 6-aa site disruption of a critical dsRBD3. (*Bottom*) Multiple paired quantified splice junction reads spanning exons 4 and 5 of Stau1 in murine HSCs; red boxes highlight 3 out of 4 paired comparisons favouring a higher level of expression of Stau1 with an intact dsRBD3 over its disrupted isoform in murine HSCs (Goldstein *et al.*, 2017). (C) BloodSpot expression profiles of STAU1 (*Top*, probe: 207320_x_at) and STAU2 (*Bottom*, probe: 204226_at) in normal human hematopoiesis (HemaExplorer) (Bagger *et al.*, 2016).

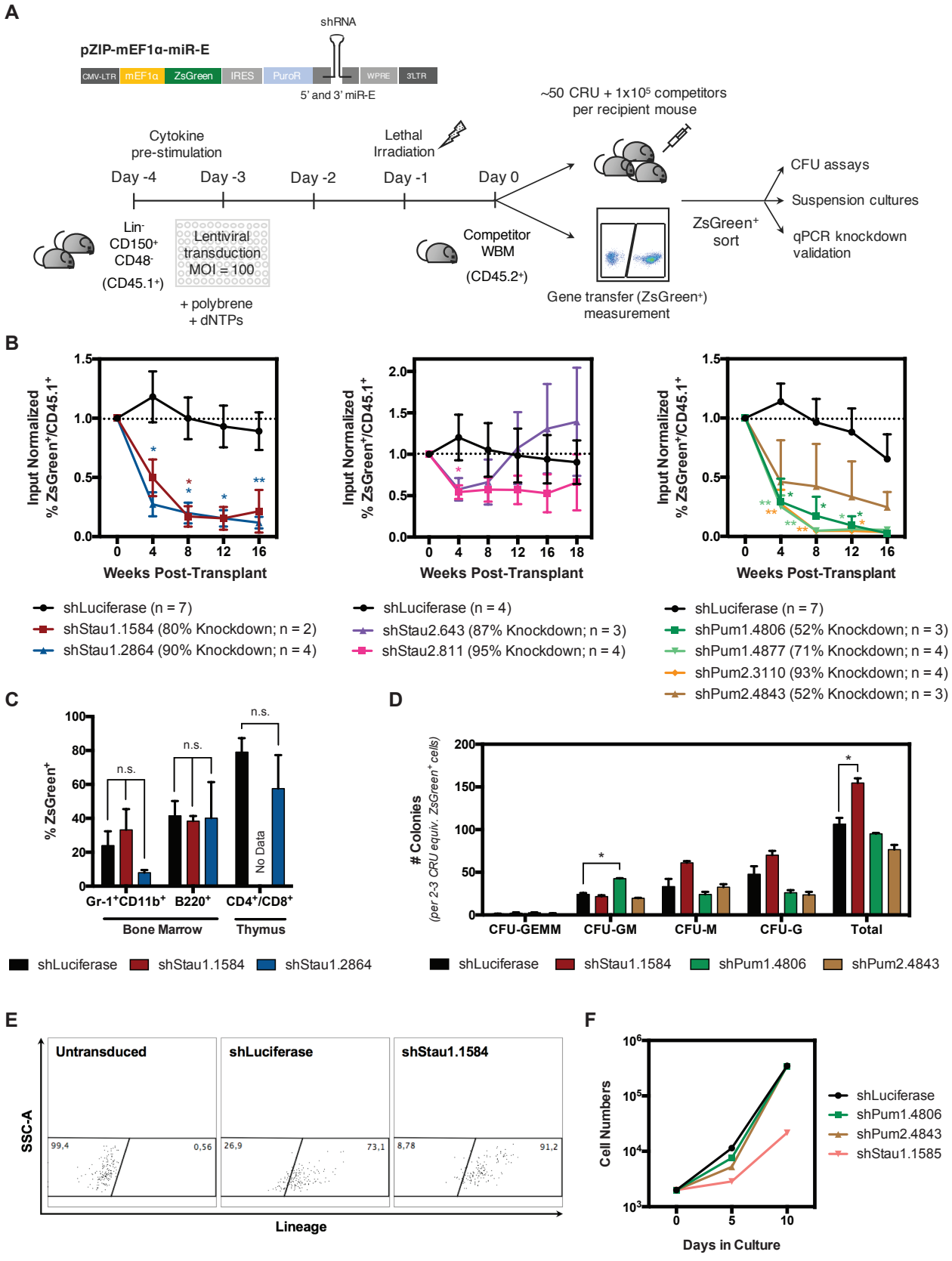
A
pZIP-mEF1α-miR-E
shRNA
CMV-LTR
mEF1α
ZsGreen
IRES
PuroR
WPRE
3LTR
5' and 3' miR-E
~50 CRU + 1x10⁵ competitors per recipient mouse
Cytokine pre-stimulation
Lethal Irradiation
Day -4
Day -3
Day -2
Day -1
Day 0
Lin⁻ CD150⁺ CD48⁻ (CD45.1⁺)
Lentiviral transduction MOI = 100
+ polybrene + dNTPs
Competitor WBM (CD45.2⁺)
Gene transfer (ZsGreen⁺) measurement
ZsGreen⁺ sort
CFU assays
Suspension cultures
qPCR knockdown validation
B
Input Normalized % ZsGreen⁺/CD45.1⁺
Weeks Post-Transplant
shLuciferase (n = 7)
shStau1.1584 (80% Knockdown; n = 2)
shStau1.2864 (90% Knockdown; n = 4)
shLuciferase (n = 4)
shStau2.643 (87% Knockdown; n = 3)
shStau2.811 (95% Knockdown; n = 4)
shLuciferase (n = 7)
shPum1.4806 (52% Knockdown; n = 3)
shPum1.4877 (71% Knockdown; n = 4)
shPum2.3110 (93% Knockdown; n = 4)
shPum2.4843 (52% Knockdown; n = 3)
C
% ZsGreen⁺
n.s.
No Data
Gr-1⁺CD11b⁺
B220⁺
CD4⁺/CD8⁺
Bone Marrow
Thymus
shLuciferase
shStau1.1584
shStau1.2864
D
Colonies (per 2-3 CRU equiv. ZsGreen⁺ cells)
CFU-GEMM
CFU-GM
CFU-M
CFU-G
Total
shLuciferase
shStau1.1584
shPum1.4806
shPum2.4843
E
Untransduced
shLuciferase
shStau1.1584
SSC-A
Lineage
99,4
0,56
26,9
73,1
8,78
91,2
F
Cell Numbers
Days in Culture
shLuciferase
shPum1.4806
shPum2.4843
shStau1.1585

Figure 2: Stau1, Pum1 and Pum2 – but not Stau2 – are essential to primary HSC functions *in vivo*.
A) Experimental pipeline using sensor-selected miR-E adapted shRNAs for downregulating gene expression in HSC-enriched $Lin^{-}CD150^{+}CD48^{-}$ populations for various functional assays. B) (*Left*) High level *Stau1* knockdown significantly compromises primary HSC repopulation activity *in vivo*; (*Centre*) *Stau2* knockdown does not compromise primary HSC repopulation *in vivo*; (*Right*) *Pum1* and *Pum2* are essential to primary HSC repopulation *in vivo*. C) Myeloid and lymphoid lineage percentages in primary recipient grafts at 16 week endpoints. D) Increased total myeloid progenitor outputs from $Lin^{-}CD150^{+}CD48^{-}$ populations with *Stau1* knockdown scored 10–14 days after plating. E) Downregulated *Stau1* in $Lin^{-}CD150^{+}CD48^{-}$ $ZsGreen^{+}$ cells results in an increased acquisition of lineage-positive markers at the end of a 7-day suspension culture F) with relatively decreased cell proliferation over a 10-day period.

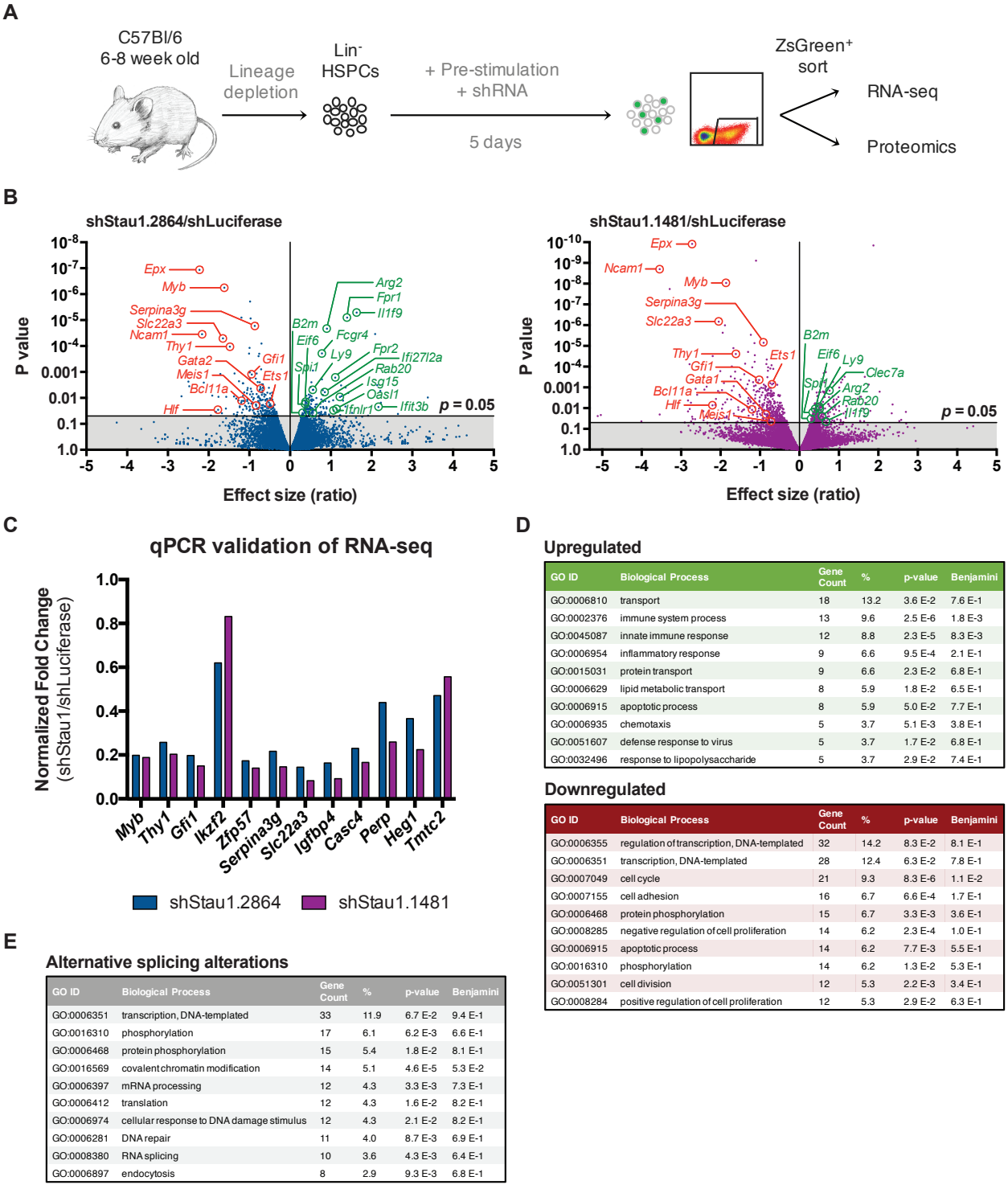

Figure 3: Downregulated *Stau1* compromises HSC-erythroid transcriptional networks and upregulates an immune/inflammatory response signature. A) Experimental schematic of *Stau1* knockdown prior to RNA-sequencing and mass spectrometry proteomic measurements. B) Volcano plot of gene expression changes derived from RNA-seq for shStau.2864 (*left*) and shStau1.1481 (*right*); sampling of differentially

expressed genes (DEGs) ($p < 0.05$) that are downregulated (*red*) or upregulated (*green*). C) qPCR validation of RNA-seq dataset with gene normalization to *Gapdh*. D) DAVID gene ontology (GO) analysis of top 10 biological processes enriched from upregulated (*top, green*) and downregulated (*bottom, red*) DEGs and E) for genes alternatively spliced (rMATS, FDR < 0.05) in shStau1.2864 samples.

A

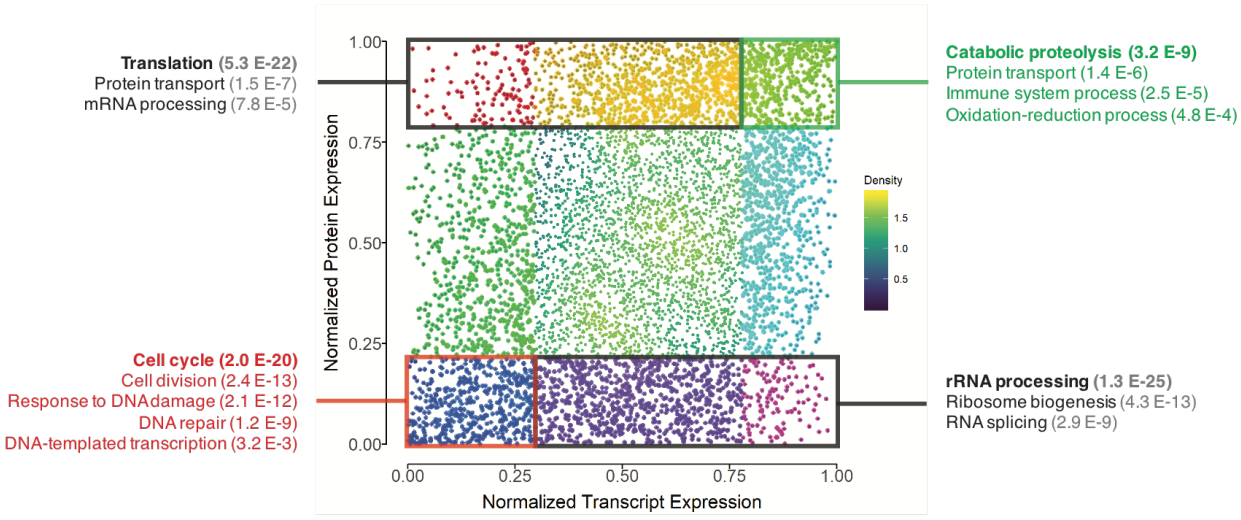

B

GO Biological Process	Genes post-transcriptionally upregulated with Stau1 downregulation
Translation	Eukaryotic translation factors (initiation, elongation, termination); mitochondrial ribosomal proteins; ribosomal proteins
Protein transport	Rab family members; adaptor complex subunits; sorting nexins
mRNA processing	RNA-binding proteins (including Adar; splicing factors)

GO Biological Process	Genes concordantly upregulated with Stau1 downregulation
Cell cycle and cell division	Cyclins, kinesins, kinases, minichromosome maintenance complex components, telomeric repeat binding factors
Response to DNA damage and DNA repair	Fanconi anemia genes, checkpoint and cohesin complex genes
DNA-templated transcription	Gata transcription factors, erythroid differentiation regulatory factor, histone deacetylases, lysine demethylases, zinc finger proteins

GO Biological Process	Genes concordantly upregulated with Stau1 downregulation
Catabolic proteolysis	Proteasome subunits, cathepsins
Protein transport	Rab family members; adaptor complex subunits; sorting nexins
Immune system process	Beta-2 microglobulin (B2m), histocompatibility complexes, interferon-induced proteins, toll-like receptors
Oxidation-reduction process	NADH dehydrogenase subcomplex units, cytochrome proteins, heme oxygenase, reductases

GO Biological Process	Genes post-transcriptionally downregulated with Stau1 downregulation
rRNA processing and ribosome biogenesis	DEAD box polypeptides, dyskeratosis congenita 1 (Dkc1), exosome components
RNA splicing	Splicing factors

Figure 4: The post-transcriptional regulatory axis of Stau1 strongly enriches for translation and ribosomal RNA processing pathways. A) Two-dimensional overlay of genes detected in both transcriptome (x-axis) and proteome (y-axis) datasets for ranked by level of normalized gene expression, representing low (closer to 0) to high (closer to 1) expressed genes in shStau1.2864 samples compared to shLuciferase controls; x and y Pearson correlation coefficient 0.26. Coloured divisions mark transition points at 1 standard deviation from the mean of each dataset within the overlay. Marked boxes represent relatively concordant upregulated (green), downregulated (red) and post-transcriptionally upregulated (top black) and downregulated (bottom black) genes annotated with top enriching gene ontology biological processes (Benjamini p-values shown). B) Sampling descriptions of genes within top enriching biological processes for each of the four quadrants.

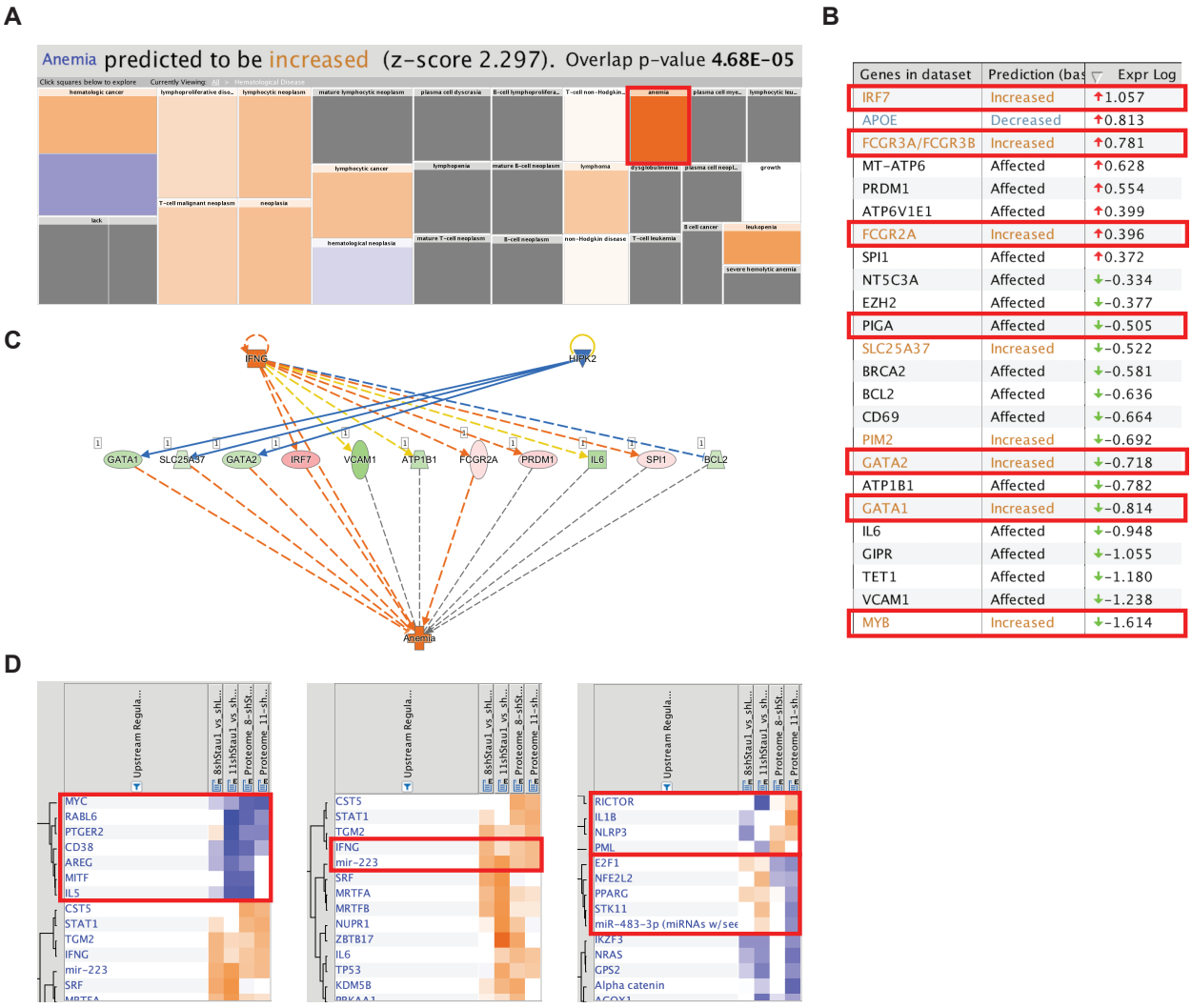

Figure 5: Stau1 downregulation elicits RNA and protein signatures consistent with immune- and inflammatory-associated anemias. A) Ingenuity pathway analysis (IPA) disease associations reveal "anemia" among top 5 global scoring entities and the first ranked association within "hematological disease" (dark orange) from significantly differentially expressed genes (non-adjusted p-value < 0.05) inputted from RNA-seq datasets (*z*-score 2.297; *p*-value 4.68E-05). B) Direction gene expression changes in RNA-seq dataset contributing to the predicted anemia signature. C) Predicted regulatory networks of activated IFN-γ (dark orange) and repressed Hipk2 (blue) upstream of directional gene expression changes reflective of predicted anemia (downregulated genes in shades of green, upregulated genes in shades of red). D) Combined IPA upstream regulator cross-analyses of both transcriptome (left two columns in each window display; 8-shStau1 = shStau.2864, 11-shStau1 = shStau.1481) and proteome DEGs (right two columns in each window display), non-supervised and hierarchically clustered, showing predicted regulators either downregulated (left window) or upregulated (middle window) at both levels, as well as those discordant between the transcriptome and proteome (right window).

References

1. Ariki R, Morikawa S, Mabuchi Y, Suzuki S, Nakatake M, Yoshioka K, et al. 2014. Homeodomain transcription factor Meis1 is a critical regulator of adult bone marrow hematopoieisis. *PLoS One*. 9:e87646.
2. Bagger FO, Sasivarevic D, Sohi SH, Laursen LG, Pundhir S, Sønderby CK, et al. 2016. BloodSpot: a database of gene expression profiles and transcriptional programs for healthy and malignant haematopoiesis. *Nucleic Acids Res*. 44:D917–24.
3. Bajaj J, Van Nostrand EL, Yeo GW, Reya T. 2017. Regulation of asymmetric division in myeloid leukemogenesis. *Blood*. 130(Suppl 1):46.
4. Becalska AN, Gavis ER. 2009. Lighting up mRNA localization in Drosophila oogenesis. *Development*. 136:2493–2503.
5. Bolger AM, Lohse M, Usadel B. 2014. Trimmomatic: a flexible trimmer for Illumina sequence data. *Bioinformatics*. 30:2114–2120.
6. Bonnet-Magnaval F, Philippe C, Van Den Berghe L, Prats H, Touriol C, Lacazette E. 2016. Hypoxia and ER stress promote Staufen1 expression through an alternative translation mechanism. *Biochem Biophys Res Commun*. 479:365–371.
7. Broadus J, Fuerstenberg S, Doe CQ. 1998. Staufen-dependent localization of prospero mRNA contributes to neuroblast daughter-cell fate. *Nature*. 391:792–795.
8. Cao L, Yang G, Gao S, Jing C, Montgomery RR, Yin Y, et al. 2019. HIPK2 is necessary for type I interferon-mediated antiviral immunity. *Sci Signal*. 12:eaau4604.
9. Chen J, Feng X, Desierto MJ, Keyvanfar K, Young NS. 2015. IFN-γ-mediated hematopoietic cell destruction in murine models of immune-mediated bone marrow failure. *Blood*. 126:2621–2631.
10. Cogswell JP, Cogswell PC, Kuehl WM, Cuddihy AM, Bender TM, Engelke U, et al. 1993. Mechanism of c-myc regulation by c-Myb in different cell lineages. *Mol Cell Biol*. 13:2858–2869.
11. Costello P, Sargent M, Maurice D, Esnault C, Foster K, Anjos-Afonso F, et al. 2015. MRTF-SRF signaling is required for seeding of HSC/Ps in bone marrow during development. *Blood*. 125:1244–1255.
12. Cutler C, Multani P, Robbins D, Kim HT, Le T, Hoggatt J, et al. 2013. Prostaglandin-modulated umbilical cord blood hematopoietic stem cell transplantation. *Blood*. 122:3074–3081.
13. de Bruin AM, Demirel Ö, Hooibrink B, Brandts CH, Nolte MA. 2013. Interferon-γ impairs proliferation of hematopoietic stem cells in mice. *Blood*. 121:3578–3585.

14. Dennis G Jr, Sherman BT, Hosack DA, Yang J, Gao W, Lane HC, et al. 2003. DAVID: Database for annotation, visualization, and integrated discovery. *Genome Biol*. 4:P3.
15. Dobin A, Davis CA, Schlesinger F, Drenkow J, Zaleski C, Jha S, et al. 2013. STAR: ultrafast universal RNA-seq aligner. *Bioinformatics*. 29:15–21
16. Dugré-Brisson S, Elvira G, Boulay K, Chatel-Chaix L, Mouland AJ, DesGroseillers L. 2005. Interaction of Staufen1 with the 5' end of mRNA facilitates translation of these RNAs. *Nucleic Acids Res*. 33:4797–4812.
17. Elbarbary RA, Li W, Tian B, Maquat LE. 2013. STAU1 binding 3'UTR IRAlus complements nuclear retention to protect cells from PKR-mediated translational shutdown. *Genes Dev*. 27:1495–1510.
18. Felli N, Pedini F, Romania P, Biffoni M, Morsilli O, Castelli G, et al. 2009. MicroRNA 223-dependent expression of LMO2 regulates normal erythropoiesis. *Haematologica*. 94:479–486.
19. Goldstein O, Meyer K, Greenshpan Y, Bujanover N, Feigin M, Ner-Gaon H, et al. 2017. Mapping whole-transcriptome splicing in mouse hematopoietic stem cells. *Stem Cell Reports*. 8:163–176.
20. Gong C, Tang Y, Maquat LE. 2013. mRNA-mRNA duplexes that autoelicit Staufen1–mediated mRNA decay. *Nat Struct Mol Biol*. 20:1214–1220.
21. Hock H, Hamblen MJ, Rooke HM, Schindler JW, Saleque S, Fujiwara Y, et al. 2004. Gfi-1 restricts proliferation and preserves functional integrity of haematopoietic stem cells. *Nature*. 431:1002–1007.
22. Hoggatt J, Singh P, Sampath J, Pelus LM. 2009. Prostaglandin E2 enhances hematopoietic stem cell homing, survival, and proliferation. *Blood*. 113:5444–5455.
23. Hope KJ, Cellot S, Ting SB, MacRae T, Mayotte N, Iscove NN, et al. 2010. An RNAi screen identifies Msi2 and Prox1 as having opposite roles in the regulation of hematopoietic stem cell activity. *Cell Stem Cell*. 7:101–113.
24. Jambor H, Surendranath V, Kalinka AT, Mejstrik P, Saalfeld S, Tomancak P. 2015. Systematic imaging reveals features and changing localization of mRNAs in Drosophila development. *eLife*. 4:e05003.
25. Jeong K, Ryu I, Park J, Hwang HJ, Ha H, Park Y, et al. 2019. Staufen1 and UPF1 exert opposite actions on the replacement of the nuclear cap-binding complex by eIF4E at the 5' end of mRNAs. *Nucleic Acids Res*. 47:9313–9328.
26. Kim YK, Furic L, Desgroseillers L, Maquat LE. 2005. Mammalian Staufen1 recruits Upf1 to specific mRNA 3'UTRs so as to elicit mRNA decay. *Cell*. 120:195–208.
27. King ML, Messitt TJ, Mowry KL. 2005. Putting RNAs in the right place at the right time: RNA localization in the frog oocyte. *Biol Cell*. 97:19–33.

28. Kocabas F, Zheng J, Thet S, Copeland NG, Jenkins NA, DeBerardinis RJ, et al. 2012. Meis1 regulates the metabolic phenotype and oxidant defense of hematopoietic stem cells. *Blood*. 120:4963–72.
29. Komorowska K, Doyle A, Wahlestedt M, Subramaniam A, Debnath S, Chen J, et al. 2017. Hepatic leukemia factor maintains quiescence of hematopoietic stem cells and protects the stem cell pool during regeneration. *Cell Rep*. 21:3514–3523.
30. Krämer A, Green J, Pollard J Jr, Tugendreich S. 2014. Causal analysis approaches in Ingenuity Pathway Analysis. *Bioinformatics*. 30:523–530.
31. Kumar A, Lee CM, Reddy EP. 2003. c-Myc is essential but not sufficient for c-Myb-mediated block of granulocytic differentiation. *J Biol Chem*. 278:11480–11488.
32. Kusek G, Campbell M, Doyle F, Tenenbaum SA, Kiebler M, Temple S. 2012. Asymmetric segregation of the double-stranded RNA binding protein Staufen2 during mammalian neural stem cell divisions promotes lineage progression. *Cell Stem Cell*. 11:505–516.
33. Lee JM, Chan K, Kan YW, Johnson JA. 2004. Targeted disruption of Nrf2 causes regenerative immune-mediated hemolytic anemia. *Proc Natl Acad Sci U S A*. 101:9751–9756.
34. Li B, Dewey CN. 2011. RSEM: accurate transcript quantification from RNA-Seq data with or without a reference genome. *BMC Bioinformatics*. 12:323.
35. Li FX, Zhu JW, Hogan CJ, DeGregori J. 2003. Defective gene expression, S phase progression, and maturation during hematopoiesis in E2F1/E2F2 mutant mice. *Mol Cell Biol*. 23:3607–3622.
36. Li P, Yang X, Wasser M, Cai Y, Chia W. 1997. Inscuteable and Staufen mediate asymmetric localization and segregation of prospero RNA during Drosophila neuroblast cell divisions. *Cell*. 90:437–447.
37. Lieu YK, Reddy EP. 2009. Conditional c-myb knockout in adult hematopoietic stem cells leads to loss of self-renewal due to impaired proliferation and accelerated differentiation. *Proc Natl Acad Sci U S A*. 106:21689–21694.
38. Lin FC, Karwan M, Saleh B, Hodge DL, Chan T, Boelte KC, et al. 2014. IFN-γ causes aplastic anemia by altering hematopoietic stem/progenitor cell composition and disrupting lineage differentiation. *Blood*. 124:3699–3708.
39. Love MI, Huber W, Anders S. 2014. Moderated estimation of fold change and dispersion for RNA-seq data with DESeq2. *Genome Biol*. 15:550.
40. Luc S, Huang J, McEldoon JL, Somuncular E, Li D, Rhodes C, et al. 2016. Bcl11a deficiency leads to hematopoietic stem cell defects with an aging-like phenotype. *Cell Rep*. 16:3181–3194.

41. Lucas BA, Lavi E, Shiue L, Cho H, Katzman S, Miyoshi K, et al. 2018. Evidence for convergent evolution of SINE-directed Staufen-mediated mRNA decay. *Proc Natl Acad Sci U S A*. 115:968–973.
42. Lécuyer E, Yoshida H, Parthasarathy N, Alm C, Babak T, Cerovina T, et al. 2007. Global analysis of mRNA localization reveals a prominent role in organizing cellular architecture and function. *Cell*. 131:174–187.
43. Menendez-Gonzalez JB, Vukovic M, Abdelfattah A, Saleh L, Almotiri A, Thomas LA, et al. 2019. Gata2 as a crucial regulator of stem cells in adult hematopoiesis and acute myeloid leukemia. *Stem Cell Reports*. 13:291–306.
44. Miller ME, Rosten P, Lemieux ME, Lai C, Humphries RK. 2016. Meis1 is required for adult mouse erythropoiesis, megakaryopoiesis and hematopoietic stem cell expansion. *PLoS One*. 11:e0151584.
45. Moon BS, Bai J, Cai M, Liu C, Shi J, Lu W. 2018. Kruppel-like factor 4-dependent Staufen1-mediated mRNA decay regulates cortical neurogenesis. *Nat Commun*. 9:401.
46. Mucenski ML, McLain K, Kier AB, Swerdlow SH, Schreiner CM, Miller TA, et al. 1991. A functional c-myb gene is required for normal murine fetal hepatic hematopoiesis. *Cell*. 65:677–689.
47. Naudin C, Hattabi A, Michelet F, Miri-Nezhad A, Benyoucef A, Pflumio F, et al. 2017. PUMILIO/FOXP1 signaling drives expansion of hematopoietic stem/progenitor and leukemia cells. *Blood*. 129:2493–2506.
48. Park E, Gleghorn ML, Maquat LE. 2013. Staufen2 functions in Staufen1-mediated mRNA decay by binding to itself and its paralog and promoting UPF1 helicase but not ATPase activity. *Proc Natl Acad Sci U S A*. 110:405–412.
49. Park E, Maquat LE. 2013. Staufen-mediated mRNA decay. *Wiley Interdiscip Rev RNA*. 4:423–435.
50. Ragu C, Elain G, Mylonas E, Ottolenghi C, Cagnard N, Daegelen D, et al. 2010. The transcription factor Srf regulates hematopoietic stem cell adhesion. *Blood*. 116:4464–4473.
51. Ravel-Chapuis A, Bélanger G, Yadava RS, Mahadevan MS, DesGroseillers L, Côté J, et al. 2012. The RNA-binding protein Staufen1 is increased in DM1 skeletal muscle and promotes alternative pre-mRNA splicing. *J Cell Biol*. 196:699–712.
52. Ravel-Chapuis A, Klein Gunnewiek A, Bélanger G, Crawford Parks TE, Côté J, Jasmin BJ. 2016. Staufen1 impairs stress granule formation in skeletal muscle cells from myotonic dystrophy type 1 patients. *Mol Biol Cell*. 27:1728–1739.
53. Ricci EP, Kucukural A, Cenik C, Mercier BC, Singh G, Heyer EE, et al. 2014. Staufen1 senses overall transcript secondary structure to regulate translation. *Nat Struct Mol Biol*. 21:26–35.

54. Sakurai M, Shiromoto Y, Ota H, Song C, Kossenkov AV, Wickramasinghe J, et al. 2017. ADAR1 controls apoptosis of stressed cells by inhibiting Staufen-1-mediated mRNA decay. *Nat Struct Mol Biol*. 24:534–543.
55. Schwartz SP, Aisenthal L, Elisha Z, Oberman F, Yisraeli JK. 1992. A 69-kDa RNA-binding protein from Xenopus oocytes recognizes a common motif in two vegetally localized maternal mRNAs. *Proc Natl Acad Sci U S A*. 89:11895–11899.
56. Shen S, Park JW, Lu ZX, Lin L, Henry MD, Wu YN, et al. 2014. rMATS: robust and flexible detection of differential alternative splicing from replicate RNA-Seq data. *Proc Natl Acad Sci U S A*. 111:E5593–5601.
57. Sloand E, Kim S, Maciejewski JP, Tisdale J, Follmann D, Young NS. 2002. Intracellular interferon-gamma in circulating and marrow T cells detected by flow cytometry and the response to immunosuppressive therapy in patients with aplastic anemia. *Blood*. 100:1185–1191.
58. Solomou EE, Keyvanfar K, Young NS. 2006. T-bet, a Th1 transcription factor, is up-regulated in T cells from patients with aplastic anemia. *Blood*. 107:3983–3991.
59. St Johnston D, Beuchle D, Nüsselein-Volhard C. 1991. Staufen, a gene required to localize maternal RNAs in the Drosophila egg. *Cell*. 66:51–63.
60. St Johnston D, Beuchle D, Nüsselein-Volhard C. 1991. Staufen, a gene required to localize maternal RNAs in the Drosophila egg. *Cell*. 66:51–63.
61. Sugimoto Y, Vigilante A, Darbo E, Zirra A, Militti C, D'Ambrogio A, et al. 2015. hiCLIP reveals the *in vivo* atlas of mRNA secondary structures recognized by Staufen 1. *Nature*. 519:491–494.
62. Takeda J, Miyata T, Kawagoe K, Iida Y, Endo Y, Fujita T, et al. 1993. Deficiency of the GPI anchor caused by a somatic mutation of the PIG-A gene in paroxysmal nocturnal hemoglobinuria. *Cell*. 73:703–711.
63. Thomas MG, Martinez Tosar LJ, Desbats MA, Leishman CC, Boccaccio GL. 2009. Mammalian Staufen 1 is recruited to stress granules and impairs their assembly. *J Cell Sci*. 122:563–573.
64. Unnisa Z, Clark JP, Roychoudhury J, Thomas E, Tessarollo L, Copeland NG, et al. 2012. Meis1 preserves hematopoietic stem cells in mice by limiting oxidative stress. *Blood*. 120:4973–4981.
65. Vessey JP, Amadei G, Burns SE, Kiebler MA, Kaplan DR, Miller FD. 2012. An asymmetrically localized Staufen2-dependent RNA complex regulates maintenance of mammalian neural stem cells. *Cell Stem Cell*. 11:517–528.

66. Vessey JP, Macchi P, Stein JM, Mikl M, Hawker KN, Vogelsang P, et al. 2008. A loss of function allele for murine Staufen1 leads to impairment of dendritic Staufen1-RNP delivery and dendritic spine morphogenesis. *Proc Natl Acad Sci U S A*. 105:16374–16379.
67. Wang C, Xu CX, Alippe Y, Qu C, Xiao J, Schipani E, et al. 2017. Chronic inflammation triggered by the NLRP3 inflammasome in myeloid cells promotes growth plate dysplasia by mesenchymal cells. *Sci Rep*. 7:4880.
68. Wilk R, Hu J, Blotsky D, Krause HM. 2016. Diverse and pervasive subcellular distributions for both coding and long noncoding RNAs. *Genes Dev*. 30:594–609.
69. Wreden C, Verrotti AC, Schisa JA, Lieberfarb ME, Strickland S. 1997. Nanos and pumilio establish embryonic polarity in Drosophila by promoting posterior deadenylation of hunchback mRNA. *Development*. 124:3015–3023.
70. Yang CC, Chen YT, Chang YF, Liu H, Kuo YP, Shih CT, et al. 2017. ADAR1-mediated 3' UTR editing and expression control of antiapoptosis genes fine-tunes cellular apoptosis response. *Cell Death Dis*. 8:e2833.
71. Zeng H, Yücel R, Kosan C, Klein-Hitpass L, Möröy T. 2004. Transcription factor Gfi1 regulates self-renewal and engraftment of hematopoietic stem cells. *EMBO J*. 23:4116–4125.
72. Zeng W, Chen G, Kajigaya S, Nunez O, Charrow A, Billings EM, et al. 2004. Gene expression profiling in CD34 cells to identify differences between aplastic anemia patients and healthy volunteers. *Blood*. 103:325–332.
73. Zoumbos NC, Gascón P, Djeu JY, Trost SR, Young NS. 1985. Circulating activated suppressor T lymphocytes in aplastic anemia. *N Engl J Med*. 312:257–265.

Chapter 4: Post-transcriptional regulation in hematopoiesis: RNA binding proteins take control

Laura P.M.H. de Rooij,[1]* Derek C.H. Chan,[1]* Ava Keyvani Chahi,[1]* and Kristin J. Hope[1]

*These authors contributed equally to this work.

[1]Department of Biochemistry and Biomedical Sciences, Stem Cell and Cancer Research Institute, McMaster University, Hamilton, ON L8S 4K1, Canada.

Abstract

Normal hematopoiesis is sustained through a carefully orchestrated balance between hematopoietic stem cell (HSC) self-renewal and differentiation. The functional importance of this axis is underscored by the severity of disease phenotypes initiated by abnormal HSC function, including myelodysplastic syndromes and hematopoietic malignancies. Major advances in the understanding of transcriptional regulation of primitive hematopoietic cells have been achieved; however, the post-transcriptional regulatory layer that may impinge on their behavior remains underexplored by comparison. Key players at this level include RNA-binding proteins (RBPs), which execute precise and highly coordinated control of gene expression through modulation of RNA properties that include its splicing, polyadenylation, localization, degradation, or translation. With the recent identification of RBPs having essential roles in regulating proliferation and cell fate decisions in other systems, there has been an increasing appreciation of the importance of post-transcriptional control at the stem cell level. Here we discuss our current understanding of RBP-driven post-transcriptional regulation in HSCs, its implications for normal, perturbed, and malignant hematopoiesis, and the most recent technological innovations aimed at RBP–RNA network characterization at the systems level. Emerging evidence highlights RBP-driven control as an underappreciated feature of primitive hematopoiesis, the greater understanding of which has important clinical implications.

Introduction

The machinery underlying stem cells' capacity to orchestrate their self-maintenance and differentiation can be represented as integrated circuits that are genetically programmed. As demonstrated by the capacity to reprogram somatic cells to pluripotency using only four key transcription factors (Takahashi and Yamanaka 2006), identification of master regulators that control critical nodes of this circuitry offers incredible opportunities to engineer cell types of interest or to reign in aberrantly renewing cancer stem cells. Of note, later work shed light on the contribution of post-transcriptional regulators to cell fate determination with the demonstration that the RNA-binding protein (RBP) Lin28 can function as a reprogramming factor in combination with the core NANOG, OCT-4, and SOX2 transcription factors (Yu et al. 2007).

The specialized multipotent nature of hematopoietic stem cells (HSCs) and their need to rapidly alter cell fate decisions to buffer the hematopoietic system in response to external cues suggests that they are likely subject to precise regulation at multiple levels. Although a wealth of research has revealed the crucial importance of transcriptional regulation in governing HSC activity (Nerlov et al. 2000; Wilson et al. 2010), HSCs are also subject to an additional critical layer of post-transcriptional control. This "RNA centric" level of regulation offers cells a way to precisely and rapidly fine-tune protein expression by modulating mRNA splicing, localization, degradation, or translation (Grech and von Lindern 2012). Key players in this level of regulation include RBPs, which achieve their function through integration with the existing transcriptional networks in the cell (Yuan and Muljo 2013). Based on RNA sequence and structure recognition, RBPs interact with their target mRNAs in RNPs to strongly influence their downstream processing. Similar to the ability of transcription factors to impact on many targets, unique RBPs can link the fates of

many mRNAs through synchronous regulation within so-called RNA operons (Keene and Tenenbaum 2002). The coordinated interplay of functionally connected RNA operons through "post-transcriptional RNA regulons" ensures a highly efficient cellular response to endogenous and environmental stimuli (Keene 2007). Post-transcriptional regulation is emerging as a vital mechanism for governing complex genetic networks and establishing cellular diversity, and more recently, light has been shed on the role of RBPs in stem cell biology specifically (Sampath et al. 2008; Anokye-Danso et al. 2011; Voronina et al. 2011). With respect to HSC control, microRNAs, also key in enacting post-transcriptional control, have been the subject of significant recent efforts. The potential of RBP–mRNA-directed post-transcriptional mechanisms functioning in primitive blood cell homeostasis, however, has been comparatively understudied. This review will outline our current understanding of the functional role played by mRNA regulating RBPs in controlling the biology of primitive hematopoietic cells in normal, perturbed, and malignant settings (see Table 1 for a list of RBPs with roles in these contexts). Finally, with an effort to detail approaches key for dissecting the systems-level mechanics of RBP action in these rare cells, we briefly discuss recent technical advances facilitating the characterization of RBP–mRNA interactomes and global outcomes for targeted RNAs.

Understanding the function of RBPs in hematopoietic stem and progenitor cells (HSPCs)

The mRNA life cycle proceeds through a series of steps within the cell. At each point, a given transcript is subject to a unique set of interactions with RBPs that may serve to modify it, alter its localization, and influence how and when it will be translated into protein. RBP-directed control of HSPCs is an emerging field. Indeed, there is a developing understanding that RBPs can influence stemness properties in these cells by impinging on mRNAs at many of the various points

of their life cycle. Below we provide key examples of some of these known HSPC regulators and detail how they operate at different levels of mRNA metabolism to enforce their effects.

RBP-directed control of HSC fate regulation via regulated mRNA splicing

Once generated in the nucleus, the splicing of mRNA transcripts is subject to regulation by RBPs. Enforcement of specific alternative splicing outputs mediated by key spliceosomal RBPs represents an important regulatory mechanism in primitive hematopoietic cells. For example, the RBP Rbm15 mediates splicing of the truncated form of the c-Mpl receptor. In turn, this influences the degree of thrombopoietin signaling and subsequent balancing of HSC quiescence and proliferation (Xiao et al. 2015). Conditional knockout mouse models of the RBP Srsf2 have also demonstrated the essentiality of certain splicing factors to HSPC populations. In these cases, decreased HSC numbers and compromised hematopoietic reconstitution upon transplantation were observed upon Srsf2 depletion (Komeno et al. 2015). Subsequent analyses demonstrated that mutant Srsf2 yielded widespread alternative splicing effects, a common set of which was shared in the Srsf2 knockdown scenario and which coalesced on gene targets that specifically associated with cancer development and apoptosis (Kim et al. 2015; Komeno et al. 2015).

Insights into splicing control have also translated into a better understanding of hematological abnormalities in humans, with the recognition that spliceosomal RBPs act as drivers of clonal hematopoiesis in older individuals (McKerrell et al. 2015). Further experimental modeling approaches have shown that in these scenarios, mutations in SF3B1, another RBP with essential roles in the HSC compartment, likely arise within HSPC subsets (Mian et al. 2015; Mortera-Blanco et al. 2017). RNA sequencing analyses show that SF3B1 mutations globally disrupt splicing

patterns with aberrant 3' splice site recognition (Obeng et al. 2016; Mupo et al. 2017). This enforces a state that recapitulates many aspects of myelodysplastic syndromes (MDS), such as impaired erythropoiesis and expansion of the HSC pool. Similarly, Kim and colleagues overlapped RNA sequencing profiles of wildtype and various mutant SRSF2-expressing backgrounds and conducted motif identification and structural analysis to demonstrate that MDS-related SRSF2 mutations result in an altered RNA-binding profile rather than a loss of normal splice site recognition activity (Kim et al. 2015).

RBPs that edit, modify, or alter transcript integrity to influence HSPC function

Throughout their life cycle, mRNAs can be subject to a variety of different modifications, sequence changes, or alterations to their stability. In primitive hematopoietic cells, RBPs appear to play an important functional role in regulating transcript outcomes in HSPCs. For example, RNA editing activity by the double-stranded RBP Adar1, which mediates adenosine-to-inosine editing of primary transcripts, has been shown through knockout mouse models to be critical for the capacity of HSCs to derive downstream progenitors (Hartner et al. 2009; XuFeng et al. 2009). Intriguingly, global gene expression profiling of Adar1 deficient mouse HSPCs revealed a significant elevation in the expression of genes known to be induced by interferon as well as a host of genes that are interferon regulatory factors. Thus, Adar1 may represent a critical suppressor of HSPC-specific loss in response to interferon activation stimulated by chronic infection or other stress-inducing disease conditions.

RNA decay and stability in HSPCs can also be directly regulated by RBPs. Weischenfeldt and colleagues, for example, conditionally deleted Upf2 within the hematopoietic system

(Weischenfeldt et al. 2008). Upf2 is a core component of the nonsense-mediated decay RNA surveillance pathway that recognizes mRNAs with premature termination codons and targets them for degradation. In this study, it was found that acute UPF2 loss mediated by Mx1-Cre deletion leads to a rapid reduction in the number of HSPCs, which the authors speculated could be due to HSPC exhaustion or clearance by apoptosis (Weischenfeldt et al. 2008). Microarray-based gene expression profiling identified intriguing expression changes including derepression of several snoRNAs and premature termination codon containing alternative splice forms; however, the extent to which these changes contributed to the pronounced HSPC defects remains to be elucidated.

Finally, Naudin et al. took advantage of knockout mouse models and experiments with human hematopoietic cells and demonstrated that PUM1 and PUM2, both members of the PUF family of RBPs, are each independently essential for HSPC growth (Naudin et al. 2017). Using a proteomics approach, the authors identified a significant decrease in expression of the FOXP1 transcription factor when PUM1 or PUM2 was repressed in either the primitive mouse or human hematopoietic context. FOXP1 loss was shown by the authors to phenocopy that of PUM1/2 knockout, indicating that it likely represents one of the major targets underlying their effects. In deciphering the post-transcriptional mechanism at play, it was found that PUM1 and PUM2 bind and promote the stability and/or translation of FOXP1.

RBP-influenced control of translation in HSPC fate regulation

When bound to the untranslated regions of mRNAs, RBPs often function to either promote or repress protein translation of their targeted transcripts. Recent work highlights the RBP Musashi-

2 (MSI2), implicated in other nonhematopoietic cell types as a repressor of translation, as an important determinant of HSC self-renewal, cell fate, and lineage bias. Using a Msi2 conditional knockout mouse, Park et al. assayed differential gene expression in HSPCs upon conditional hematopoietic Msi2 deletion and showed particular modulatory effects at various nodes of the TGF- signaling pathway (Park et al. 2014). In the human system, Rentas et al. overexpressed MSI2 and integrated both transcriptome and global MSI2–RNA interaction data to link its translational repression of aryl hydrocarbon receptor pathway targets to aspects of MSI2-induced HSC expansion *ex vivo* (Rentas et al. 2016).

Renewed interest in the field of epitranscriptomics has also resulted in the identification of the N6-methyladenosine (m6A) forming RBP METTL3 as a critical regulator of human HSPCs (Vu et al. 2017a). When knocked down, METTL3 drives HSC differentiation and reduced proliferation, while when overexpressed, it promotes their growth. By coupling RNA sequencing based methods with ribosome profiling, it has been possible to map the m6A-modified transcripts to those that similarly show an enhanced level of translation. Key target genes included C-MYC, BCL2, and PTEN (Vu et al. 2017a).

Influence of the translational machinery on HSPC homeostasis

The ribosome is itself an RBP complex that when dysregulated can cause productivity defects among HSPCs that underlie some of the key features of various bone marrow failures. In certain cases like 5q− syndrome, a subtype of MDS characterized by ineffective hematopoiesis due to mutations incurred in HSCs, RPS14 loss-of-function defects compromise 18S rRNA processing (Ebert et al. 2008). Similarly, in Schwachman–Diamond syndrome, where neutropenia and

defects in erythroid cell production are characteristic, mutations in the ribosome biogenesis Shwachman–Bodian–Diamond syndrome protein result in dysregulated 60S subunit biogenesis and impaired ribosome assembly (Ganapathi et al. 2007; Wong et al. 2011). Defects in dyskeratosis congenita are also caused by mutations in the RBP DKC1 that affect H/ACA RNP-mediated rRNA pseudouridylation in HSCs (Bellodi et al. 2013).

Altogether, the above studies highlight many key RBP functions that post-transcriptionally regulate normal hematopoiesis. These studies also provide insights into the global changes that occur at the levels of both the transcriptome and proteome in response to alterations in the levels of expression and/or mutations of various RBPs. Related recent efforts have integrated global transcriptome, proteome, and DNA methylome data of purified primitive HSPC subsets in the mouse system (Cabezas-Wallscheid et al. 2014). This resource provides a valuable platform from which to analyze correlative and discordant gene expression levels that will likely inform future studies of post-transcriptional regulation in the hematopoietic system.

The importance of RBPs and RBP–interactomes in leukemia

Leukemia stem cells and the hierarchical organization of malignant hematopoiesis

Given the complex interplay between transcriptional and post-transcriptional mechanisms regulating the self-renewal and differentiation axis in normal HSCs, dysregulation of these mechanisms has the potential to result in leukemic transformation, leading to the genesis of leukemic stem cells (LSCs). By means of alterations in their self-renewal capacities, LSCs drive leukemic maintenance, chemoresistance, and relapse and are implicated in the low overall survival

rates observed for leukemia patients (Lapidot et al. 1994; Shlush et al. 2017). Evidence has highlighted the potential of HSCs or early myeloid progenitors to function as the cell of origin for leukemia (Miyamoto et al. 2000; Jamieson et al. 2004; Abrahamsson et al. 2009; Jan et al. 2012; Krivtsov et al. 2013; Shlush et al. 2014). As such, the networks and signaling pathways regulating HSPC self-renewal and differentiation might also be essential for their transformation into LSCs. Given the key role of RBP-directed posttranscriptional regulation for HSPC fates as described above, RBPs represent interesting candidate drivers of leukemic transformation. Although thus far relatively understudied, a handful of RBPs and the networks they regulate have indeed been found associated with the stem cell compartment of leukemia.

LSC dependencies on RBP-directed post-transcriptional regulatory networks

LSC-related gene expression signatures strongly correlate with an overall poor prognosis in acute myeloid leukemia (AML) patients (Gentles et al. 2010; Eppert et al. 2011; Ng et al. 2016). However, integrative analyses at multiple regulatory levels to connect LSC-specific transcriptional signatures with their corresponding translatome, for example, could reveal more complete insights into the exact regulators of LSC biology and the central networks involved. A handful of recent studies are pioneering the start of a more multilevel approach of characterizing LSCs. Interestingly, these studies collectively hint towards a highly specific dependence of LSCs on post-transcriptional regulatory processes. For instance, in AML, a role for snoRNAs, which catalyze RNA base modifications, was ultimately uncovered by integrative profile analysis of RNA transcript expression, rRNA pseudouridylation, rRNA methylation, and RNA–protein interactions. Here, snoRNA/RNP formation was found to be regulated by the RBP DDX21 as an essential pathway for self-renewal in AML1–ETO-driven leukemogenesis and AML clonogenicity

(Zhou et al. 2017). Similarly, a multilevel comparative analysis of treatment naïve chronic myeloid leukemia (CML) and normal $CD34^+$ cells identified TP53 and C-MYC as central nodes in an LSC-enriched CML network that is comprised of 30 proteins, indicating a potential differential dependency of CML LSCs on this network (Abraham et al. 2016). Interestingly, 15% of this network is comprised of RBPs, which further suggests an important role for RBP-directed post-transcriptional regulation within this system. Below we present several from amongst only a handful of bona fide RBP regulators of leukemia transformation and LSCs and their defined molecular pathways of action. Together with the above-mentioned studies, these findings hint at the potential for an underappreciated role of RBP-driven post-transcriptional regulation for LSC function. Unraveling novel key RBP-directed networks in LSCs may therefore improve our abilities to selectively study and target this leukemic population in the future.

RBPs that function as master regulators of LSCs and leukemic transformation

The MSI2 RBP has been shown to have prognostic relevance in various solid cancers. In addition, its overexpression strongly associates with poor prognosis in acute and chronic leukemias (Ito et al. 2010; Kharas et al. 2010; Mu et al. 2013). Various mechanisms have been proposed to explain the important role that MSI2 plays in leukemia and its stem cell compartment. Through RNA sequencing and RNA immunoprecipitation in AML and CML cell lines, Hattori and colleagues described a direct interaction of MSI2 with FLT3, a receptor tyrosine kinase frequently altered in AML (Hattori et al. 2017). While genetic loss of MSI2 led to a downregulation of FTL3 protein and impairments in leukemic growth, binding of MSI2 was predicted to stabilize FLT3 transcripts, providing evidence for post-transcriptional regulation as a mechanism contributing to leukemogenesis. Comparative analysis of gene expression signatures from LSCs derived from

Msi2-deficient CML and MLL–AF9-driven mouse leukemias revealed that this RBP regulates a large fraction of genes belonging to pathways involved in cell differentiation and apoptosis (Kwon et al. 2015). The analysis also revealed the Msi2 target Tspan3 as a key gene involved in self-renewal of LSCs in murine leukemias and required for propagation of human AML in xenograft assays. In addition, high-throughput sequencing and cross-linking immunoprecipitation experiments in K562 cells revealed that MSI2 directly interacts with targets involved in pathways associated with an MLL–AF9-driven self-renewal gene expression signature shared between leukemic progenitors and HSCs (Park et al. 2015).

A screening effort focusing on MSI2 interacting proteins identified SYNCRIP as another RBP selectively essential for the stem cell compartment of leukemia (Vu et al. 2017b). In murine leukemia models, depletion of Syncrip resulted in reduced colony formation, increased differentiation, and impairment of *in vivo* engraftment, whereas normal HSPCs were unaffected. Mechanistically, Syncrip was shown to post-transcriptionally maintain steady-state levels of the oncogenic transcription factor Hoxa9, partially explaining its relevance for leukemia. Collectively, these results indicate that the MSI2-driven post-transcriptional regulatory network might play a major role in malignant HSCs, paving the way for novel therapeutic strategies aimed at selective eradication of LSCs.

Besides MSI2 and its interacting partners, a handful of other RBPs have been identified as important putative regulators of LSCs. For example, the methyltransferase METTL14, which catalyzes the m6A modification of target mRNAs, is elevated in expression in human AML relative to normal bone marrow. METTL4 depletion in the leukemic scenario leads to cell differentiation and death, a reduced capacity to propagate the disease *in vivo*, and a loss of LSC function (Weng

et al. 2018). Global mapping of METTL14-mediated m6A marks showed that it is through this modification on target transcripts including MYC and MYB that METTL14 achieves a heightened translation of these factors, which directly contributes to its proleukemic effects.

Targeted inhibition of RBPs for selective eradication of LSCs in leukemia patients

Whereas the therapeutic relevance of RBP networks may not have been extensively studied in the context of LSCs, individual RBPs have been associated with poor clinical outcome in leukemias (Byers et al. 2011; Kechavarzi and Janga 2014; Pan et al. 2017). Although there are few examples, small molecule inhibitors specifically targeting RBPs have successfully entered clinical studies, suggesting that the networks regulated by these RBPs might play an essential and targetable role in cancer maintenance and progression. For instance, altered EIF4E-dependent nuclear export of transcripts was shown to contribute to leukemogenesis, partially by blocking myeloid differentiation (Topisirovic et al. 2003). By inhibiting the mRNA export and translation functions of the protein, the EIF4E inhibitor ribavirin was shown to result in cytoplasmic relocalization of the protein and remissions in poor-prognosis AML patients with increased EIF4E levels. Patients resistant to ribavirin retained EIF4E in the nucleus, indicating a correlation of disease progression and the mRNA export function of EIF4E in leukemia (Assouline et al. 2009). Interestingly, preclinical studies suggest a cooperative effect of ribavirin with several established AML therapies including cytarabine, which is now being tested in Phase I/II clinical trials (Assouline et al. 2015).

Increased expression of the nuclear exporter CRM1/XPO1, which has protein-binding propensities in addition to validated mRNA binding capacity, has been reported in hematopoietic malignancies (Walker et al. 2013). In these cases, dysregulations in the nuclear export of certain

proteins and RNAs have strong oncogenic effects that contribute to poor prognosis and resistance to therapy (Kojima et al. 2013). A first-generation compound, selinexor, which inhibits the interaction of CRM1 with its cargo, thereby inhibiting nuclear export, is currently being tested in several Phase I/II clinical trials for AML and MDS (Savona et al. 2013; Fiedler et al. 2015; Garzon et al. 2017). Disease remissions in patients with chemoresistant or relapsed AML upon treatment with selinexor alone or in combination with chemotherapy have been reported; however, severe side effects have limited the maximum tolerated dose and therefore efficacy of this inhibitor in patients (Hing et al. 2016). A second-generation CRM1 inhibitor, KPT-8602, was recently developed and tested in xenograft models of high-risk human AML. These studies reported a high efficacy in targeting bulk leukemic cells as well as the more stem-like leukemia-initiating cells. Importantly, normal HSPCs were minimally affected upon treatment, which could support usage of this therapy as one that could avoid the toxic side effects of treatment on normal hematopoiesis (Etchin et al. 2017). Altogether, these findings strengthen the idea of specific dependencies of LSCs on RBP-directed post-transcriptional programs and provide a good rationale to pursue the clinical testing of high-confidence RBPs as targets for LSC-focused therapeutic strategies.

Therapy-induced activation of RBP-directed networks

Resistance to common chemotherapeutic regimens is one of the main features that distinguish LSCs from their bulk leukemic counterparts, yet the underlying mechanism remains to be identified. Studies centering around targeted treatment of BCR–ABL-driven CML with imatinib indeed hint towards interesting associations between RBPs and treatment response. The BCR–ABL oncogenic fusion gene has been shown to alter the expression and activity of the RBPs La/SSB, multiple hnRNPs, TLS/FUS, and the pathways they regulate (Perrotti et al. 1998; Perrotti

and Calabretta 2002; Trotta et al. 2003; Notari et al. 2006). This results in enhanced activity of proliferation and survival pathways and an arrest in differentiation, aspects of which are required for CML disease progression. However, imatinib-driven inhibition of BCR–ABL also causes specific changes in the expression levels of certain RBPs that could be exploited for their potential synergistic therapeutic relevance. Assessment of protein level alterations in K562 cells treated with imatinib, for instance, revealed that the RBP DDX3X was strongly upregulated (Arvaniti et al. 2014). Interestingly, a genome-wide CRISPR-mediated knockout screen uncovered DDX3X as an essential gene for K562 cells (Wang et al. 2015), and mutations in this gene have been frequently observed in various hematopoietic malignancies, including CLL (Ojha et al. 2015) and natural killer/T-cell lymphomas (Jiang et al. 2015).

Additionally, imatinib has been shown to decrease the total amount of polysome-bound mRNA and mRNA ribosome density in Ba/F3–Bcr–Abl and K562 cells. Simultaneous inhibition of mRNA polysome assembly (CPG57380) and BCR–ABL (imatinib) showed synergistic activity between both compounds and revealed reductions in the levels of the 5'-cap RBP EIF4E and impairment of RPS6 phosphorylation as the main mechanisms underlying the increased cell death observed (Zhang et al. 2008). This effect was also observed in imatinib-resistant cell lines, suggesting that interfering with RBPs involved in cap-dependent translation could represent a novel strategy to overcome imatinib resistance. Interestingly, synergistic antiproliferative effects were shown upon combined ribavirin and imatinib treatment of K562 cells *in vitro* (Shi et al. 2015). This further supports the concept that combinatorial inhibition of RBPs and BCR–ABL represents a promising therapeutic approach for BCR–ABL-driven leukemias. Although not extensively studied in combination with antileukemic agents, these findings indicate the potential importance of RBPs and the networks they regulate as mechanisms for treatment response and/or

resistance in leukemia. Altogether, the studies discussed so far highlight the emerging key role of RBP-driven post-transcriptional control in the regulation of hematopoietic cell fate.

Techniques and approaches for dissecting RBP-driven regulons

The modified transcriptome

As can be appreciated from the existing literature that has begun to dissect RBP-driven control of both normal and malignant stem cells in the blood system, many techniques and approaches have been developed to facilitate the global integrated view of their functionality. RBPs mediate a diverse set of functions and to deconstruct their mechanism of action, the canvas upon which these events occur is first defined by profiling the global transcriptome.

RNA-seq-based transcriptional profiling has been applied to sorted populations of the hematopoietic hierarchy (Cabezas-Wallscheid et al. 2014; Chen et al. 2014; Klimmeck et al. 2014) and more recently has been carried out in these cell types at single-cell resolution (Kowalczyk et al. 2015; Wilson et al. 2015; Povinelli et al. 2018). Notably, RNA-seq analysis of sorted populations from human umbilical cord blood uncovered significant differential usage of alternative splicing and novel splicing events throughout the hematopoietic hierarchy, emphasizing cell type specific posttranscriptional mechanisms at work (Chen et al. 2014). Single-cell RNA-seq has a limited sequencing depth in comparison to population-level RNA-seq. Nonetheless, it represents a promising technology worth building upon to better dissect regulatory systems underlying cell type specific capacities and is an ideal approach for use with rare cell populations. To this end, coupling single-cell RNA-seq to functional screening approaches has successfully uncovered

molecular circuitries governing cellular behavior in other contexts (Dixit et al. 2016; Jaitin et al. 2016). Through similar coupling with biochemical techniques, RNA-seq is now recognized as a central pillar for systems-level profiling and is a key approach for the decoding of post-transcriptional regulatory networks.

Mapping transcriptome secondary structure

The secondary structure of transcripts is a feature that plays critical roles in regulating or directing post-transcriptional processes. Dimethyl sulfate-seq (Rouskin et al. 2014), Structure-seq (Ding et al. 2015; Ritchey et al. 2017), and Mod-seq (Lin et al. 2015) are all approaches that exploit imethyl sulfate labeling of unpaired adenine and cytosine to inform on the location of RNA duplexes or regions of RNA that are unreactive due to protein association. Although it would be useful to define the structural features unique to specific cell types within the blood system, comparative RNA structural analysis of the hematopoietic hierarchy or malignant hematopoiesis has not yet been done. A major challenge of performing Structure-seq in these cell types is the requirement for large amounts of input sample. Of note, alternative protocols to advance the characterization of RNA secondary structure are being developed and have been discussed in other reviews (Bevilacqua et al. 2016).

Studying RBP–RNA interactomes

Transcriptome-wide maps of RNA-binding sites for RBPs are also essential for decoding RNA regulons. Cross-linking immunoprecipitation and high-throughput sequencing (CLIP-seq or HITSCLIP) was first used to interrogate the RNA interactome of the RBP FOXB in human

embryonic stem cells. Here, interacting RNA and proteins are covalently (UV) cross-linked before the RBP of interest is immobilized by immunoprecipitation and unoccupied strands of coprecipitated RNA are enzymatically sheared. RNA elements occupied by the RBP are protected during fragmentation and adaptors or tags are ligated to their ends to facilitate downstream cDNA library preparation for subsequent RNA-seq (Yeo et al. 2009). The fundamental CLIP biochemical approach was described well before high-throughput sequencing (Ule et al. 2003, 2005), but its coupling with RNA-seq rendered it a powerful tool for mapping RBP targets transcriptome-wide.

Despite its power, prototypical CLIP-seq still suffers from certain limitations such as the readout of nonspecific sequences (false positives) and low sequence complexity. For these reasons, this procedure typically requires massive cell inputs that are prohibitive for researchers investigating rare cell populations. To overcome these barriers and advance its potential, modified protocols have been developed. Photoactivatable ribonucleoside enhanced CLIP (PAR-CLIP) supplements cultured cells with a photoactivatable nucleoside analog (e.g., 4sU) and subsequent irradiation of cells with 365 nm UV light. The resultant point mutations at the site of cross-linking in the reverse transcribed sequencing library provide one mechanism for assigning nonspecific sequences (Hafner et al. 2010a, 2010b), but also have an effect of frequently terminating reverse transcription at the site of cross-linking leading to truncated sequences discarded from downstream analyses. Individual nucleotide resolution CLIP (iCLIP) likewise leverages cross-linking-induced mutation sites to elucidate RBP binding sites to single nucleotide resolution and resolves the truncated sequence problem by making use of iCLIP cDNA library circularization with a cleavable 5' adaptor. This results in both fully reverse-transcribed and truncated cDNA being flanked by 5' and 3' adaptors amenable to sequencing (König et al. 2010; Bahrami-Samani et al. 2015). iCLIP-seq was further enhanced as eCLIP-seq, which introduced technical optimizations of RNA

fragmentation and adaptor ligation steps to reduce requisite amplification by approximately 1000-fold (Van Nostrand et al. 2016). The method also includes a size-matched input control that enables accurate identification of truly enriched sequences. Overall, these improvements ultimately allow for reduced input cell numbers, an exciting advancement for rendering CLIP accessible for investigations of rare stem and progenitor cell populations.

While CLIP-based protocols take a protein-centric view of deciphering RNA regulons, the reverse procedure, known as mRNA interactome capture, allows for the identification of RBPs (Castello et al. 2012, 2013; Kwon et al. 2013). Polyadenylated RNA is precipitated by oligo(dT) beads and coprecipitated proteins are identified by mass spectrometry. mRNA interactome capture has been instrumental in elucidating novel RBPs, particularly those lacking canonical RNA-binding domains. Identification of specific RNA-binding domains or peptides is now possible due to refinements to this technique, which capitalize on exploitation of structural changes induced by cross-linking (Kramer et al. 2014; Castello et al. 2016) or protease treatment of precipitated RBPs (Castello et al. 2017). Overall, application of interactome capture has the potential to inform globally on aberrant RBP regulons in disease-state hematopoiesis; however, due to the input requirement of tens of millions of cells, this technique has not yet been accessible to HSPC or LSC contexts.

Measuring RNA stability

Temporal regulation of RNA stability and turnover has been traditionally measured by individual transcript (qPCR) or transcriptome profiling after transcription is inhibited using chemicals such as actinomycin D. A major caveat of this approach is these drugs have profound effects on normal

cell signaling. An alternative approach involves metabolic pulse-chase labeling of newly transcribed RNA with 4-thiouracile or 4-thiouridine (4tU or 4sU) followed by high-throughput sequencing (RATE-seq) (Neymotin et al. 2014). Both 4tU and 4sU are nontoxic nucleoside analogs incorporated in place of uridine into nascent transcripts. Biotinylation of the 4t/sU thiol group allows for subsequent highly efficient separation of labeled (newly transcribed) and unlabeled (preexisting) RNA by streptavidin affinity purification. Isolated RNA can be indexed for RNA-seq and a global perspective on RNA half-life can be measured mathematically taking into consideration the ratios between newly transcribed, preexisting, and total RNA (Chen et al. 2008; Pérez-Ortín et al. 2013; Palumbo et al. 2015).

Profiling translation

In the hematopoietic system, control at the level of protein translation has been inferred through correlation of the transcriptome and proteome (Cabezas-Wallscheid et al. 2014). While comparisons of this nature offer important insights, they overlook the potentially significant effects that mRNA or protein stability may have on concordant or discordant transcript to protein ratios. To conclusively understand translational control, the translatome, meaning the global profile of transcripts being translated, can be measured specifically by profiling transcripts or nascent peptides associated with translational machinery.

Polysome profiling is achieved by gradient isolation of polysomes and RNA-seq of associated transcripts (Sterne-Weiler et al. 2013; Martinez-Nunez and Sanford 2016). Both polysome profiling and Ribo-seq approaches (discussed below) make use of a whole transcriptome input control to accurately assess and quantify enrichment of transcripts within the translational

machinery. However, because polysome profiling does not delineate the precise position of ribosomes or their presence at regular intervals on transcripts, sequenced reads could represent transcripts associated with stalled ribosomes and not those necessarily undergoing productive active translation.

Ribosome profiling or foot printing (Ribo-seq) is the preferred approach to elucidate the specific RNA region occupied by translating ribosomes. Similar to CLIP-procedures, Ribo-seq involves fragmentation of free RNA and isolation of ribosomes and ribosome-protected RNA fragments for RNA-seq (Ingolia et al. 2009, 2012). By virtue of the ribosome "footprint" spanning approximately 30 nucleotides, Ribo-seq decodes the translatome to a high subcodon resolution. This is a powerful tool capable of informing on specific translation sites, such as alternative and near-cognate start sites and translational pause sites, alternative translation of multiple open reading frames within a single transcript, and translational stalling (Michel et al. 2012; Menschaert et al. 2013).

Conclusion

The self-renewal and differentiation axis underlying HSC fate is controlled by a complex and multilayered cascade of intracellular events. Influenced by the wealth of data generated by systems biology focused experimental approaches, our current understanding of the regulatory networks that orchestrate hematopoietic lineage commitment continues to evolve. Recent advances in high-throughput genomic tools and computational models aimed at identifying genome-wide RBP–RNA interactions have paved the way for the exploration of post-transcriptional networks and their functional relevance in stem cell biology. Individual nodes within intricate regulatory

circuitries are being revealed, providing us with a more accurate grasp on the cooperative regulatory mechanisms underlying HSC biology. A remaining challenge, however, is to reliably integrate and organize these highly complex data into our current understanding of HSC behavior. By balancing accurate network modeling algorithms and more low-throughput biochemical approaches, it remains to be unraveled which interactions identified on a global scale are truly functionally relevant for the stem cell in its *in vivo* environment. Variables including combinations of microenvironmental cues, indirect interactors, competitors, and/or multiple feedback and forward loops certainly contribute to ongoing cell intrinsic mechanisms to tailor the ultimate outcome of RBP–RNA interactions. In addition, it remains to be elucidated how these mechanisms are utilized, coopted, or repressed in the malignant setting. LSCs might, for example, rewire or hijack these intricate circuitries at multiple levels. Further experimental dissection of key nodes within post-transcriptional networks could thus pave the way for more efficient LSC-focused therapeutic approaches.

Moving forward, the unmistakably important role of RBP-directed post-transcriptional regulatory networks for the regenerative potential of HSCs should continue to inspire us to achieve a more complete understanding of their collective dynamics and how this can be harnessed for therapeutic means.

Table 1. RBPs with key roles in hematopoietic cell fate.

RBP	RNA-binding motif	Role in normal hematopoiesis	Role in aberrant hematopoiesis
ADAR1	*A_deamin*, *z-alpha*, *dsrm*	Suppresses interferon signaling in HSCs and regulates their differentiation via its base editing activity (Hartner et al. 2009; XuFeng et al. 2009)	Enhanced editing activity in CML impairs biogenesis of developmentally regulated family of miRNAs that normally limits self-renewal capacity (Zipeto et al. 2016)
AGO2	*DUF1785*, *PAZ*, *Piwi*	Forms minimal RISC complex; promotes HSC exit from quiescence and regulates both erythropoiesis and lymphopoiesis (O'Carroll et al. 2007)	
DDX21	*Helicase*, *DEAD*, *GUCT*		Regulates LSC self-renewal in AML–ETO1 driven leukemogenesis (Zhou et al. 2017)
DDX3X	*Helicase*, *DEAD*		Frequently mutated in hematopoietic malignancies and upregulated upon imatinib treatment (Jiang et al. 2015; Ojha et al. 2015)
DICER1	*Helicase*, *dsrm*, *PAZ*, *DEAD*, *Ribonuclease*	Maintains HSC reservoirs and promotes erythro- and myelopoiesis (Guo et al. 2010; Buza-Vidas et al. 2012)	
DKC1	*PUA*, *DKCLD*, *TruB*	Regulates HSC differentation through its pseudouridylation activity on small noncoding RNAs (Bellodi et al. 2013)	Mutations found in dyskeratosis congenita result in defective rRNA pseudouridylation (Bellodi et al. 2013)
DPPA5	*KH*-like *RBD*	Downregulates endoplasmic reticulum stress in HSCs (Miharada et al. 2014)	
DROSHA	*Ribonuclease*, *dsrm*	Promotes myelopoiesis by repressing mRNAs through a non-miRNA pathway (Johanson et al. 2015)	
EIF4E	*IF4E*		Contributes to leukemogenesis in part by blocking myeloid differentiation (Topisirovic et al. 2003); target for phase I/II clinical trials with ribavirin and (or) cytarabine (Assouline et al. 2009, 2015); reduced levels of eIF4E upon simultaneous inhibition of BCR–ABL and polysome assembly (Zhang et al. 2008)
FUS	*zf-RanBP*, *RRM_1*	Radioprotects and maintains fetal HSC self-renewal (Sugawara et al. 2010)	Upregulated by BCR–ABL; enhances proliferation and survival signaling (Perrotti et al. 1998)
HNRNPA0	*RRM_1*, *RRM_6*	Shifts myeloid lineage fate upon functional knockdown (Young et al. 2014)	del(5q) haploinsufficient gene in patients; alters mRNAs associated with increased growth and proliferation (Young et al. 2014)
HNRNPA1	*HnRNPA1*, *RRM_1*	Regulates granulocytic differentiation (Song et al. 2017)	Upregulated upon imatinib treatment (Breitkopf et al. 2015)
HNRNPK	*ROKNT*, *KH_1*	Acts as a tumour suppressor (Gallardo et al. 2013, 2015)	Haploinsufficiency contributes to myeloproliferation and lymphomas (Gallardo et al. 2013, 2015); overexpression in CML is associated with therapy resistance (Breitkopf et al. 2015)
LIN28B	*zf-CCHC*, *CSD*	Expands fetal liver HSC pool by repression of a family of miRNAs (Lee et al. 2013)	Expression associated with CML progression in some patients; maintains and regulates LSC self-renewal (Zipeto et al. 2016)
METTL3	*MT-A70*	Regulates HSPC proliferation and differentiation through m^{6}A-mediated translational regulation (Vu et al. 2017*a*)	
METTL14	*MT-A70*	Regulates HSPC proliferation and differentiation through m^{6}A-mediated translational regulation (Weng et al. 2018)	Promotes leukemogenesis through m^{6}A-mediated translational regulation (Weng et al. 2018)
MSI2	*RRM_1*	Promotes HSC self-renewal through modulation of several key signaling pathways (Park et al. 2014; Rentas et al. 2016)	Maintains and regulates LSC self-renewal in AML and CML models (Ito et al. 2010; Kharas et al. 2010; Mu et al. 2013; Hattori et al. 2017)
PKR	*Pkinase*	Regulates HSPC proliferation, differentiation, and survival through downstream target phosphorylation (Liu et al. 2013)	

Table 1 (*concluded*).

RBP	RNA-binding motif	Role in normal hematopoiesis	Role in aberrant hematopoiesis
PUM1 PUM2	*Shadoo*, *PUF* *PUF*	Regulates HSPC growth by stabilizing key transcription factor expression (Naudin et al. 2017)	Sustains myeloid leukemic growth by the same pathway in HSPCs (Naudin et al. 2017)
RBM15	*RRM_5*, *RRM_1*, *SPOC*	Regulates balance between HSC quiescence and differentiation through alternative splicing (Xiao et al. 2015)	RBM15–MKL1 fusion present in (t(1;22)(p13;q13) acute megakaryoblastic leukemias (Ma et al. 2001)
RPS14	*Ribosomal_S11*		Mutations cause MDS with defects in erythroid differentiation due to compromised rRNA processing (Ebert et al. 2008)
SBDS	*SBDS_C*, *SBDS*		Defects result in neutropenia and erythroid production deficiencies due to impaired ribosome assembly (Ganapathi et al. 2007)
SF3B1	*HEAT_2*, *SF3b1*	Maintains HSPCs and normal hematopoiesis through wildtype splicing profile (Mian et al. 2015; Mortera-Blanco et al. 2017)	SF3B1 mutations impair erythropoiesis and expand the HSC pool (Obeng et al. 2016; Mupo et al. 2017)
SRSF2	*RRM_1*	Maintains HSPCs and normal hematopoiesis through wildtype splicing profile (Kim et al. 2015; Komeno et al. 2015)	SRSF2 mutations result in myelodysplasia due to altered binding and splicing profiles (Kim et al. 2015; Komeno et al. 2015)
SSB	*La*, *RRM_1*, *RRM_3*		Upregulated by BCR–ABL; enhances proliferation and survival signaling (Trotta et al. 2003)
SYNCRIP	*RRM_1*	Not essential for fetal liver hematopoiesis (Vu et al. 2017*b*)	Regulates LSC gene expression programs in conjunction with MSI2 (Vu et al. 2017*b*)
U2AF1	*RRM_5*, *zf-CCCH*	Maintains HSPCs and normal hematopoiesis through wildtype splicing profile (Shirai et al. 2015; Wadugu et al. 2017)	U2AF1 mutations result in leukopenia and progenitor expansion (Shirai et al. 2015)
UPF2	*MIF4 G*, *Upf2*	Core component of NMD pathway; maintains HSPCs (Weischenfeldt et al. 2008)	
XPO1	*IBN_N*, *Xpo1*, *CRM1_C*		Inhibition may result in remissions in chemoresistant or relapsed AML patients by selective targeting of LSCs (Kojima et al. 2013; Savona et al. 2013; Walker et al. 2013; Fiedler et al. 2015; Hing et al. 2016; Etchin et al. 2017; Garzon et al. 2017)

Note: RNA-binding motifs adapted from Gerstberger et al. (2014).

References

1. Abraham, S.A., Hopcroft, L.E., Carrick, E., Drotar, M.E., Dunn, K., Williamson, A.J., et al. 2016. Dual targeting of p53 and c-Myc selectively eliminates leukaemic stem cells. Nature, **534**(7607): 341–346. doi:10.1038/ nature18288. PMID:27281222.
2. Abrahamsson, A.E., Geron, I., Gotlib, J., Dao, K.H., Barroga, C.F., Newton, I.G., et al. 2009. Glycogen synthase kinase 3 missplicing contributes to leukemia stem cell generation. Proc. Natl. Acad. Sci. U.S.A. **106**(10): 3925–3929. doi:10. 1073/pnas.0900189106. PMID:19237556.
3. Anokye-Danso, F., Trivedi, C.M., Juhr, D., Gupta, M., Cui, Z., Tian, Y., et al. 2011. Highly efficient miRNA-mediated reprogramming of mouse and human somatic cells to pluripotency. Cell Stem Cell, **8**(4): 376–388. doi:10.1016/j.stem. 2011.03.001. PMID:21474102.
4. Arvaniti, K., Papadioti, A., Kinigopoulou, M., Theodorou, V., Skobridis, K., and Tsiotis, G. 2014. Proteome changes induced by imatinib and novel imatinib derivatives in K562 human chronic myeloid leukemia cells. Proteomes, **2**(3): 363–381. doi:10.3390/proteomes2030363. PMID:28250386.
5. Assouline, S., Culjkovic, B., Cocolakis, E., Rousseau, C., Beslu, N., Amri, A., et al. 2009. Molecular targeting of the oncogene eIF4E in acute myeloid leukemia (AML): a proof-of-principle clinical trial with ribavirin. Blood, **114**(2): 257–260. doi:10.1182/blood-2009-02-205153. PMID:19433856.
6. Assouline, S., Culjkovic-Kraljacic, B., Bergeron, J., Caplan, S., Cocolakis, E., Lambert, C., et al. 2015. A phase I trial of ribavirin and low-dose cytarabine for the treatment of relapsed and refractory acute myeloid leukemia with elevated eIF4E. Haematologica, **100**(1): e7–e9. doi:10.3324/haematol.2014.111245. PMID:25425688.
7. Bahrami-Samani, E., Penalva, L.O., Smith, A.D., and Uren, P.J. 2015. Leveraging cross-link modification events in CLIP-seq for motif discovery. Nucleic Acids Res. **43**(1): 95–103. doi:10.1093/nar/gku1288. PMID:25505146.
8. Bellodi, C., McMahon, M., Contreras, A., Juliano, D., Kopmar, N., Nakamura, T., et al. 2013. H/ACA small RNA dysfunctions in disease reveal key roles for noncoding RNA modifications in hematopoietic stem cell differentiation. Cell Rep. **3**(5): 1493–1502. doi:10.1016/j.celrep.2013.04.030. PMID:23707062.
9. Bevilacqua, P.C., Ritchey, L.E., Su, Z., and Assmann, S.M. 2016. Genome-wide analysis of RNA secondary structure. Annu. Rev. Genet. **50**: 235–266. doi:10. 1146/annurev-genet-120215-035034. PMID:27648642.

10. Breitkopf, S.B., Yuan, M., Helenius, K.P., Lyssiotis, C.A., and Asara, J.M. 2015. Triomics analysis of imatinib-treated myeloma cells connects kinase inhibition to RNA processing and decreased lipid biosynthesis. Anal. Chem. **87**(21): 10995–11006. doi:10.1021/acs.analchem.5b03040. PMID:26434776.
11. Buza-Vidas, N., Cismasiu, V.B., Moore, S., Mead, A.J., Woll, P.S., Lutteropp, M., et al. 2012. Dicer is selectively important for the earliest stages of erythroid development. Blood, **120**(12): 2412–2416. doi:10.1182/blood-2011-10-383653. PMID:22869792.
12. Byers, R.J., Currie, T., Tholouli, E., Rodig, S.J., and Kutok, J.L. 2011. MSI2 protein expression predicts unfavorable outcome in acute myeloid leukemia. Blood, **118**(10): 2857–2867. doi:10.1182/blood-2011-04-346767. PMID:21753187.
13. Cabezas-Wallscheid, N., Klimmeck, D., Hansson, J., Lipka, D.B., Reyes, A., Wang, Q., et al. 2014. Identification of regulatory networks in HSCs and their immediate progeny via integrated proteome, transcriptome, and DNA methylome analysis. Cell Stem Cell, **15**(4): 507–522. doi:10.1016/j.stem.2014. 07.005. PMID:25158935.
14. Castello, A., Fischer, B., Eichelbaum, K., Horos, R., Beckmann, B.M., Strein, C., et al. 2012. Insights into RNA biology from an atlas of mammalian mRNA binding proteins. Cell, **149**(6): 1393–1406. doi:10.1016/j.cell.2012.04.031. PMID: 22658674.
15. Castello, A., Horos, R., Strein, C., Fischer, B., Eichelbaum, K., Steinmetz, L.M., et al. 2013. System-wide identification of RNA-binding proteins by interactome capture. Nat. Protoc. **8**(3): 491–500. doi:10.1038/nprot.2013.020. PMID: 23411631.
16. Castello, A., Fischer, B., Frese, C.K., Horos, R., Alleaume, A.M., Foehr, S., et al. 2016. Comprehensive identification of RNA-binding domains in human cells. Mol. Cell, **63**(4): 696–710. doi:10.1016/j.molcel.2016.06.029. PMID:27453046.
17. Castello, A., Frese, C.K., Fischer, B., Järvelin, A.I., Horos, R., Alleaume, A.M., et al. 2017. Identification of RNA-binding domains of RNA-binding proteins in cultured cells on a system-wide scale with RBDmap. Nat. Protoc. **12**(12): 2447– 2464. doi:10.1038/nprot.2017.106. PMID:29095441.
18. Chen, C.Y., Ezzeddine, N., and Shyu, A.B. 2008. Messenger RNA half-life measurements in mammalian cells. Methods Enzymol. **448**: 335–357. doi:10.1016/ S0076-6879(08)02617-7. PMID:19111184.
19. Chen, L., Kostadima, M., Martens, J.H.A., Canu, G., Garcia, S.P., Turro, E., et al. 2014. Transcriptional diversity during lineage commitment of human blood progenitors. Science, **345**(6204): 1251033. doi:10.1126/science.1251033. PMID: 25258084.
20. Ding, Y., Kwok, C.K., Tang, Y., Bevilacqua, P.C., and Assmann, S.M. 2015. Genomewide profiling of *in vivo* RNA structure at single-nucleotide resolution using structure-seq. Nat. Protoc. **10**(7): 1050–1066. doi:10.1038/nprot.2015.064. PMID: 26086407.

21. Dixit, A., Parnas, O., Li, B., Chen, J., Fulco, C.P., Jerby-Arnon, L., et al. 2016. Perturb-seq: dissecting molecular circuits with scalable single-cell RNA profiling of pooled genetic screens. Cell, **167**(7): 1853–1866.e17. doi:10.1016/j.cell. 2016.11.038. PMID:27984732.
22. Ebert, B.L., Pretz, J., Bosco, J., Chang, C.Y., Tamayo, P., Galili, N., et al. 2008. Identification of RPS14 as a 5q– syndrome gene by RNA interference screen. Nature, **451**(7176): 335–339. doi:10.1038/nature06494. PMID:18202658.
23. Eppert, K., Takenaka, K., Lechman, E.R., Waldron, L., Nilsson, B., van Galen, P., et al. 2011. Stem cell gene expression programs influence clinical outcome in human leukemia. Nat. Med. **17**(9): 1086–1093. doi:10.1038/nm.2415. PMID: 21873988.
24. Etchin, J., Berezovskaya, A., Conway, A.S., Galinsky, I.A., Stone, R.M., Baloglu, E., et al. 2017. KPT-8602, a second-generation inhibitor of XPO1-mediated nuclear export, is well tolerated and highly active against AML blasts and leukemia-initiating cells. Leukemia, **31**(1): 143–150. doi:10.1038/leu.2016.145. PMID:27211268.
25. Fiedler, W., Chromik, J., Kebenko, M., Thol, F., Trummer, A., Schunemann, C., et al. 2015. Selinexor, ara-c and idarubicin: an effective and tolerable combination in patients with relapsed/refractory AML: a multicenter phase II study. Blood, **126**: 3789.
26. Gallardo, M., Lee, H.J., Zhang, X., Nazha, A., Pageon, L.R., Kornblau, S.M., et al. 2013. hnRNP K: a novel regulator of hematopoiesis and a potential predictive biomarker in acute myeloid leukemia. Blood, **122**(21): 226.
27. Gallardo, M., Lee, H.J., Zhang, X., Bueso-Ramos, C., Pageon, L.R., McArthur, M., et al. 2015. hnRNP K is a haploinsufficient tumor suppressor that regulates proliferation and differentiation programs in hematologic malignancies. Cancer Cell, **28**(4): 486–499. doi:10.1016/j.ccell.2015.09.001. PMID:26412324.
28. Ganapathi, K.A., Austin, K.M., Lee, C.S., Dias, A., Malsch, M.M., Reed, R., and Shimamura, A. 2007. The human Shwachman–Diamond syndrome protein, SBDS, associates with ribosomal RNA. Blood, **110**(5): 1458–1465. doi:10.1182/ blood-2007-02-075184. PMID:17475909.
29. Garzon, R., Savona, M., Baz, R., Andreeff, M., Gabrail, N., Gutierrez, M., et al. 2017. A phase 1 clinical trial of single-agent selinexor in acute myeloid leukemia. Blood, **129**(24): 3165–3174. doi:10.1182/blood-2016-11-750158. PMID: 28336527.
30. Gentles, A.J., Plevritis, S.K., Majeti, R., and Alizadeh, A.A. 2010. Association of a leukemic stem cell gene expression signature with clinical outcomes in acute myeloid leukemia. JAMA, **304**(24): 2706–2715. doi:10.1001/jama.2010.1862. PMID:21177505.
31. Gerstberger, S., Hafner, M., and Tuschl, T. 2014. A census of human RNA binding proteins. Nat. Rev. Genet. **15**(12): 829–845. doi:10.1038/nrg3813. PMID:25365966.

32. Grech, G., and von Lindern, M. 2012. The role of translation initiation regulation in haematopoiesis. Comp. Funct. Genomics, **2012**: 576540. doi:10.1155/2012/ 576540. PMID:22649283.
33. Guo, S., Lu, J., Schlanger, R., Zhang, H., Wang, J.Y., Fox, M.C., et al. 2010. MicroRNA miR-125a controls hematopoietic stem cell number. Proc. Natl. Acad. Sci. U.S.A. **107**(32): 14229–14234. doi:10.1073/pnas.0913574107. PMID: 20616003.
34. Hafner, M., Landthaler, M., Burger, L., Khorshid, M., Hausser, J., Berninger, P., et al. 2010a. PAR-CliP — a method to identify transcriptome-wide the binding sites of RNA binding proteins. J. Vis. Exp. **41**: e2034. doi:10.3791/2034. PMID: 20644507.
35. Hafner, M., Landthaler, M., Burger, L., Khorshid, M., Hausser, J., Berninger, P., et al. 2010b. Transcriptome-wide identification of RNA-binding protein and microRNA target sites by PAR-CLIP. Cell, **141**(1): 129–141. doi:10.1016/j.cell.2010. 03.009. PMID:20371350.
36. Hartner, J.C., Walkley, C.R., Lu, J., and Orkin, S.H. 2009. ADAR1 is essential for the maintenance of hematopoiesis and suppression of interferon signaling. Nat. Immunol. **10**(1): 109–115. doi:10.1038/ni.1680. PMID:19060901.
37. Hattori, A., McSkimming, D., Kannan, N., and Ito, T. 2017. RNA binding protein MSI2 positively regulates FLT3 expression in myeloid leukemia. Leuk. Res. **54**: 47–54. doi:10.1016/j.leukres.2017.01.015. PMID:28107692.
38. Hing, Z.A., Fung, H.Y., Ranganathan, P., Mitchell, S., El-Gamal, D., Woyach, J.A., et al. 2016. Next-generation XPO1 inhibitor shows improved efficacy and *in vivo* tolerability in hematologic malignancies. Leukemia, **30**(12): 2364–2372. doi:10.1038/leu.2016.136. PMID:27323910.
39. Ingolia, N.T., Ghaemmaghami, S., Newman, J.R.S., and Weissman, J.S. 2009. Genome-wide analysis *in vivo* of translation with nucleotide resolution using ribosome profiling. Science, **324**(5924): 218–223. doi:10.1126/science.1168978. PMID:19213877.
40. Ingolia, N.T., Brar, G.A., Rouskin, S., McGeachy, A.M., and Weissman, J.S. 2012. The ribosome profiling strategy for monitoring translation *in vivo* by deep sequencing of ribosome-protected mRNA fragments. Nat. Protoc. **7**(8): 1534– 1550. doi:10.1038/nprot.2012.086. PMID:22836135.
41. Ito, T., Kwon, H.Y., Zimdahl, B., Congdon, K.L., Blum, J., Lento, W.E., et al. 2010. Regulation of myeloid leukaemia by the cell-fate determinant Musashi. Nature, **466**(7307): 765–768. doi:10.1038/nature09171. PMID:20639863.
42. Jaitin, D.A., Weiner, A., Yofe, I., Lara-Astiaso, D., Keren-Shaul, H., David, E., et al. 2016. Dissecting immune circuits by linking CRISPR-pooled screens with single-cell RNA-seq. Cell, **167**(7): 1883–1896.e15. doi:10.1016/j.cell.2016.11.039. PMID:27984734.

43. Jamieson, C.H., Ailles, L.E., Dylla, S.J., Muijtjens, M., Jones, C., Zehnder, J.L., et al. 2004. Granulocyte–macrophage progenitors as candidate leukemic stem cells in blast-crisis CML. N. Engl. J. Med. **351**(7): 657–667. doi:10.1056/ NEJMoa040258. PMID:15306667.
44. Jan, M., Snyder, T.M., Corces-Zimmerman, M.R., Vyas, P., Weissman, I.L., Quake, S.R., and Majeti, R. 2012. Clonal evolution of preleukemic hematopoietic stem cells precedes human acute myeloid leukemia. Sci. Transl. Med. **4**(149): 149ra118. doi:10.1126/scitranslmed.3004315. PMID:22932223.
45. Jiang, L., Gu, Z.H., Yan, Z.X., Zhao, X., Xie, Y.Y., Zhang, Z.G., et al. 2015. Exome sequencing identifies somatic mutations of DDX3X in natural killer/T-cell lymphoma. Nat. Genet. **47**(9): 1061–1066. doi:10.1038/ng.3358. PMID:26192917.
46. Johanson, T.M., Keown, A.A., Cmero, M., Yeo, J.H., Kumar, A., Lew, A.M., et al. 2015. Drosha controls dendritic cell development by cleaving messenger RNAs encoding inhibitors of myelopoiesis. Nat. Immunol. **16**(11): 1134–1141. doi:10.1038/ni.3293. PMID:26437240.
47. Kechavarzi, B., and Janga, S.C. 2014. Dissecting the expression landscape of RNA-binding proteins in human cancers. Genome Biol. **15**(1): R14. doi:10.1186/ gb-2014-15-1-r14. PMID:24410894.
48. Keene, J.D. 2007. RNA regulons: coordination of post-transcriptional events. Nat. Rev. Genet. **8**(7): 533–543. doi:10.1038/nrg2111. PMID:17572691.
49. Keene, J.D., and Tenenbaum, S.A. 2002. Eukaryotic mRNPs may represent posttranscriptional operons. Mol. Cell, **9**(6): 1161–1167. doi:10.1016/S1097-2765(02) 00559-2. PMID:12086614.
50. Kharas, M.G., Lengner, C.J., Al-Shahrour, F., Bullinger, L., Ball, B., Zaidi, S., et al. 2010. Musashi-2 regulates normal hematopoiesis and promotes aggressive myeloid leukemia. Nat. Med. **16**(8): 903–908. doi:10.1038/nm.2187. PMID: 20616797.
51. Kim, E., Ilagan, J.O., Liang, Y., Daubner, G.M., Lee, S.C., Ramakrishnan, A., et al. 2015. SRSF2 mutations contribute to myelodysplasia by mutant-specific effects on exon recognition. Cancer Cell, **27**(5): 617–630. doi:10.1016/j.ccell.2015. 04.006. PMID:25965569.
52. Klimmeck, D., Cabezas-Wallscheid, N., Reyes, A., von Paleske, L., Renders, S., Hansson, J., et al. 2014. Transcriptome-wide profiling and posttranscriptional analysis of hematopoietic stem/progenitor cell differentiation toward myeloid commitment. Stem Cell Rep. **3**(5): 858–875. doi:10.1016/j.stemcr.2014.08. 012. PMID:25418729.
53. Kojima, K., Kornblau, S.M., Ruvolo, V., Dilip, A., Duvvuri, S., Davis, R.E., et al. 2013. Prognostic impact and targeting of CRM1 in acute myeloid leukemia. Blood, **121**(20): 4166–4174. doi:10.1182/blood-2012-08-447581. PMID:23564911.

54. Komeno, Y., Huang, Y.J., Qiu, J., Lin, L., Xu, Y., Zhou, Y., et al. 2015. SRSF2 is essential for hematopoiesis, and its myelodysplastic syndrome-related mutations dysregulate alternative pre-mRNA splicing. Mol. Cell Biol. **35**(17): 3071–3082. doi:10.1128/MCB.00202-15. PMID:26124281.
55. König, J., Zarnack, K., Rot, G., Curk, T., Kayikci, M., Zupan, B., et al. 2010. iCLIP reveals the function of hnRNP particles in splicing at individual nucleotide resolution. Nat. Struct. Mol. Biol. **17**(7): 909–915. doi:10.1038/nsmb.1838. PMID:20601959.
56. Kowalczyk, M.S., Tirosh, I., Heckl, D., Rao, T.N., Dixit, A., Haas, B.J., et al. 2015. Single-cell RNA-seq reveals changes in cell cycle and differentiation programs upon aging of hematopoietic stem cells. Genome Res. **25**(12): 1860– 1872. doi:10.1101/gr.192237.115. PMID:26430063.
57. Kramer, K., Sachsenberg, T., Beckmann, B.M., Qamar, S., Boon, K.L., Hentze, M.W., et al. 2014. Photo-cross-linking and high-resolution mass spectrometry for assignment of RNA-binding sites in RNA-binding proteins. Nat. Methods, **11**(10): 1064–1070. doi:10.1038/nmeth.3092. PMID:25173706.
58. Krivtsov, A.V., Figueroa, M.E., Sinha, A.U., Stubbs, M.C., Feng, Z., Valk, P.J., et al. 2013. Cell of origin determines clinically relevant subtypes of MLL-rearranged AML. Leukemia, **27**(4): 852–860. doi:10.1038/leu.2012.363. PMID:23235717.
59. Kwon, H.Y., Bajaj, J., Ito, T., Blevins, A., Konuma, T., Weeks, J., et al. 2015. Tetraspanin 3 is required for the development and propagation of acute myelogenous leukemia. Cell Stem Cell, **17**(2): 152–164. doi:10.1016/j.stem.2015.06.006. PMID:26212080.
60. Kwon, S.C., Yi, H., Eichelbaum, K., Föhr, S., Fischer, B., You, K.T., et al. 2013. The RNA-binding protein repertoire of embryonic stem cells. Nat. Struct. Mol. Biol. **20**(9): 1122–1130. doi:10.1038/nsmb.2638. PMID:23912277.
61. Lapidot, T., Sirard, C., Vormoor, J., Murdoch, B., Hoang, T., Caceres-Cortes, J., et al. 1994. A cell initiating human acute myeloid leukaemia after transplantation into SCID mice. Nature, **367**(6464): 645–648. doi:10.1038/367645a0. PMID:7509044.
62. Lee, Y.T., de Vasconcellos, J.F., Yuan, J., Byrnes, C., Noh, S.J., Meier, E.R., et al. 2013. LIN28B-mediated expression of fetal hemoglobin and production of fetal-like erythrocytes from adult human erythroblasts *ex vivo*. Blood, **122**(6): 1034–1041. doi:10.1182/blood-2012-12-472308. PMID:23798711.
63. Lin, Y., May, G.E., and McManus, C.J. 2015. Mod-seq: a high-throughput method for probing RNA secondary structure. Methods Enzymol. **558**: 125–152. doi:10.1016/bs.mie.2015.01.012. PMID:26068740.
64. Liu, X., Bennett, R.L., Cheng, X., Byrne, M., Reinhard, M.K., and May, W.S., Jr. 2013. PKR regulates proliferation, differentiation, and survival of murine hematopoietic

stem/progenitor cells. Blood, **121**(17): 3364–3374. doi:10.1182/ blood-2012-09-456400. PMID:23403623.

65. Ma, Z., Morris, S.W., Valentine, V., Li, M., Herbrick, J.A., Cui, X., et al. 2001. Fusion of two novel genes, RBM15 and MKL1, in the t(1;22)(p13;q13) of acute megakaryoblastic leukemia. Nat. Genet. **28**(3): 220–221. doi:10.1038/90054. PMID: 11431691.
66. Martinez-Nunez, R.T., and Sanford, J.R. 2016. Studying isoform-specific mRNA recruitment to polyribosomes with Frac-seq. Methods Mol. Biol. **1358**: 99–108. doi:10.1007/978-1-4939-3067-8_6. PMID:26463379.
67. McKerrell, T., Park, N., Moreno, T., Grove, C.S., Ponstingl, H., Stephens, J., et al. 2015. Leukemia-associated somatic mutations drive distinct patterns of agerelated clonal hemopoiesis. Cell Rep. **10**(8): 1239–1245. doi:10.1016/j.celrep. 2015.02.005. PMID:25732814.
68. Menschaert, G., Van Criekinge, W., Notelaers, T., Koch, A., Crappé, J., Gevaert, K., and Van Damme, P. 2013. Deep proteome coverage based on ribosome profiling aids mass spectrometry-based protein and peptide discovery and provides evidence of alternative translation products and near-cognate translation initiation events. Mol. Cell Proteomics, **12**(7): 1780–1790. doi:10.1074/ mcp.M113.027540. PMID:23429522.
69. Mian, S.A., Rouault-Pierre, K., Smith, A.E., Seidl, T., Pizzitola, I., Kizilors, A., et al. 2015. SF3B1 mutant MDS-initiating cells may arise from the haematopoietic stem cell compartment. Nat. Commun. **6**: 10004. doi:10.1038/ncomms10004. PMID:26643973.
70. Michel, A.M., Choudhury, K.R., Firth, A.E., Ingolia, N.T., Atkins, J.F., and Baranov, P.V. 2012. Observation of dually decoded regions of the human genome using ribosome profiling data. Genome Res. **22**(11): 2219–2229. doi: 10.1101/gr.133249.111. PMID:22593554.
71. Miharada, K., Sigurdsson, V., and Karlsson, S. 2014. Dppa5 improves hematopoietic stem cell activity by reducing endoplasmic reticulum stress. Cell Rep. **7**(5): 1381–1392. doi:10.1016/j.celrep.2014.04.056. PMID:24882002.
72. Miyamoto, T., Weissman, I.L., and Akashi, K. 2000. AML1/ETO-expressing nonleukemic stem cells in acute myelogenous leukemia with 8;21 chromosomal translocation. Proc. Natl. Acad. Sci. U.S.A. **97**(13): 7521–7526. doi:10.1073/pnas. 97.13.7521. PMID:10861016.
73. Mortera-Blanco, T., Dimitriou, M., Woll, P.S., Karimi, M., Elvarsdottir, E., Conte, S., et al. 2017. SF3B1-initiating mutations in MDS-RSs target lymphomyeloid hematopoietic stem cells. Blood, **130**(7): 881–890. doi:10.1182/blood2017-03-776070. PMID:28634182.
74. Mu, Q., Wang, Y., Chen, B., Qian, W., Meng, H., Tong, H., et al. 2013. High expression of Musashi-2 indicates poor prognosis in adult B-cell acute lymphoblastic leukemia. Leuk. Res. **37**(8): 922–927. doi:10.1016/j.leukres.2013.05. 012. PMID:23759245.

75. Mupo, A., Seiler, M., Sathiaseelan, V., Pance, A., Yang, Y., Agrawal, A.A., et al. 2017. Hemopoietic-specific Sf3b1-K700E knock-in mice display the splicing defect seen in human MDS but develop anemia without ring sideroblasts. Leukemia, **31**(3): 720–727. doi:10.1038/leu.2016.251. PMID:27604819.
76. Naudin, C., Hattabi, A., Michelet, F., Miri-Nezhad, A., Benyoucef, A., Pflumio, F., et al. 2017. PUMILIO/FOXP1 signaling drives expansion of hematopoietic stem/progenitor and leukemia cells. Blood, **129**(18): 2493–2506. doi:10.1182/ blood-2016-10-747436. PMID:28232582.
77. Nerlov, C., Querfurth, E., Kulessa, H., and Graf, T. 2000. GATA-1 interacts with the myeloid PU.1 transcription factor and represses PU.1-dependent transcription. Blood, **95**(8): 2543–2551. PMID:10753833.
78. Neymotin, B., Athanasiadou, R., and Gresham, D. 2014. Determination of *in vivo* RNA kinetics using RATE-seq. RNA, **20**(10): 1645–1652. doi:10.1261/rna.045104. 114. PMID:25161313.
79. Ng, S.W., Mitchell, A., Kennedy, J.A., Chen, W.C., McLeod, J., Ibrahimova, N., et al. 2016. A 17-gene stemness score for rapid determination of risk in acute leukaemia. Nature, **540**(7633): 433–437. doi:10.1038/nature20598. PMID: 27926740.
80. Notari, M., Neviani, P., Santhanam, R., Blaser, B.W., Chang, J.S., Galietta, A., et al. 2006. A MAPK/HNRPK pathway controls BCR/ABL oncogenic potential by regulating MYC mRNA translation. Blood, **107**(6): 2507–2516. doi:10.1182/ blood-2005-09-3732. PMID:16293596.
81. Obeng, E.A., Chappell, R.J., Seiler, M., Chen, M.C., Campagna, D.R., Schmidt, P.J., et al. 2016. Physiologic expression of Sf3b1K700E causes impaired erythropoiesis, aberrant splicing, and sensitivity to therapeutic spliceosome modulation. Cancer Cell, **30**(3): 404–417. doi:10.1016/j.ccell.2016.08.006. PMID:27622333.
82. O'Carroll, D., Mecklenbrauker, I., Das, P.P., Santana, A., Koenig, U., Enright, A.J., et al. 2007. A Slicer-independent role for Argonaute 2 in hematopoiesis and the microRNA pathway. Genes Dev. **21**(16): 1999–2004. doi:10.1101/gad. 1565607. PMID:17626790.
83. Ojha, J., Secreto, C.R., Rabe, K.G., Van Dyke, D.L., Kortum, K.M., Slager, S.L., et al. 2015. Identification of recurrent truncated DDX3X mutations in chronic lymphocytic leukaemia. Br. J. Haematol. **169**(3): 445–448. doi:10.1111/bjh.13211. PMID:25382417.
84. Palumbo, M.C., Farina, L., and Paci, P. 2015. Kinetics effects and modeling of mRNA turnover. Wiley Interdiscip. Rev.: RNA, **6**(3): 327–336. doi:10.1002/wrna. 1277. PMID:25727049.
85. Pan, L., Li, Y., Zhang, H.Y., Zheng, Y., Liu, X.L., Hu, Z., et al. 2017. DHX15 is associated with poor prognosis in acute myeloid leukemia (AML) and regulates cell apoptosis via the

NF- signaling pathway. Oncotarget, **8**(52): 89643–89654. doi:10.18632/oncotarget.20288. PMID:29163777.

86. Park, S.M., Deering, R.P., Lu, Y., Tivnan, P., Lianoglou, S., Al-Shahrour, F., et al. 2014. Musashi-2 controls cell fate, lineage bias, and TGF-beta signaling in HSCs. J. Exp. Med. **211**(1): 71–87. doi:10.1084/jem.20130736. PMID:24395885.
87. Park, S.M., Gönen, M., Vu, L., Minuesa, G., Tivnan, P., Barlowe, T.S., et al. 2015. Musashi2 sustains the mixed-lineage leukemia-driven stem cell regulatory program. J. Clin. Invest. **125**(3): 1286–1298. doi:10.1172/JCI78440. PMID: 25664853.
88. Pérez-Ortín, J.E., Alepuz, P., Chávez, S., and Choder, M. 2013. Eukaryotic mRNA decay: methodologies, pathways, and links to other stages of gene expression. J. Mol. Biol. **425**(20): 3750–3775. doi:10.1016/j.jmb.2013.02.029. PMID: 23467123.
89. Perrotti, D., and Calabretta, B. 2002. Post-transcriptional mechanisms in BCR/ ABL leukemogenesis: role of shuttling RNA-binding proteins. Oncogene, **21**(56): 8577–8583. doi:10.1038/sj.onc.1206085. PMID:12476304.
90. Perrotti, D., Bonatti, S., Trotta, R., Martinez, R., Skorski, T., Salomoni, P., et al. 1998. TLS/FUS, a pro-oncogene involved in multiple chromosomal translocations, is a novel regulator of BCR/ABL-mediated leukemogenesis. EMBO J. **17**(15): 4442–4455. doi:10.1093/emboj/17.15.4442. PMID:9687511.
91. Povinelli, B.J., Rodriguez-Meira, A., and Mead, A.J. 2018. Single cell analysis of normal and leukemic hematopoiesis. Mol. Aspects Med. **59**: 85–94. doi:10. 1016/j.mam.2017.08.006. PMID:28863981.
92. Rentas, S., Holzapfel, N., Belew, M.S., Pratt, G., Voisin, V., Wilhelm, B.T., et al. 2016. Musashi-2 attenuates AHR signaling to expand human hematopoietic stem cells. Nature, **532**(7600): 508–511. doi:10.1038/nature17665. PMID: 27121842.
93. Ritchey, L.E., Su, Z., Tang, Y., Tack, D.C., Assmann, S.M., and Bevilacqua, P.C. 2017. Structure-seq2: sensitive and accurate genome-wide profiling of RNA structure *in vivo*. Nucleic Acids Res. **45**(14): e135. doi:10.1093/nar/gkx533. PMID:28637286.
94. Rouskin, S., Zubradt, M., Washietl, S., Kellis, M., and Weissman, J.S. 2014. Genome-wide probing of RNA structure reveals active unfolding of mRNA structures *in vivo*. Nature, **505**(7485): 701–705. doi:10.1038/nature12894. PMID: 24336214.
95. Sampath, P., Pritchard, D.K., Pabon, L., Reinecke, H., Schwartz, S.M., Morris, D.R., and Murry, C.E. 2008. A hierarchical network controls protein translation during murine embryonic stem cell self-renewal and differentiation. Cell Stem Cell, **2**(5): 448–460. doi:10.1016/j.stem.2008.03.013. PMID: 18462695.
96. Savona, M., Garzon, R., Brown, P.D., Yee, K., Lancet, J.E., Gutierrez, M., et al. 2013. Phase I trial of Selinexor (KPT-330), a first-in-class oral selective inhibitor of nuclear export

(SINE) in patients (pts) with advanced acute myelogenous leukemia (AML). Blood, **122**(21): 1440.

97. Shi, F., Len, Y., Gong, Y., Shi, R., Yang, X., Naren, D., and Yan, T. 2015. Ribavirin inhibits the activity of mTOR/eIF4E, ERK/Mnk1/eIF4E signaling pathway and synergizes with tyrosine kinase inhibitor Imatinib to impair Bcr-Abl mediated proliferation and apoptosis in Ph+ leukemia. PLoS One, **10**(8): e0136746. doi:10.1371/journal.pone.0136746. PMID:26317515.
98. Shirai, C.L., Ley, J.N., White, B.S., Kim, S., Tibbitts, J., Shao, J., et al. 2015. Mutant U2AF1 expression alters hematopoiesis and pre-mRNA splicing *in vivo*. Cancer Cell, **27**(5): 631–643. doi:10.1016/j.ccell.2015.04.008. PMID:25965570.
99. Shlush, L.I., Zandi, S., Mitchell, A., Chen, W.C., Brandwein, J.M., Gupta, V., et al. 2014. Identification of pre-leukaemic haematopoietic stem cells in acute leukaemia. Nature, **506**(7488): 328–333. doi:10.1038/nature13038. PMID: 24522528.
100. Shlush, L.I., Mitchell, A., Heisler, L., Abelson, S., Ng, S.W.K., Trotman-Grant, A., et al. 2017. Tracing the origins of relapse in acute myeloid leukaemia to stem cells. Nature, **547**(7661): 104–108. doi:10.1038/nature22993. PMID:28658204.
101. Song, L., Lin, H.S., Gong, J.N., Han, H., Wang, X.S., Su, R., et al. 2017. microRNA451-modulated hnRNP A1 takes a part in granulocytic differentiation regulation and acute myeloid leukemia. Oncotarget, **8**(33): 55453–55466. doi:10. 18632/oncotarget.19325. PMID:28903433.
102. Sterne-Weiler, T., Martinez-Nunez, R.T., Howard, J.M., Cvitovik, I., Katzman, S., Tariq, M.A., et al. 2013. Frac-seq reveals isoform-specific recruitment to polyribosomes. Genome Res. **23**(10): 1615–1623. doi:10.1101/gr.148585.112. PMID:23783272.
103. Sugawara, T., Oguro, H., Negishi, M., Morita, Y., Ichikawa, H., Iseki, T., et al. 2010. FET family proto-oncogene Fus contributes to self-renewal of hematopoietic stem cells. Exp. Hematol. **38**(8): 696–706. doi:10.1016/j.exphem.2010.04.006. PMID:20412831.
104. Takahashi, K., and Yamanaka, S. 2006. Induction of pluripotent stem cells from mouse embryonic and adult fibroblast cultures by defined factors. Cell, **126**(4): 663–676. doi:10.1016/j.cell.2006.07.024. PMID:16904174.
105. Topisirovic, I., Guzman, M.L., McConnell, M.J., Licht, J.D., Culjkovic, B., Neering, S.J., et al. 2003. Aberrant eukaryotic translation initiation factor 4E-dependent mRNA transport impedes hematopoietic differentiation and contributes to leukemogenesis. Mol. Cell. Biol. **23**(24): 8992–9002. doi:10.1128/ MCB.23.24.8992-9002.2003. PMID:14645512.
106. Trotta, R., Vignudelli, T., Candini, O., Intine, R.V., Pecorari, L., Guerzoni, C., et al. 2003. BCR/ABL activates mdm2 mRNA translation via the La antigen. Cancer Cell, **3**(2): 145–160. doi:10.1016/S1535-6108(03)00020-5. PMID:12620409.

107. Ule, J., Jensen, K.B., Ruggiu, M., Mele, A., Ule, A., and Darnell, R.B. 2003. CLIP identifies Nova-regulated RNA networks in the brain. Science, **302**(5648): 1212–1215. doi:10.1126/science.1090095. PMID:14615540.
108. Ule, J., Jensen, K., Mele, A., and Darnell, R.B. 2005. CLIP: a method for identifying protein–RNA interaction sites in living cells. Methods, **37**(4): 376–386. doi:10.1016/j.ymeth.2005.07.018. PMID:16314267.
109. Van Nostrand, E.L., Pratt, G.A., Shishkin, A.A., Gelboin-Burkhart, C., Fang, M.Y., Sundararaman, B., et al. 2016. Robust transcriptome-wide discovery of RNAbinding protein binding sites with enhanced CLIP (eCLIP). Nat. Methods, **13**(6): 508–514. doi:10.1038/nmeth.3810. PMID:27018577.
110. Voronina, E., Seydoux, G., Sassone-Corsi, P., and Nagamori, I. 2011. RNA granules in germ cells. Cold Spring Harbor Perspect. Biol. **3**(12): a002774. doi:10.1101/cshperspect.a002774. PMID:21768607.
111. Vu, L.P., Pickering, B.F., Cheng, Y., Zaccara, S., Nguyen, D., Minuesa, G., et al. 2017a. The N6-methyladenosine (m6A)-forming enzyme METTL3 controls myeloid differentiation of normal hematopoietic and leukemia cells. Nat. Med. **23**(11): 1369–1376. doi:10.1038/nm.4416. PMID:28920958.
112. Vu, L.P., Prieto, C., Amin, E.M., Chhangawala, S., Krivtsov, A., Calvo-Vidal, M.N., et al. 2017b. Functional screen of MSI2 interactors identifies an essential role for SYNCRIP in myeloid leukemia stem cells. Nat. Genet. **49**(6): 866–875. doi:10.1038/ng.3854. PMID:28436985.
113. Wadugu, B., Heard, A., Bradley, J., Ndonwi, M., and Walter, M.J. 2017. Normal hematopoiesis is dependent on the expression of U2af1, a spliceosome gene commonly mutated in MDS. Blood, **130**(Suppl. 1): 3747.
114. Walker, C.J., Oaks, J.J., Santhanam, R., Neviani, P., Harb, J.G., Ferenchak, G., et al. 2013. Preclinical and clinical efficacy of XPO1/CRM1 inhibition by the karyopherin inhibitor KPT-330 in Ph+ leukemias. Blood, **122**(17): 3034–3044. doi:10.1182/blood-2013-04-495374. PMID:23970380.
115. Wang, T., Birsoy, K., Hughes, N.W., Krupczak, K.M., Post, Y., Wei, J.J., et al. 2015. Identification and characterization of essential genes in the human genome. Science, **350**(6264): 1096–1101. doi:10.1126/science.aac7041. PMID:26472758.
116. Weischenfeldt, J., Damgaard, I., Bryder, D., Theilgaard-Mönch, K., Thoren, L.A., Nielsen, F.C., et al. 2008. NMD is essential for hematopoietic stem and progenitor cells and for eliminating by-products of programmed DNA rearrangements. Genes Dev. **22**(10): 1381–1396. doi:10.1101/gad.468808. PMID:18483223.

117. Weng, H., Huang, H., Wu, H., Qin, X., Zhao, B.S., Dong, L., et al. 2018. METTL14 inhibits hematopoietic stem/progenitor differentiation and promotes leukemogenesis via mRNA m6A modification. Cell Stem Cell, **22**(2): 191–205.e9. doi:10.1016/j.stem.2017.11.016. PMID:29290617.
118. Wilson, N.K., Foster, S.D., Wang, X., Knezevic, K., Schütte, J., Kaimakis, P., et al. 2010. Combinatorial transcriptional control in blood stem/progenitor cells: genome-wide analysis of ten major transcriptional regulators. Cell Stem Cell, **7**(4): 532–544. doi:10.1016/j.stem.2010.07.016. PMID:20887958.
119. Wilson, N.K., Kent, D.G., Buettner, F., Shehata, M., Macaulay, I.C., Calero-Nieto, F.J., et al. 2015. Combined single-cell functional and gene expression analysis resolves heterogeneity within stem cell populations. Cell Stem Cell, **16**(6): 712–724. doi:10.1016/j.stem.2015.04.004. PMID:26004780.
120. Wong, C.C., Traynor, D., Basse, N., Kay, R.R., and Warren, A.J. 2011. Defective ribosome assembly in Shwachman–Diamond syndrome. Blood, **118**(16): 4305–4312. doi:10.1182/blood-2011-06-353938. PMID:21803848.
121. Xiao, N., Laha, S., Das, S.P., Morlock, K., Jesneck, J.L., and Raffel, G.D. 2015. Ott1 (Rbm15) regulates thrombopoietin response in hematopoietic stem cells through alternative splicing of c-Mpl. Blood, **125**(6): 941–948. doi:10.1182/blood2014-08-593392. PMID:25468569.
122. XuFeng, R., Boyer, M.J., Shen, H., Li, Y., Yu, H., Gao, Y., et al. 2009. ADAR1 is required for hematopoietic progenitor cell survival via RNA editing. Proc. Natl. Acad. Sci. U.S.A. **106**(42): 17763–17768. doi:10.1073/pnas.0903324106. PMID:19805087.
123. Yeo, G.W., Coufal, N.G., Liang, T.Y., Peng, G.E., Fu, X.D., and Gage, F.H. 2009. An RNA code for the FOX2 splicing regulator revealed by mapping RNA–protein de Rooij et al. 19 Published by NRC Research Press interactions in stem cells. Nat. Struct. Mol. Biol. **16**(2): 130–137. doi:10.1038/ nsmb.1545. PMID:19136955.
124. Young, D.J., Stoddart, A., Nakitandwe, J., Chen, S.C., Qian, Z., Downing, J.R., and Le Beau, M.M. 2014. Knockdown of Hnrnpa0, a del(5q) gene, alters myeloid cell fate in murine cells through regulation of AU-rich transcripts. Haematologica, **99**(6): 1032–1040. doi:10.3324/haematol.2013.098657. PMID:24532040.
125. Yu, J., Vodyanik, M.A., Smuga-Otto, K., Antosiewicz-Bourget, J., Frane, J.L., Tian, S., et al. 2007. Induced pluripotent stem cell lines derived from human somatic cells. Science, **318**(5858): 1917–1920. doi:10.1126/science.1151526. PMID:18029452.
126. Yuan, J., and Muljo, S.A. 2013. Exploring the RNA world in hematopoietic cells through the lens of RNA-binding proteins. Immunol. Rev. **253**(1): 290–303. doi:10.1111/imr.12048. PMID:23550653.

127. Zhang, M., Fu, W., Prabhu, S., Moore, J.C., Ko, J., Kim, J.W., et al. 2008. Inhibition of polysome assembly enhances imatinib activity against chronic myelogenous leukemia and overcomes imatinib resistance. Mol. Cell. Biol. **28**(20): 6496–6509. doi:10.1128/MCB.00477-08. PMID:18694961.
128. Zhou, F., Liu, Y., Rohde, C., Pauli, C., Gerloff, D., Köhn, M., et al. 2017. AML1-ETO requires enhanced C/D box snoRNA/RNP formation to induce self-renewal and leukaemia. Nat. Cell. Biol. **19**(7): 844–855. doi:10.1038/ncb3563. PMID: 28650479.
129. Zipeto, M.A., Court, A.C., Sadarangani, A., Delos Santos, N.P., Balaian, L., Chun, H.J., et al. 2016. ADAR1 activation drives leukemia stem cell selfrenewal by impairing let-7 biogenesis. Cell Stem Cell, **19**(2): 177–191. doi:10. 1016/j.stem.2016.05.004. PMID:27292188.

Chapter 5: Concluding Remarks

The novel connection reported in this thesis between ACD-associated genes with defects in HSCs and the pathogenesis of benign blood disorders uniquely highlights how alterations to critical developmental pathways can effectively compromise hematopoiesis in diverse ways. Indeed, much of the heterogeneity and idiopathic nature of bone marrow failure syndromes remain to be better understood at the molecular level. To date, exemplar pathways classically known to be disrupted in inherited bone marrow failure syndromes include defects in DNA repair in Fanconi anemia (Kottemann and Smogorzewska, 2013; Longerich *et al.*, 2014), defective ribosomal biogenesis and assembly in Diamond-Blackfan anemia (Choesmel *et al.*, 2007; Khajuria *et al.*, 2018) and Shwachman-Diamond syndrome (Burwick *et al.*, 2012), and dysfunctions in telomere maintenance and small noncoding RNAs in dyskeratosis congenita (Mitchell *et al.*, 1999; Vulliamy *et al.*, 2001; Bellodi *et al.*, 2013), among others. However, as suggested by results from this work, there may exist a wider landscape to which other developmentally-linked genes may contribute to and/or explain the pathogenesis of certain bone marrow failure syndromes.

For example, our identification of Arhgef2 as an essential spindle orienting factor in HSCs highlights the importance of integrating extrinsic and intrinsic crosstalk. Interestingly, we also recently learned that unpublished work by another research group has found a broader polarity network disrupted in Shwachman-Diamond syndrome potentially consistent with our findings. In the case of aplastic anemia, while the most favoured model supports a dysregulated immune system that elicits autoreactive T cell destruction of HSPCs, clear lines of evidence also point toward intrinsic defects within affected HSCs that may arise from germline mutations not yet fully appreciated (Kallen *et al.*, 2019). Our data on Stau1 at least supports the concept that disruptions

to a post-transcriptional landscape in HSCs can independently predispose or lead towards anemia, and in combination of a growing body of literature on RBP effects in HSCs, opens up doors to a relatively uncharted territory. Recent sequencing efforts have also identified clonal mutations in paroxysmal nocturnal hemoglobinuria, previously thought of as a monogenic disorder, that predate or follow acquisition of canonical *PIGA* mutations, demonstrating similar architectures to those found in malignant neoplasms, the significance of which has yet to be elucidated (Shen *et al.*, 2014).

These observations of broader network alterations, alternative pathways that potentially lead to similar phenotypes, and overlapping landscapes between benign and malignant hematopoietic diseases suggest a rich and complex landscape intrinsic to HSCs yet to be annotated for significance across the full spectrum of benign to malignant hematopoietic disorders. Efforts at the frontier of bone marrow failure research now include studying earlier defects in fetal hematopoiesis (Kurre, 2018), the role of surrounding microenvironment to both disease process and transplant outcomes (Zha *et al.*, 2019), induced pluripotent stem cell-based modelling strategies (Elbadry *et al.*, 2019), studies of clonal evolution in related settings (Shen *et al.*, 2014; Babushok *et al.*, 2015; Yoshizato *et al.*, 2015), single cell based profiling of rare cell populations (Joyce *et al.*, 2019) and genetic studies of germline mutations (Bluteau *et al.*, 2018), as well as applications of gene editing (Wu *et al.*, 2019; Humbert *et al.*, 2019) and gene therapy (Ribeil *et al.*, 2017; Thompson *et al.*, 2018). Future work should recognize the former on this benign-to-malignant continuum of defective hematopoiesis more fully, not only to better capture deviations from normal hematopoiesis across the developmental lifespan of an organism or individual, but to ultimately leverage and harness such insight for applications that may one day reach and treat even these rarest of diseases.

References

1. Babushok DV, Perdigones N, Perin JC, Olson TS, Ye W, Roth JJ, et al. 2015. Emergence of clonal hematopoiesis in the majority of patients with acquired aplastic anemia. Cancer Genet. 208:115–128.
2. Bellodi C, McMahon M, Contreras A, Juliano D, Kopmar N, Nakamura T, et al. 2013. H/ACA small RNA dysfunctions in disease reveal key roles for noncoding RNA modifications in hematopoietic stem cell differentiation. Cell Rep. 3:1493–1502.
3. Bluteau O, Sebert M, Leblanc T, Peffault de Latour R, Quentin S, Lainey E, et al. 2018. A landscape of germ line mutations in a cohort of inherited bone marrow failure patients. Blood. 131:717–732.
4. Burwick N, Coats SA, Nakamura T, Shimamura A. 2012. Impaired ribosomal subunit association in Shwachman-Diamond syndrome. Blood. 120:5143–5152.
5. Choesmel V, Bacqueville D, Rouquette J, Noaillac-Depeyre J, Fribourg S, Crétien A, et al. 2007. Impaired ribosome biogenesis in Diamond-Blackfan anemia. Blood. 109:1275–1283.
6. Elbadry MI, Espinoza JL, Nakao S. 2019. Disease modeling of bone marrow failure syndromes using iPSC-derived hematopoietic stem progenitor cells. Exp Hematol. 71:32–42.
7. Humbert O, Radtke S, Samuleson C, Carrillo RR, Perez AM, Reddy SS, et al. 2019. Therapeutically relevant engraftment of a CRISPR-Cas9-edited HSC-enriched population with HbF reactivation in nonhuman primates. Sci Transl Med. 11:eaaw3768.
8. Joyce CE, Saadatpour A, Ruiz-Gutierrez M, Bolukbasi OV, Jiang L, Thomas DD, et al. 2019. TGFβ signalling underlies hematopoietic dysfunction and bone marrow failure in Shwachman-Diamond syndrome. J Clin Invest. 130:3821–3826.
9. Kallen ME, Dulau-Florea A, Wang W, Calvo KR. 2019. Acquired and germline predisposition to bone marrow failure: diagnostic features and clinical implications. Semin Hematol. 56:69–82.
10. Khajuria RK, Munschauer M, Ulirsch JC, Fiorini C, Ludwig LS, McFarland SK, et al. 2018. Ribosome levels selectively regulate translation and lineage commitment in human hematopoiesis. Cell. 173:90–103.
11. Kottemann MC, Smogorzewska A. 2013. Fanconi anaemia and the repair of Watson and Crick DNA crosslinks. Nature. 493:356–363.
12. Kurre P. 2018. Hematopoietic development: a gap in our understanding of inherited bone marrow failure. Exp Hematol. 59:1–8.

13. Lian Y, Shi J, Nie N, Huang Z, Shao Y, Zhang J, et al. 2019. Evolution patterns of paroxysmal nocturnal hemoglobinuria clone and clinical implications in acquired bone marrow failure. Exp Hematol. 77:41–50.
14. Longerich S, Li J, Xiong Y, Sung P, Kupfer GM. 2014. Stress and DNA repair biology of the Fanconi anemia pathway. Blood. 124:2812–2819.
15. Mitchell JR, Wood E, Collins K. 1999. A telomerase component is defective in the human disease dyskeratosis congenita. Nature. 402:551–555.
16. Ribeil JA, Hacein-Bey-Abina S, Payen E, Magnani A, Semeraro M, Magrin E, et al. 2017. Gene therapy in a patient with sickle cell disease. N Engl J Med. 376:848–855.
17. Shen W, Clemente MJ, Hosono N, Yoshida K, Przychodzen B, Yoshizato T, et al. 2014. Deep sequencing reveals stepwise mutation acquisition in paroxysmal nocturnal hemoglobinuria. J Clin Invest. 124:4529–4538.
18. Thompson AA, Walters MC, Kwiatkowski J, Rasko JEJ, Ribeil JA, Hongeng S, et al. 2018. Gene therapy in patients with transfusion-dependent β–thalassemia. N Engl J Med. 378:1479–1493.
19. Vulliamy T, Marrone A, Goldman F, Dearlove A, Bessler M, Mason PJ, et al. 2001. The RNA component of telomerase is mutated in autosomal dominant dyskeratosis congenita. Nature. 413:432–435.
20. Wu Y, Zeng J, Roscoe BP, Liu P, Yao Q, Lazzarotto CR, et al. 2019. Highly efficient therapeutic gene editing of human hematopoietic stem cells. Nat Med. 25:776–783.
21. Yoshizato T, Dumitriu B, Hosokawa K, Makishima H, Yoshida K, Townsley D, et al. 2015. Somatic mutations and clonal hematopoiesis in aplastic anemia. N Engl J Med. 373:35–47.
22. Zha J, Kunselman L, Fan JM, Olson TS. 2019. Bone marrow niches of germline FANCC/FANCG deficient mice enable efficient and durable engraftment of hematopoietic stem cells after transplantation. Haematologica. 104:e284–e287.